SPRING-PINS AS A TIMBER CONNECTOR IN PARALLEL STRAND LUMBER

by

MARK ROBERTSON

B.A.Sc., The University of British Columbia, 2003

A THESIS SUBMITTED IN PARTIAL FULFILLMENT OF THE REQUIREMENTS FOR THE DEGREE OF

MASTER OF APPLIED SCIENCE

in

THE FACULTY OF GRADUATE STUDIES

(Civil Engineering)

THE UNIVERISTY OF BRITISH COLUMBIA

October, 2006

ABSTRACT

The spring pin timber connection was developed by Structurecraft Builders Inc. to meet an architectural need for a high profile project involving a large glass timber façade. Traditionally, bolts would be used for such connections, however these were not acceptable from an architectural standpoint due to the aesthetic statement of the nut and bolt. The spring pin is an "off the shelf" fastener with a compressible diameter so that it fits tightly in the connection hole eliminating the need for highly visible nuts and bolts.

Aside from its architectural benefits, the tight-fitting nature of the spring-pin connection has suitable stiffness performance characteristics required for a glass façade. Bolts would have been insufficient because the bolthole tolerance involved would allow for too much slop in the connection posing a hazard to the glazing system. Furthermore, current research has indicated that there is a potential for a strength advantage of tight-fitting pins over bolts with required bolthole tolerances.

This thesis examines the strength and stiffness characteristics of these tight-fitting pins with ramifications for all tight-fitting pins. A simple Monte-Carlo simulation is presented that provides insight into the effect of bolthole tolerances. The research includes a discussion of the physical testing of the spring-pin connection, and determines the statistical implications of testing twin ended wood connections in which only one end fails. The physical testing is used as tool to determine the fastener stiffness and bearing strength both perpendicular to grain and parallel to

grain. Testing is conducted on multiple pin connections, and ultimately on moment connections to reflect the load demands predicted in the structural model.

It was found that the spring-pin connection is stiff and strong enough to be used in the façade structural system as a light-duty moment connection. Although the stiffness of the connection is greatly enhanced over tradition bolts, the effect of removing bolthole tolerances on the axial strength of a wood connection is not found to be significant for the connection of interest. The influence of the hole-tolerance is likely to be more profound with brittle connections and diminishes with increased slenderness/ductility of the timber fastener.

TABLE OF CONTENTS

LIST OF TABLES

LIST OF FIGURES

ACKNOWLEDGEMENTS

I would like to thank Dr. Helmut Prion for getting me started on the right path, and for the many hours of discussion that helped me focus my energies. I would also like to thank Dr. Carlos Ventura and Dr. Terje Haukaas for taking me under their wing and helping me get to the finish line. I would also like to express my gratitude to Gerald Epp, owner of Structurecraft Builders, was it not for his inspiration and dedication to quality this thesis would certainly not exist. I also give a special thanks to my family for their support during all my years at University. Finally, an extra special thank-you to my loving wife Anna for putting up with my late nights of research during our first years of life together.

1.0 INTRODUCTION

The research presented in this thesis was conducted in conjunction with an industrial sponsor, Structurecraft Builders Inc of British Columbia. This company specializes in design-build contracts for architectural heavy timber. In heavy timber construction, the majority of the structural cost comes from the joinery of the timber members. There are many connection options available to the engineer in wood, but situations arise in which research is necessary to prove the viability of a structural system. This might be important to control escalating construction costs or even make the architectural system a possibility at all, leading to some exciting opportunities for research and development. My research is focused on the implementation of a heavy timber structural system for a proposed design-build project, but many general contributions to the body of timber engineering were made as a by-product of this process. This thesis refers to many different research issues in the field of Timber Engineering, although not solving all of them rigorously may provide some information to other research.

1.1 DEVELOPMENT OF THE SPRING-PIN

The spring pin is an "off the shelf" fastener typically used in the automotive industry, which has caught the attention of the structural engineers at Fast + Epp for it's potential in timber as a fastener. The spring-pin is a hollow tube with a longitudinal gap running along its entire length allowing the diameter of the connector to be compressed (See Figure 1.1). The pin is installed by jamming it into a pre-drilled hole slightly smaller

than its diameter. The pin will compress during the installation process and therefore be tight fitting and snug in its final position.

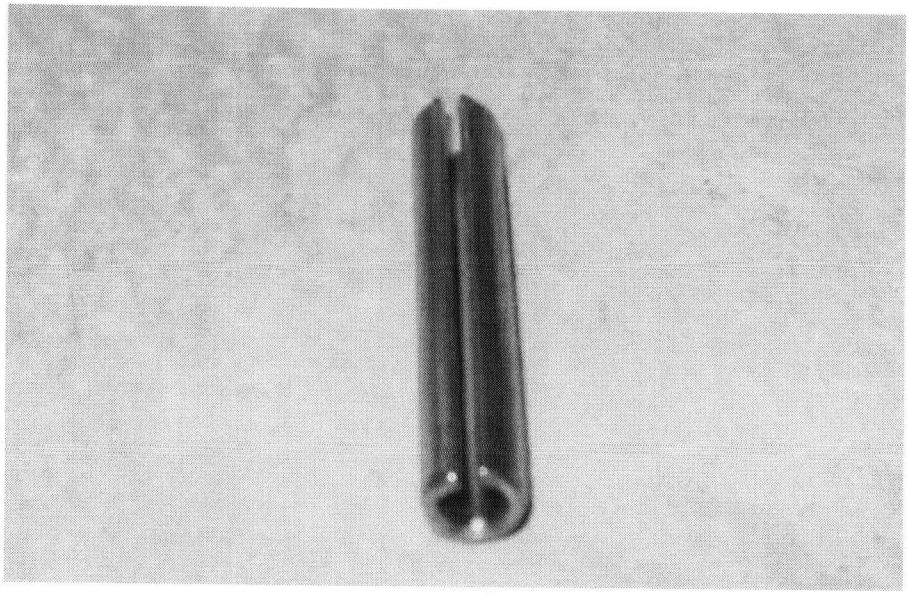

Figure 1.1 A ½" diameter spring-pin

The spring pin timber connection was developed by Structurecraft to meet the architectural requirements for a large glass timber façade at Surrey City Centre (See Figure 1.2 & 1.3). The spring pin connections were used to connect the bracing arms to the columns and to the mullion beams. A low level of visibility was desired for the highly exposed connections between the refined timber mullion beams. The connection plates were mortised into the receiving wood member to reduce the visibility of the joinery by means of what is called a knife-plate connection (See Figure 1.2 & 1.3).

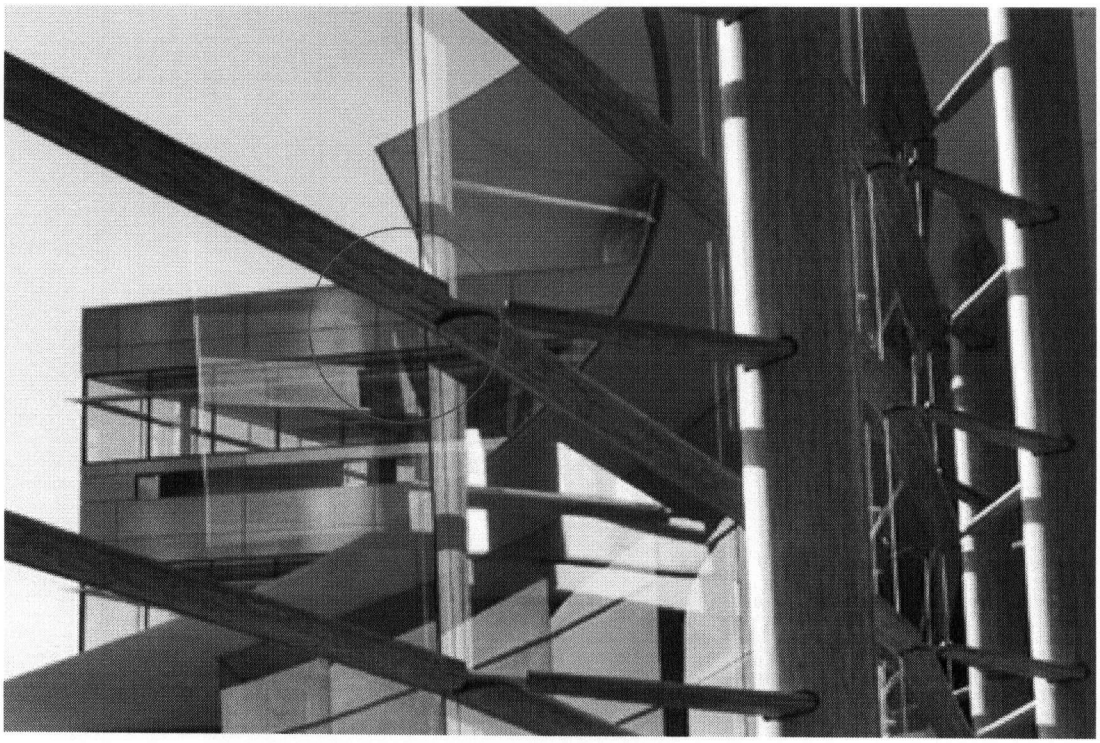

Figure 1.2 The Surrey City Façade. Note the low visibility of the spring-pin knife-plate connections.

Traditionally, bolts would be used for such connections, however these would have been unacceptable from a visual standpoint. Since spring pins are compressible, they can be installed into the connection in a tight fitting manner negating the need for highly visible mechanical fasteners such as nuts & bolts. Furthermore, bolted connections are quite insufficient because of the required tolerances inherently involved with bolt installation and resulting loss of stiffness and quite possibly strength. Bolts have been observed to fail in a manner analogous to a zipper with one bolt reaching peak capacity at a time. The tight fit of the spring-pin would, in theory, encourage all fasteners to reach peak strength at the same time.

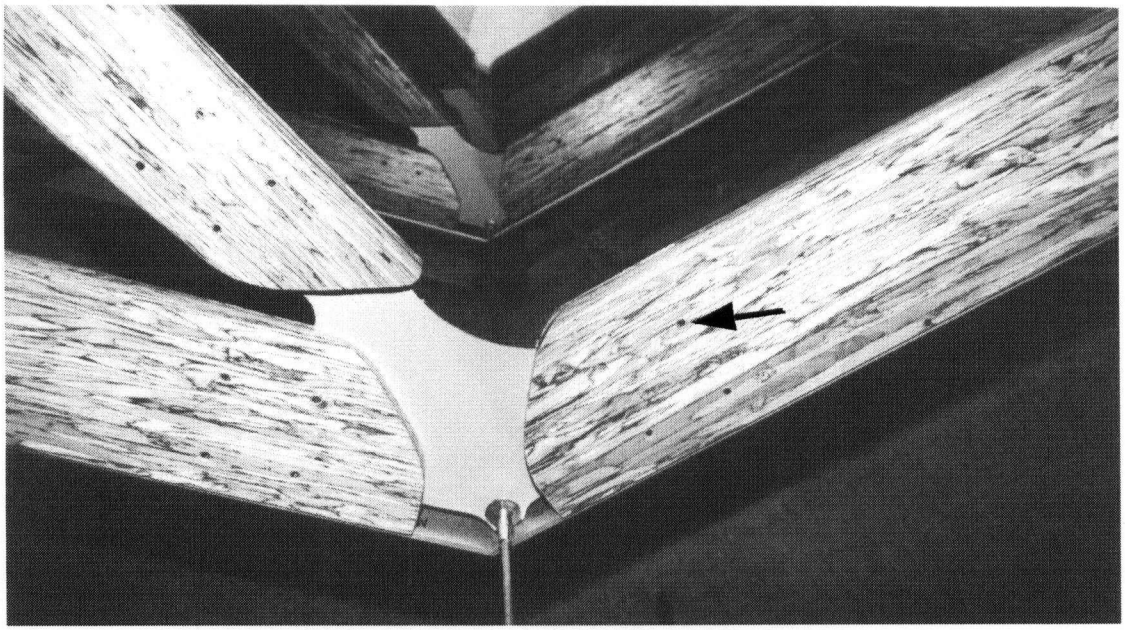

Figure 1.3 Close-up of the Spring-pin connection at Surrey City Center. The cable takes the vertical weight of the glass in this system.

1.2 INITIAL TESTING FOR SURREY CITY CENTRE

To confirm that the spring-pins met or exceeded the CSA–086 design code on bolted connections, a modest testing program was conducted to observe the behaviour of the spring-pin connections. The testing program consisted of tension tests on 12 test specimens with a 4-pin configuration with the same curve shaped cross-section as the in-situ connections (See Figure 1.3).

Further tests were also conducted to explore the effect of eccentricity on the axial capacity of the connection because of concerns that the structural system could be compromised by some unintended bending moments that would be distributed to the connections. This called for the testing of an additional 6 connections of the same configuration, but with the load applied at an eccentricity of 1.5 inches.

1.2.1 Testing Specifications

The original test specimens were made to model exactly what was used in the Surrey City Centre Project. The test specimens consisted of shaped PSL with outside dimensions of 89x180. Two materials were investigated for the embedded knife plate, namely 3 sets of ¼" steel and 3 sets of 5/8" aluminium plate. The pin configuration, row spacing and end/edge distances can be seen in Figure 1.4. The row and fastener spacing were twice what the Canadian code recommends, and the loaded end distance was 8 diameters or 1 diameter larger than the minimum required. The test specimens were all twin-ended, which means that the machine actually tests two connections at once with only one connection failing. The connection that did not fail was, for the purpose of statistics, given the same capacity as the connection that failed even though

it may hold more load. The statistical effect of this double set of data was not investigated until work began on this thesis in 2004.

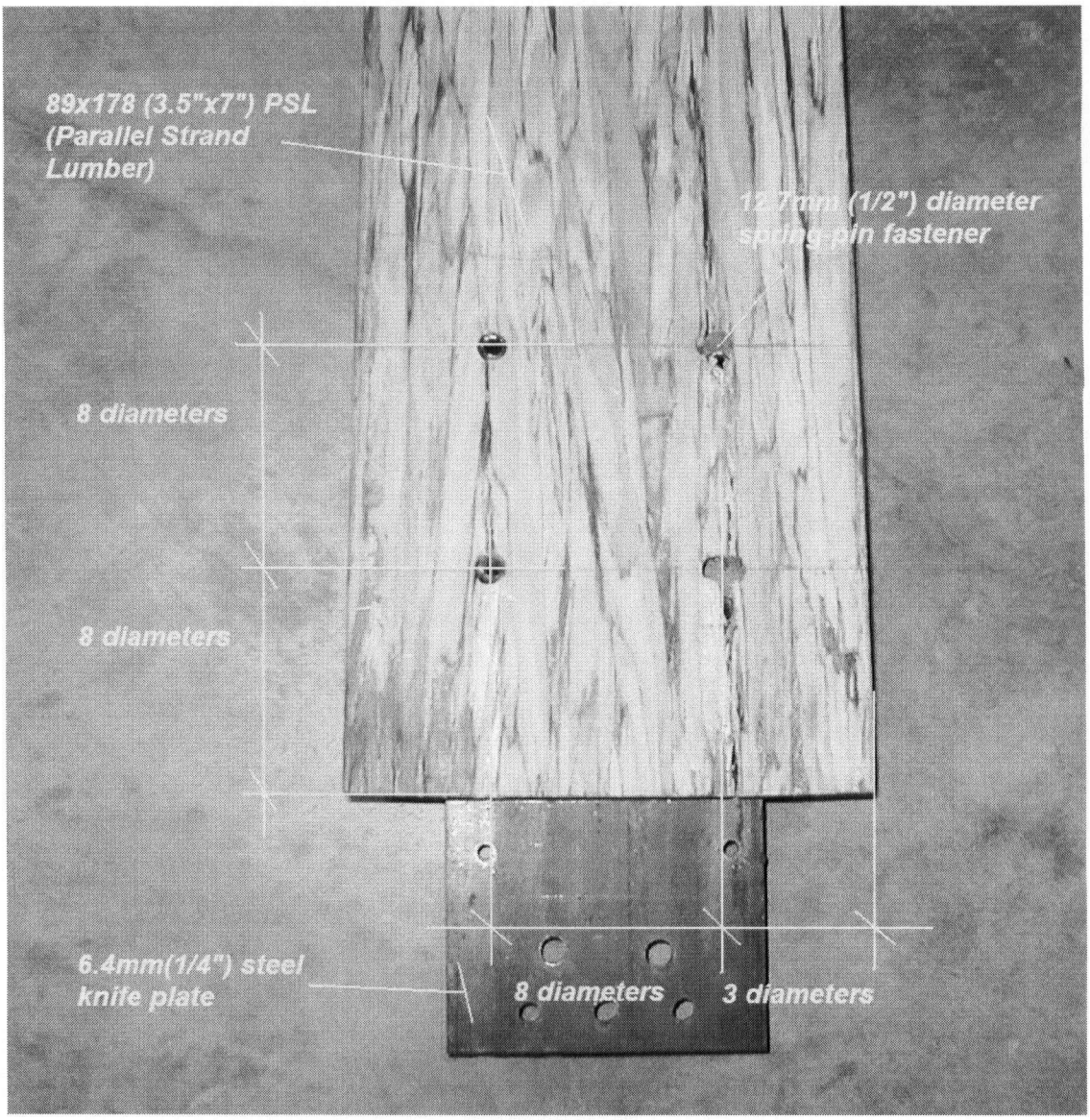

Figure 1.4 *Geometry of initial test specimens*

1.2.2 Measurement Error

Accurate displacement measurements were not of primary importance to this testing and the only recorded displacement was that of the stroke of the testing machine. This is highly inaccurate because there was significant movement between the machine grips that is not considered part of the connection. The following are sources of error:

- Significant yielding around the large diameter bolthole connecting the test specimens to the grips of the machine. Approximately 6mm each side.
- Since there are two connections being tested, it is difficult to know the true stiffness of the individual connections. Assuming equal stiffness for both is not acceptable since wood connections have a large coefficient of variance (approximately 30-50%). Furthermore, once one side would start yielding, any further deformations are likely to be concentrated on the failing connection, while the intact side might actually experience a reduction in displacement as the load decreases after the peak load has been passed.

1.2.3 Interpretation of Results By Others

The results of the tests indicated a significant increase in strength for the spring-pin connections over the code values for equivalent bolted connections.

Code Capacity (CSA O86-01)

SPECIFIED STRENGTH = 70 KN

FAILURE MODE: Embedding Failure without Plastic Hinging

GROUP EFFECTS (FACTORS):

Row factor J_R = 0.8,

End distance factor for 8 diameters J_L = 0.83,

which yields a cumulative configuration factor of $J_F = J_G * J_R * J_L = 0.66$

Test Results:

Number of Specimens = 12 (6 twin ended)

Mean Strength of Tests = 114 kN

Standard Deviation = 8 kN

5^{th} Percentile of Tests = 102 kN

C.O.V. = 6.7%

The direct comparison to the test results to the code value shows that the code for bolted connections has 66% of the capacity of the spring-pin connection. This number just happened to be exactly the same as the group factor, JF = 0.66, calculated by the code. At this stage in the spring-pin development the following hypothesis presents itself: The superior performance of the tight-fit spring-pins can be ascribed to the elimination of the configuration (group) effect.

1.2.4 Design Resistance Used

The Engineers at Structurecraft Builders performing the structural calculations were encouraged with the highly consistent test and felt comfortable using the 5th percentile for design. To establish a resistance per pin, a four pin connection load of 105kN was divided by the number of pins, 4, giving a single-pin strength of 26 kN. Using the CSA-086-01 code on bolted connections as a model, the resistance of the spring-pin connection can be written as:

$$\Pr = \phi \cdot P_{0.05} \cdot N \cdot 0.85 \cdot K_t \cdot K_d \qquad [1.1]$$

Where,

- *N, number of fasteners, provided that no more than 4 spring-pins are to be used.*
- *$P_{0.05}$ = 26KN, 5th percentile strength for the individual fastener.*
- *ϕ is the same as that used for bolted connections in CSA 086-01, namely 0.7*
- *Loaded end, edge, and fastener spacing distances are to conform to the minimum specimen specifications used in test specimens.*
- *Kt is the treatment factor (not applicable) as recommended by CSA 086*
- *Kd is the load duration factor (1.15 for wind) as recommended by CSA 086*
- *The factor 0.85 is to reduce the 5th percentile of a 5-minute test duration strength to a normal load duration*

1.2.5 Topics for Further Research

Although the strength values are dependable, there are some concerns about the performance of the spring-pin connections especially if the engineers intend to deviate from the original connection specifications. Questions raised were:

- Is the tight fitting nature of the spring-pin responsible for the perceived advantage in performance of spring-pins over the code for bolts?
- What is the physical difference of strength and stiffness between spring-pins and bolted connections?
- How do the spring-pin connections perform with more than 4 pins
- What is the effect of eccentricity on the spring-pin connections
- Can the perceived advantage of spring-pins be attributed to the overly conservative conversion of bolt capacities in sawn lumber to that of Parallel Strand Lumber?

1.3 SCOPE AND OBJECTIVES

Structurecraft Builders were invited to bid on a job in Washington DC as part of a larger project for the Arena Stage theatres. The overall project involves the retrofit of three theatres and the construction of a large canopy to shelter all three theatres. Structurecraft is bidding on a portion of the project; a heavy timber glass façade that surrounds all three theatres. The architects were inspired by the previous work Structurecraft had done at Surrey City Centre. The proposed façade was intended to be much larger in scale and complexity.

Because of the complexity of the structure and the high profile of the work, Structurecraft did not feel comfortable with the limited scope of the technical information they had acquired on the spring-pin timber connectors. Further research and testing into their performance was mandatory.

The purpose of my work was to design the timber façade for Arena Stage and to ensure the connections will perform as expected by developing and executing a testing program. As the thesis research evolved, many issues relating to testing and timber engineering presented themselves.

Firstly, it was suggested by Structurecraft that the connections be tested in pairs as shown in Figure 1.5 in order to save costs. Two statistical methods are presented in Section 2.0 that interpret the statistical implications of this test setup. Section 2.0 also describes the methodology used to convert test results to design values with guidance from the Canadian wood design manual CSA-086.

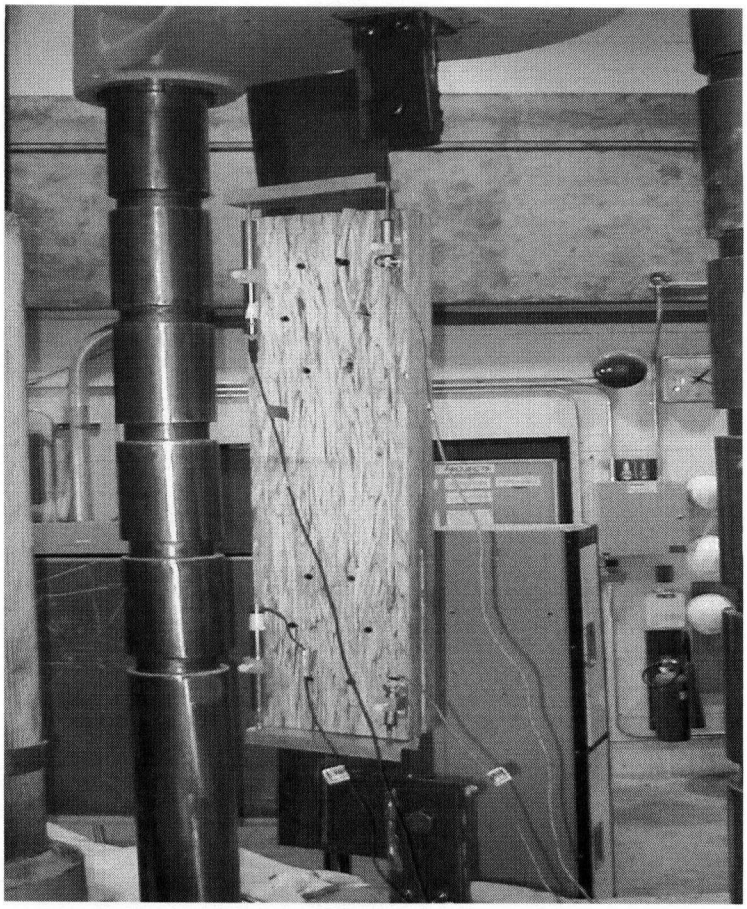

Figure 1.5 *Photograph of Test Specimen with two connections top and bottom. Note the top connection has failed while the bottom remains relatively undisturbed.*

The structural model for the Arena Stage project was a central focus to this thesis and is discussed in Section 3.0. The structural model was highly sensitive to the rotational stiffness of the spring-pin connection. The structural model incorporates the rotational stiffness of the connection as a variable, the value of which was confirmed by physical testing discussed in section 6.0. Using the flexibility of a connection as a variable is an unusual practice in structural analysis. Section 3.0 illustrates how, for some unusual structures, this approach is necessary.

The scope of this research is also required to encompass the behaviour of dowelled connections in Parallel Strand Lumber (a proprietary wood product). Some existing literature was used to aid in the understanding of this material and is discussed in Section 4.0. Section 4.0 primarily focuses on the impact of the spring-pin dowel itself. The single fastener response of the spring-pin connector in wood is predicted by the well-established European yield theory. The testing done to confirm the single pin capacity is summarized and discussed in Section 4.0.

Section 5.0 focuses on the statistical advantage of tight-fitting dowels in a wood connection. A statistical model used to compare tight-fitting dowels to loose bolts is presented in this section. Some conclusions are made, but the analysis is not rigorous enough to end the ongoing debate on this subject.

Section 6.0 focuses entirely on the rotational response of the spring-pin connection. This section uses and extends a model presented in two previous M.A.Sc. Thesis at U.B.C to predict the response of the connection to moment loads. The model uses the value of single fastener stiffness to predict the connection behaviour under bending moments. The single fastener stiffness parameters were determined in section 4.0 from single pin testing. This prediction model was compared to observations from physical testing of connections subjected to bending moments.

Although at first this seemed an overly optimistic task for a M.A.Sc program, much of the issues had been addressed in previous studies, and were merely applied to the specifics of the project. These issues were all addressed with a varying degree of rigor. At the end of the study, the ultimate objective remained to ensure that the timber façade was designed to meet the desired level of performance and safety.

2.0 STATISTICS OF TESTING WOOD CONNECTIONS

Most research in the field of timber engineering is focused on the reduction of uncertainty through repetitive testing programs. There are many published test results for strength parameters in wood products and the variability of these results is well known. However, there still remains a significant amount of uncertainty in engineering design. Some uncertainty cannot easily be understood and characterized by a simple set of random variables. An example of this type of uncertainty would be the following:

- Are the patterns of loads applied to the structure in a distribution representative of the loads the structure would see in service?
- Is the deflection criteria used in design adequate for protecting unique architectural façades?
- Will the structure be built as it is designed on paper, or will the contractor/ builder not meet the specifications?

These types of questions cannot be studied and described by stochastic random variables. The remaining uncertainty must be dealt with by good engineering judgment or empirical rules of thumb. Most of the work on this project is epistemic (can be reducible by testing ever more connections), but it is also necessary to discuss the aleatory uncertainty (inherent, irreducible), such as those listed above.

2.1 STATISTICS OF TESTING TWIN ENDED TEST SPECIMENS

One of the unique aspects of the testing program is that the test specimens are twin ended. Physically speaking, this means that the test specimen is gripped at either end. The machine is testing two connections at once, with one connection failing before the peak strength of the other can be recorded (see Figure 2.1).

Failure load of a given test specimen is recorded as the failure of the weaker of the two wood connections in a given test specimen. Therefore the individual connection strength is different from the test specimen strength. If we define these two variables as follows

Z: Capacity of the test specimen, the lesser of two connections

X: Capacity of an individual connection

We are only interested in the connection capacity, X, but are only given the statistical distribution of the specimen strength, *Z*. We know that *Z* will be slightly lower than that of the connection of interest because it is the lesser of two connections, but we don't know by how much. This section looks at the differences in the distributions of *X* and *Z* and how this affects the calculation of design strength (5th percentile).

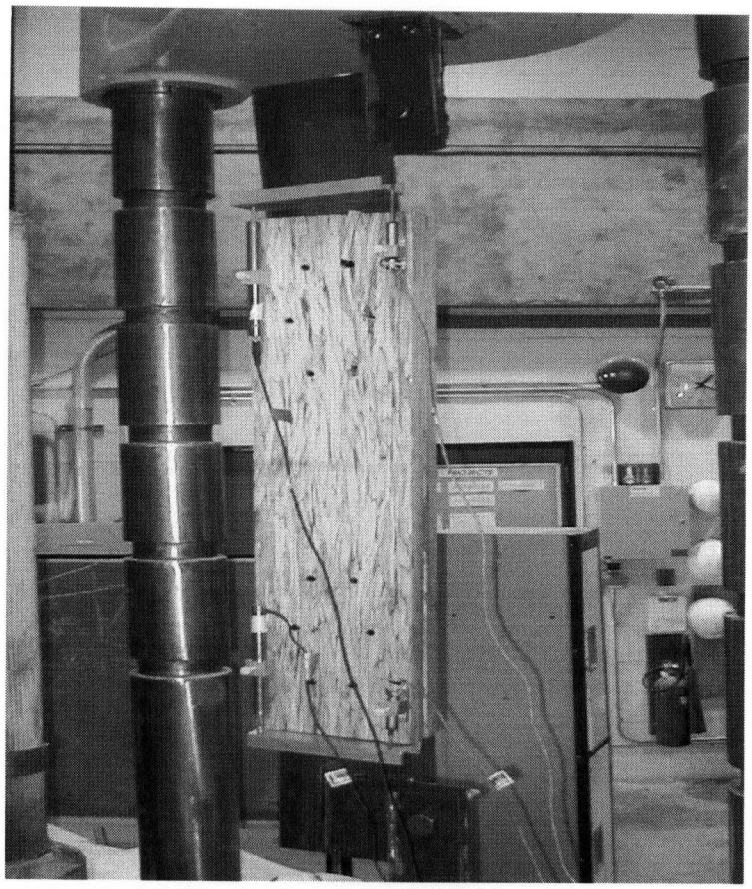

Figure 2.1: *Photograph of Test Specimen with two connections top and bottom. Note the top connection has failed while the bottom remains relatively undisturbed.*

2.1.1 Data Set

The data set (See Table 2.1) consists of six failure strengths for existing tests on 4-pin connections. Note that each failure strength value refers to the failure of the lesser of two connections.

Table 2.1: *Data Set*

Z (kN):	107	116	111	124	120	105

$\overline{Z} = 114kN$, $s_Z = 7.5kN$, *where Z is defined in Section 2.1.0*

Although six tests might appear to be a small number of experiments, the actual number of wood connections tested is 12 since the specimens are twin ended. This results in a higher degree of confidence in the estimate of the mean and standard deviation. ASTM D-5652 recommends 10 specimens for sawn lumber that has a higher coefficient of variation.

2.1.2 Statistical Theory

From the second moment information about the capacity of the test specimen *Z*, it is possible to determine the probability of a test specimen exceeding any value of interest. In structural design, the 5th-percentile strength is used as the characteristic strength in LRFD codes. Assuming *Z* is a normal random variable the design strength can be calculated.

$$Z_{0.05} = Z\left(5^{th} - Percentile\right) = \overline{Z} + \left(\Phi^{-1}[0.05]\right)s_z \qquad [2.1]$$

$$Z_{0.05} = 114kN - 1.64 \cdot 7.5kN = 101kN \qquad [2.2]$$

In practice it is the value of $Z_{0.05}$ that would be used to ultimately determine the design value for a connection. However, as stated before, the design capacity of *Z* is

actually the failure capacity of the test specimen with two ends, not the individual connection strength. Since the test specimen failure strength Z takes the lesser of the two wood connection strengths, the high strength capacities of the connection strength X are filtered out. The likelihood of seeing a high strength outlier is effectively non-existent. Because there are twice as many test samples, the likelihood of *observing* a low strength outlier is increased. If X is a normal random variable, the PDF of Z will have a smaller average value, smaller standard deviation, and will be skewed due to the filtering of the higher end values.

To quantify and study this effect, two numerical approaches were considered.

1. From X to Z: A random number generator was used to compose Z from the random variable X. The advantage of this method is that the distribution of X could be assumed based on what is appropriate in literature for the distribution of connection strength. The disadvantage is that there is no equation relating the CDF of X to the CDF of Z.

2. From Z to X: We used order statistics to relate the probability of X to the probability of Z. This had the distinct advantage that we can write the equation for the CDF of X given Z. However we had to assume the probability distribution of Z prior to transformation. The distribution of Z is different than that of the already established distribution of a single wood connection, X.

Using these two approaches it was possible to study and determine effect of using two-ended test specimens to determine the actual connection capacity.

2.1.3 Statistical Distributions

Timber connection strength is often modeled by a normal distribution (for ease of calculations) or by a skewed lower bound distribution such as Gumble, Weibel, or Type I smallest distribution. The skewed distribution is often selected to better represent the nature of wood. This is because knots have a detrimental effect on the connection, but the chances of having one test in a critical area are small. This results in a distribution that is shifted to the right with a thin but far reaching lower tail due to the low strength outliers.

PSL does not have knots due to the nature of fabrication. PSL, however, has voids that are more randomly scattered amongst the wood. This might result in a distribution that closer to a normal distribution than sawn lumber due to a perhaps higher uniformity of defects. For this investigation, the distribution for the wood connection of interest was modeled as both normal distribution and the Type I smallest distribution.

There is another reason the Type I "lower bound" distribution was chosen. According to the literature on Order Statistics, the distribution of the minimum of *n* random variables will approach a Type I "lower bound" distribution as n approaches infinity. This is regardless of the statistical distribution for the component random variables. This means that even if you take the lesser of infinity normal random variable, the result will be a type 1 distribution.

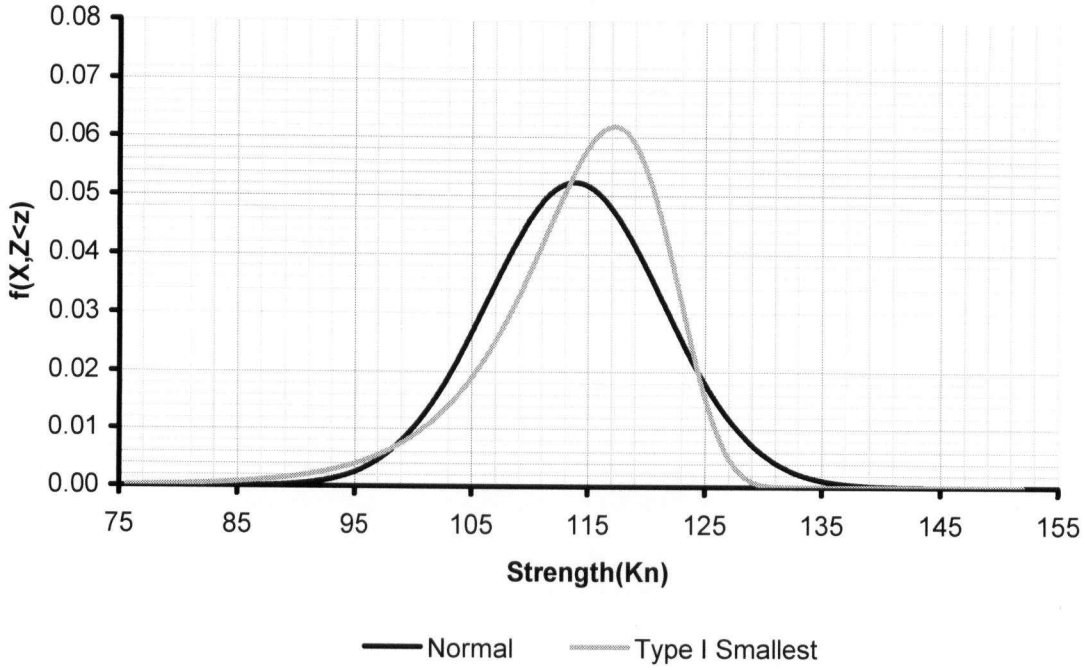

Figure 2.2: *Comparison of a Normal distribution to a Type 1 smallest distribution that have the same mean and standard deviation.*

2.1.4 Probability Preserving Transformation: From *Z* to *X*

The first method used to predict the connection resistance, *X*, was based on first principal arithmetic operations to equate the probability distribution of *X* to *Z*. Statistical notation can be hard to follow and is made more complex here because I have two different random variables for the connections on either end of the test specimen, and one random variable for the test specimen itself. The arithmetic done here is not very advanced or complicated, but the notation is somewhat subtle.

Defining the variables:

Let *Z* be the random variable for the test specimen strength.

Note: Statistical notation defines small z is the actual outcome, whereas big Z is the random variable. This applies for all statistical random variables herein.

Let X1 be the random variable for the connection on side 1 of the specimen

Let X2 be the random variable for the connection on side 2 of the specimen

The above 2 random variables are really the same variable and will soon be dropped in favor of the single random variable, X.

Writing the probability preserving statistical equation:

$$P(Z < z) = P(X_1 \cup X_2 < z). \qquad [2.3]$$

In written language this states that the probability that Z is less than z, is equal to the probability that X1 or X2 is less than z, where z is an input variable.

Solving the equation to relate X to Z:

Applying the union rule of probability theory,

$$P(Z \le z) = P(X_1 \le x1) + P(X_2 \le x2) - P(X_1 \le x1 \text{ I } X_2 \le x2). \qquad [2.4]$$

Now, there is some question as to whether X_1 and X_2 are truly independent random variables; however, for the purposes of this study, X_1 and X_2 were treated as

independent for the following reasons: the resistance of each individual connection is based largely on the properties of the PSL and the spring pins, and both connections were built to be the same within construction tolerances. Since PSL is an engineered lumber product and is designed to high tolerances, the likelihood of their being flaws in the PSL which would effect both connections, at opposite ends of the test specimen, is remote. Thus, the connection resistances at each end of the test specimen may be treated as being independent. Thus, the probability of the intersection of two independent events is simply the product of the individual probabilities. I am now invoking the notation for the CDF of Z. The CDF is defined as,

$$F_Z(z) = P(z \le Z \le z)$$

$$F_z(z) = F_{x1}(z) + F_{x2}(z) - F_{x1}(z)F_{x2}(z). \qquad [2.5]$$

Now, noting that the random variables X_1 and X_2 are essentially the same random variable, X, the expression may be rewritten in terms of X and Z:

$$F_x(z) = 2F_x(z) - [F_x(z)]^2. \qquad [2.6]$$

Rearranging into the quadradic form we get,

$$[F_X(z)]^2 - 2F_X(z) + F_Z(z) = 0. \qquad [2.7]$$

Finally, using the quadratic formula, we find an expression for the CDF of X, $F_X(z)$, in terms of the CDF of Z, $F_Z(z)$,

$$F_X(z) = 1 - \sqrt{1 - F_Z(z)}\,. \qquad [2.8]$$

Thus, from the CDF of Z, the measured failure strength, it is possible to write an expression for the CDF of X, the expected connection resistance.

Alternate Calculation for Proof of Correctness:

To prove the correctness of this formulation, I will show the derivation of the same expression derived using order statistics found in Benjamin and Cornell (1970).

For the key random variable Z which is the smallest of n random variables X_1, X_2, through X_n, we may observe that the probability of $Z > z$,

$$P(Z > z) = P\left(\prod_i^n X_i > z\right). \qquad [2.9]$$

Now, if the individual X_i are statistically independent, for reasons discussed above, we may simply multiply the individual probabilities of each X_i,

$$P(Z > z) = P(X_1 > z)P(X_2 > z)P(X_3 > z)...P(X_n > z). \qquad [2.10]$$

Now, applying de Morgan's rule, we may derive the probability of the complement of $P(Z > z)$ and $P(X_i > z)$,

$$1 - P(Z \le z) = [1 - P(X_1 \le z)] \cdot [1 - P(X_2 \le z)] \cdot [1 - P(X_3 \le z)] \cdot \ldots [1 - P(X_n \le z)]. \quad [2.11]$$

Thus the expression is now in a more useful form and it may be noted that $P(Z \le z) \equiv F_Z(Z \le z)$, likewise for the individual X_i. Thus Equation 12 can now be expressed in terms of the CDF of X_i and Z,

$$1 - F_Z(z) = [1 - F_{X_1}(z)] \cdot [1 - F_{X_2}(z)] \cdot [1 - F_{X_3}(z)] \cdot \ldots [1 - F_{X_n}(z)]. \quad [2.12]$$

As before, noting that the individual connections are described by the same random variable, X, the expression may be rewritten in terms of X:

$$1 - F_Z(z) = [1 - F_X(z)]^n. \quad [2.13]$$

From which it is possible to solve for the CDF of X,

$$F_X(z) = 1 - \sqrt[n]{1 - F_Z(z)}. \quad [2.14]$$

Finally, for this paper, there are two connections per specimen and thus two X random variables. Thus, Equation 15 specializes to:

$$F_X(z) = 1 - \sqrt{1 - F_Z(z)}. \quad [2.15]$$

Results of Transformation Effects:

Equation 9 has been confirmed from Order Statistics (Eq. 2.15), thus providing a simple expression for the relating the CDF of the measured connection failure with the predicted connection strength. The power of Equation 2.8 and Equation 2.16 lies in the ability to relate the probability of specimen strength to connection strength with a simple equation.

Now, from the distribution developed for *Z*, Equation (2.16) was employed to determine the distribution for the connection resistance *X*. As expected, the effect of the transformation is to broaden the distribution of X (compared to Z), which increases the standard deviation of X, and to shift the distribution to the right thereby increasing the mean connection strength over the specimen strength (See Figure 2.3). Therefore the mean connection strength *X* of each connection is actually larger than the mean specimen strength *Z*. The transformation also effects the third moment, or skew of the transformation. Due to the filtering out of the high strength outliers, the distribution of Z would be more skewed to the right than X. Since we produced X from a normally distributed Z with no skew, X is in fact skewed to the left. This skew cannot be seen in the Figure 2.3, but it is evident in the calculation for the 3^{rd} moment the result of which can be seen in Table 2.2.

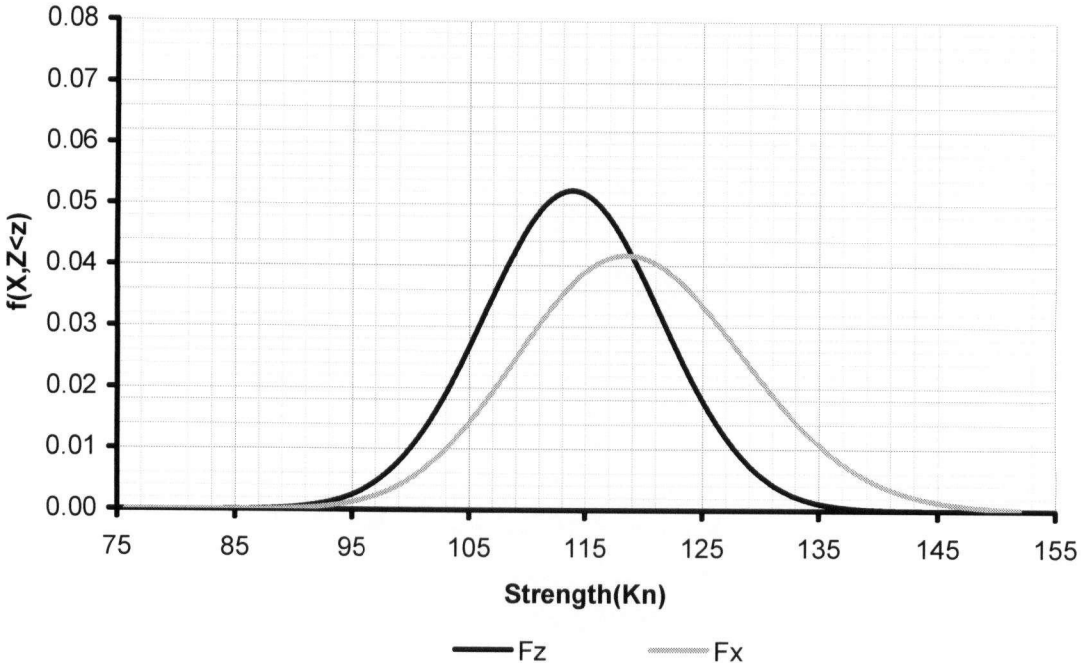

Figure 2.3: *CDF of the* ***normally*** *distributed test data Z, and the distribution of the connection strength, X, found from the transformation.*

Figure 2.4 depicts the Type I distributed *Z* and the resulting distribution for *X* based on the transformation. Note that there is no difference in skewness between the two distributions, merely a shift to the right suggesting a higher mean value but the same standard deviation. When assuming a Type I distributed specimen strength *Z*, the transformation from Z to X results in a Type I distributed connection strength, *X* with no change in skew. This distribution of X is observed to have roughly the same skewness and standard deviation but a higher mean.

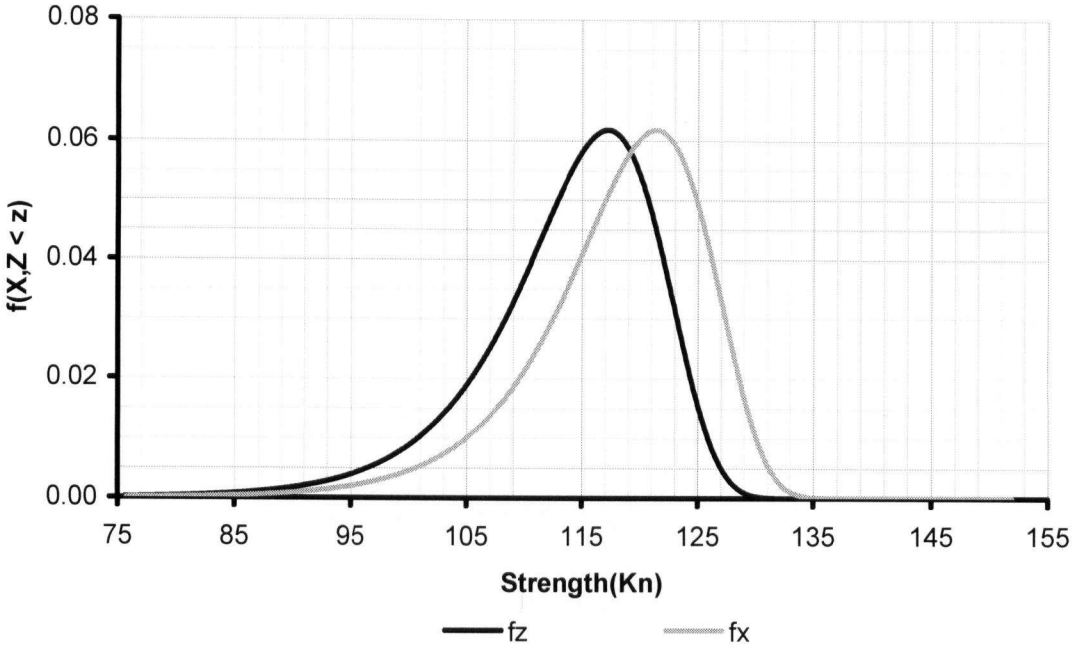

***Figure 2.4**: CDF of the **Type 1** distributed test data Z, and the distribution of the connection strength, X, found from the transformation.*

Table 2.2: *Summary of effect of probability preserving transformation, Z to X, on the 1st, 2nd, and 3rd statistical moments.*

	Mean (KN)	**Standard Deviation (KN)**	**Skewness**
Z is *normally* distributed			
Z (input)	114	7.64	0
X (output)	119	9.50	0.136
Z is *Type 1* distributed			
Z (input)	114	7.52	-0.971
X (output)	118	8.68	-0.971

2.1.5 Random Number Generation Transformation: From X to Z

The random number approach is more of a brute force method to relate X to Z. It is important to have two approaches to ensure the correctness of the findings. The transformation is conducted by generating two normally, or type 1 distributed sets of random numbers based on the 1st and 2nd moments of the test specimen data. The smallest of each pair of random numbers [X1(i), X2(i)] was stored in a third vector, Z(i). This vector Z represents the specimen failure strength, which is the lesser of the two individual connection resistances.

Note: The results of the connection specimen strength data from section 2.1.1 is employed to create the connection strength distribution for X.

The probability mass function (PMF), Figure 2.5, is plotted for both X data sets and the artificially generated Z distribution. Also included is the smoother plot of the CDF, Cumulative density Function Figure 2.6, due to the difficulty in acquiring a smooth PMF.

Figure 2.5 and 2.6 are both constructed using a data set consisting of 25 000 random number experiments. Observe that the PMF is more jagged in appearance than the CDF. Generally for experimental data, the CDF will be smoother than the PMF because the CDF is the integral of the PMF and integration has the effect of smoothing the data. It is interesting to note that even after 25 000 normally distributed random samples the PMF curve is still jagged, even though the first and second moments could be known with far less number of samples. Note that the X PMF distributions are roughly equivalent, as observed in both figures, and that the Z PMF distribution is skewed slightly to the Right. The slight skew observed in the Z PMF distribution can be explained by the effect of choosing the smaller of two values, the filtering of the high strength outliers. Observe also that the PMF of Z is a much tighter distribution than the PMF of X. This is again due to the fact that the PMF of Z represents the smaller of two random variables and will thus filter out some higher strength values resulting in a more compact distribution over the lower strength values.

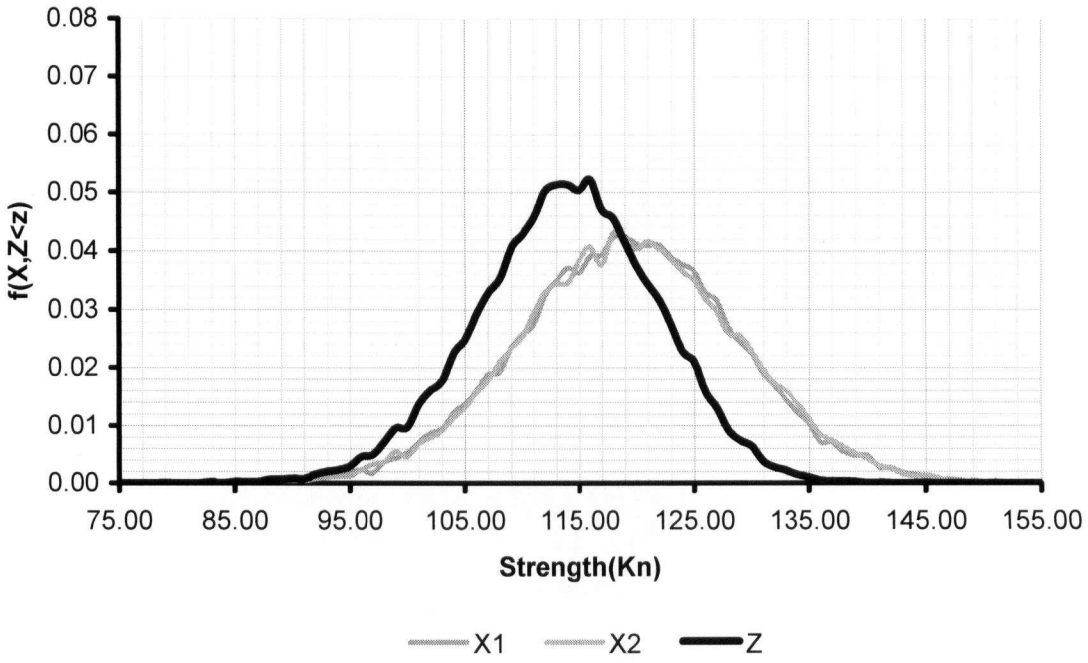

Figure 2.5: *PMF of* ***normally*** *distributed connection strength X, and the corresponding transformed Z distribution.*

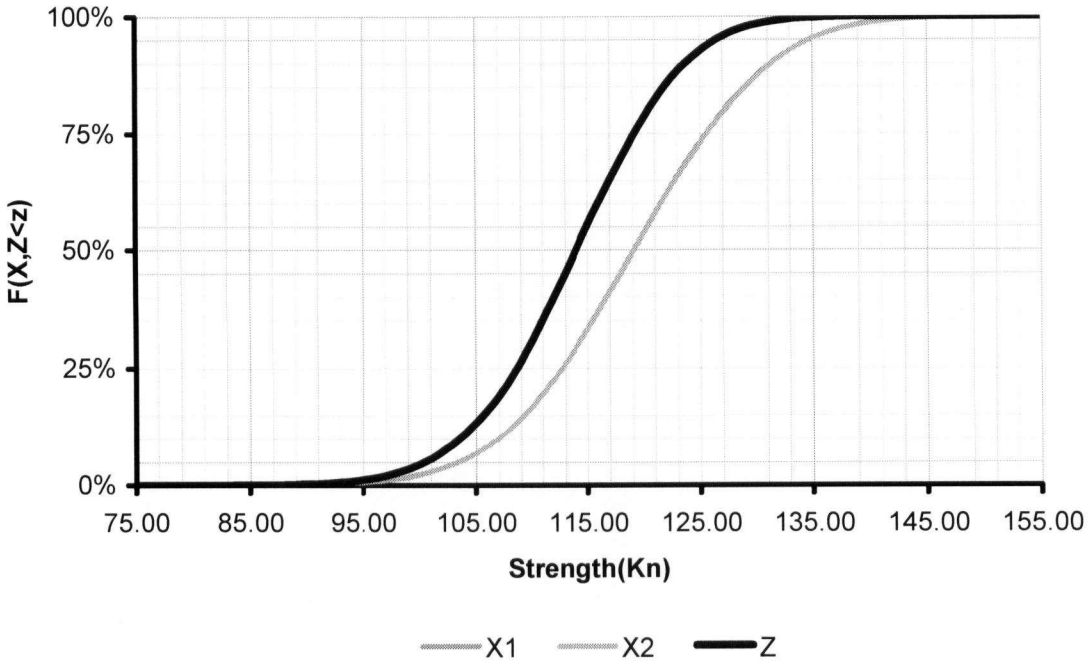

Figure 2.6: *The CDF representation of figure 2.5*

The study of Order statistics proves that as we add more random variables X, the smallest of n random variables will be strongly skewed to the right and will resemble a Type I smallest distribution In any case, Figure 2.5 and Figure 2.6 confirms that taking the smallest of two random variables results in a slightly skewed distribution. Had there been more connections in series, a more dramatic skew to the right would have been observed.

Although we are considering only two X random variables, it is instructive to observe the effect of taking the smallest of a series of random variables that have the Type I smallest distribution. To that end, the random number experiment was repeated with both X random variables having the Type I smallest distribution. Having only a normal random variable generator available for use, a probability preserving transform was employed to generate a type 1 distribution.

$$F_{T1}(x_i) = \Phi(z_i) \qquad [2.16]$$

$$x_i = F_{T1}^{-1}(\Phi[z_i]) \qquad [2.17]$$

$$x_i = \frac{1}{\alpha}(\alpha \cdot u + \ln[-\ln(1 - \Phi[z_i])]) \qquad [2.18]$$

Where x_i and z_i are the Type I distributed and normally distributed random variables (respectively) and α and u are coefficients for the Type I smallest distribution (see the previous section) based on the mean and standard deviation of z_i.

With the ability to create type 1 random variables, X_1 and X_2, the same procedure was employed as with the normal distribution to create the random variable Z (the lesser of X1 or X2). Figure 2.7 and Figure2.8 present the PMF and CDF distributions of X_1, X_2, and Z. Observe that, unlike the normally distributed data, the Z distribution is not any more skewed than the X distributions.

This is expected given that the Type I distribution is the distribution that would result from evaluating the smallest connection strength from an infinite number of connections. Since the X distribution is already Type 1, the Z cannot be shaped any more like a type 1 distribution and will remain the same shape. Thus, as observed in Figure 2.1f, the Z PMF distribution is shifted, but retains the same overall shape as the X PMF distributions.

There is a large body of literature that suggests the connection strength of PSL connections is normally distributed. However, observations made in this study suggest that the true connection behaviour may be somewhere between normally distributed and Type I distributed.

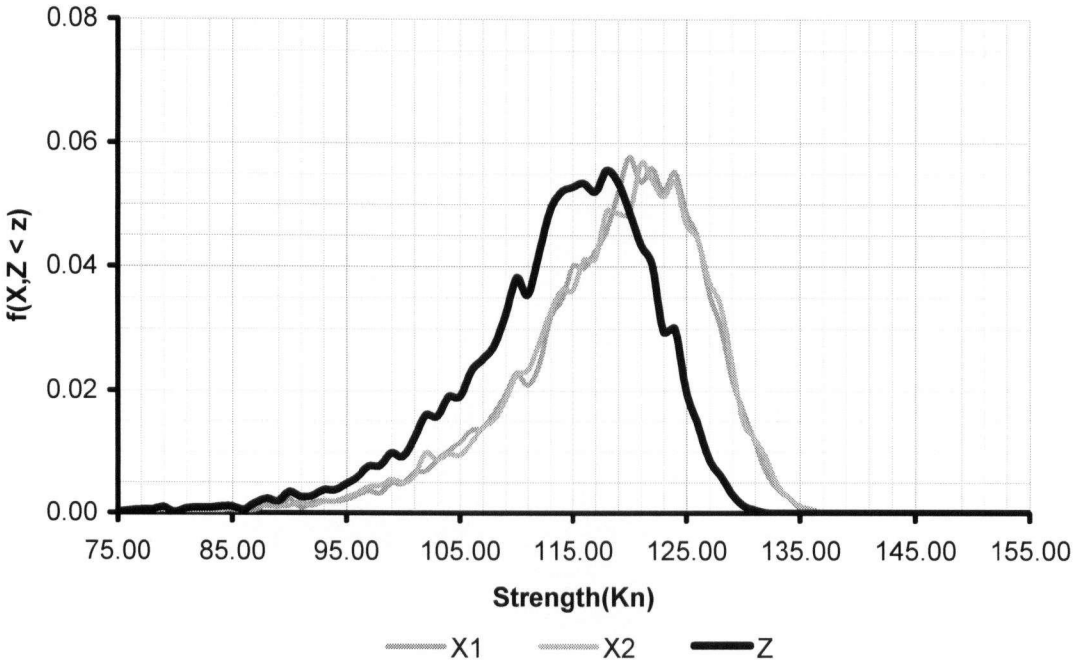

Figure 2.7: *PMF of type 1 distributed connection strength X, and the corresponding transformed Z distribution.*

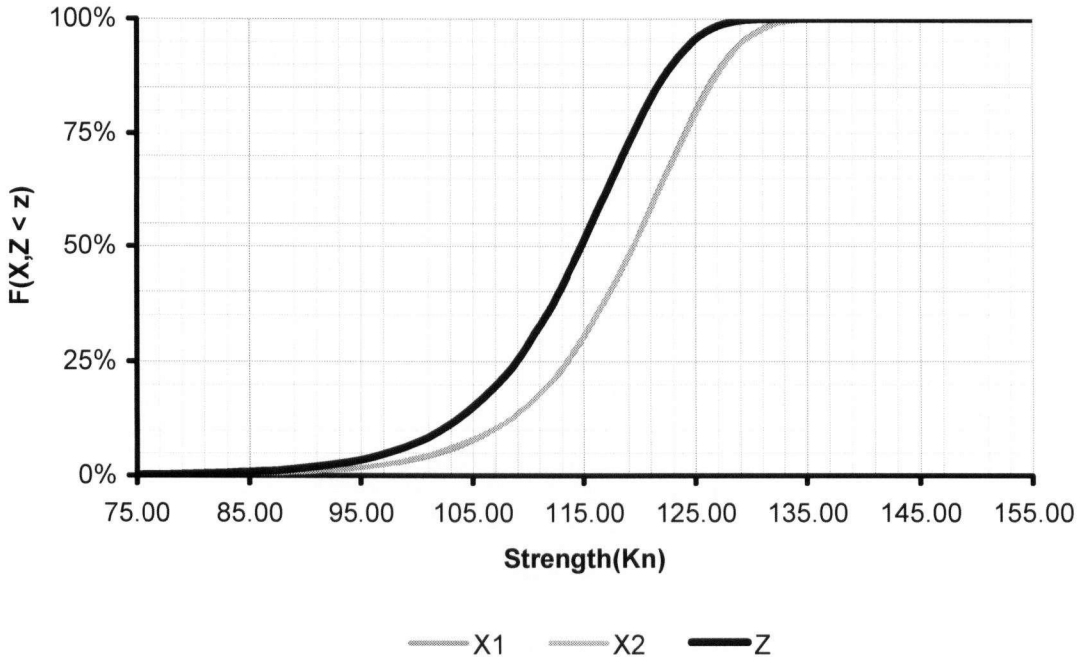

Figure 2.8: *The CDF representation of figure 2.7*

The results from the random number generator process were compared to the Order Statistic approach in order to assess the accuracy of the numerical simulation. There are inherent differences between the approaches because distribution for the probability preserving method method was skewed when transformed from Z to X. In the case of the random number generator, the distribution of consideration was skewed from X to Z.

Table 2.3: *Summary of effect of the number generator transformation on the 1st, 2nd, and 3rd statistical moments*

	Mean (KN)	**Standard Deviation (KN)**	**Skew-ness**
X is normally distributed			
X (input)	120	9.49	0
Z (output)	114	7.90	-0.16
X is type 1 distributed			
X (input)	118	8.78	-1.21
Z (output)	113	8.69	-1.16

2.1.6 Ramifications Of Twin Ended Testing For Design Strength

After studying the ramifications of testing with twin end test specimens, the effect on the 5th percentile is ultimately what affects the design strength. There was an increase in the mean strength that would increase the 5th percentile, but this was coupled with an increase in the standard deviation that would result in lower 5th percentile strength. The effect of the transformation on the skewness of the distribution was very small when taking the lesser of 2 connections. This change can be neglected especially when considering the approximations involved when assigning a distribution to the set of test data in the first place. In reality neither X nor Z will be normal or type 1. They are probably somewhere in between, but the results indicate that it makes little

difference what the distribution really is. The comparison of the 5th percentiles can be seen in Table 2.4.

Table 2.4: *5th-Percentile design strength predictions*

5th-Precentile Design Strength		
Random Variable	Normally Distributed Assumption	Type 1 Distributed Assumption
$Z_{0.05}$ *(Twin-Ended)*	101 kN	99 kN
$X_{0.05}$ *(Single Conn.)*	104 kN	104 kN

It is interesting to note that the mean and standard deviation of the Type I smallest distribution and normal distribution for X are not the same. However, the 5th percentile is the same. It seems that 104 KN is a reasonable estimate for the 5th percentile strength of the connection. This translates into a 3-4% increase over the 5th percentile of the original twin-ended test specimens. This is not a significant increase, but if similar testing was done on a failure mode with a higher standard deviation this difference might be more significant.

2.1.7 Discussion

We have shown that it is possible to calculate the statistical properties of a connection component, X, given that we know the statistical properties of the twin ended test specimen, Z. Although the results of our study did not have a significant effect on the design strength (5^{th}-percentile strength) in this particular case, this effect might have more impact in the following situations:

- Testing similar wood connections with a larger variability, say 20%
- Obtaining average values or upper percentile values from test results of the same configuration

2.2 CONFIDENCE INTERVAL REDUCTION

The confidence interval is a basic statistical concept regarding the accuracy in which the mean can be estimated. If we take N test samples, the average value theoretically converges to the mean value with an infinite number of test samples. This means that with a finite number of test samples the average of the test values will not necessarily coincide with the mean value. ASTM testing standards suggest that a 75% level of confidence of the mean value is required. This means that the theoretical "true" mean should have a 75% chance of being equal to or greater than the mean value determined from a limited number of tests. To reduce the "design mean" to this appropriate level basic statistics must be used to determine this 75% confidence level.

The mean value can be considered to be a random variable with a dispersion in proportion to the number of test samples taken, N and the natural variability of the test subject. The variance of the mean value is known to be:

$$\sigma_{\mu} = \frac{\sigma_X}{\sqrt{N}} \qquad [2.19]$$

The distribution of the random variable σ_X is considered to be the same as the distribution of the random variable X. From this knowledge we can then formulate a confidence interval of the mean over which we know the mean will be between given a probabilistic level of confidence. For example, if X is normally distributed then the 75% confidence interval of μ_X is,

$$\mu_X - \Phi^{-1}(0.05)\cdot\frac{\sigma_X}{\sqrt{N}} < \mu_X < \mu_X + \Phi^{-1}(0.95)\cdot\frac{\sigma_X}{\sqrt{N}} \qquad [2.20]$$

$$\Phi^{-1}(0.05) = -1.64 \text{ and } \Phi^{-1}(0.95) = 1.64 \qquad [2.21]$$

As can be seen in Figure 2.9, the difference between the lower bound confidence interval and thus the mean value, decreases quickly with an increasing number of test specimens.

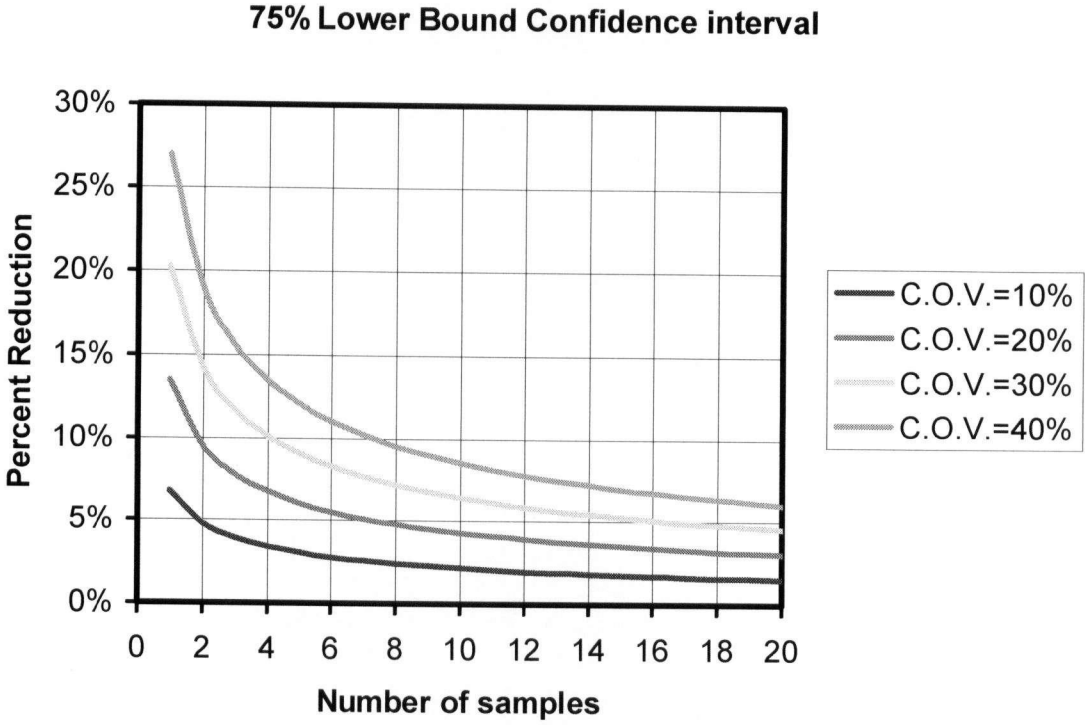

Figure 2.9: *Percent reduction required of mean to a 75% confidence level*

Figure 2.9 depicts a reasonable reduction for the mean value. However the 5th percentile is a function of the standard deviation as well as the mean. Uncertainty in the standard deviation is minimized with the use of literature from previous testing programs. For bolted connections in Parallam the coefficient of variation of 10% is typically determined for axial strength. This is in agreement with the tests I have conducted.

For the testing done in 2005, 8 connections are used in order to estimate the mean and standard deviation. The mean differed from connection to connection and must be reduced by 2.5% for a 75% level of confidence. Since all the specimens had a 10% coefficient of variation regardless of the loading, I felt comfortable testing fewer specimens than I would otherwise have done for a single unique connection.

2.3 LOAD DURATION AND MOISTURE CONTENT

For a code equivalency, the design strength must be normalized to a typical service load duration. The test load duration is 5 minutes resulting in higher strength than a typical snow load or dead load duration. A reduction factor of 0.8 is applied to the 5^{th} percentile to normalize the strength to a normal load duration.

The moisture content for Parallam is well documented in previous test programs. The equilibrium moisture content will not be affected unless Parallam is subjected to exposed conditions. Parallam is not meant for this type of use and therefore moisture content is of little concern to this project.

2.4 APPLICABILITY OF PARTIAL SAFETY FACTORS

The design capacity is defined by multiplying the 5^{th} percentile strength by the appropriate partial safety factor. The partial safety factor ϕ is 0.7 in wood doweled connections. The partial safety factor is not dependant upon the variability of material properties. It is a rule of thumb safety factor that reflects the sensitivity of wood connections to errors in fabrication, simplifying assumptions in an engineering analysis, and the issue of durability of the structure. Canisius, T. (2001) stated that the partial safety factors are calibrated to match current design methodology. The overall design process in engineering is always in a state of change. More refined structural analysis, such as the one discussed in Section 3.0, may lead to more refined and rational results. The more refined analysis may lead to a "sharpening of the pencil" in terms of force level demands on each element in the structure. Since the partial safety factors were

implemented when there was a fatter line to the pencil, perhaps the safety margin has in fact been reduced by a more sophisticated estimation of the structural behavior.

Canisius, T (2001). states that, when these more sophisticated techniques are used, so too should the level of diligence of inspections and quality control be increased. By increasing the quality control on the project the safety margin, which was perhaps compromised, is now put back into balance.

In the Arena Stage Project, Structurcraft will be responsible for the construction of the façade. The carpenters working in the fabrication shop are intimately involved with the design process and understand the implications of their construction tolerances. The control the designer has over this process will ensure the highest degree of quality control over the design to ensure the safety and performance of the structure.

2.5 DESIGN CAPACITY

The design capacity, be it pure axial force or combined axial and bending moment, is found directly from the 5th percentile of the twin ended test specimens. As discussed above, the 5th percentile of the twin-ended test specimens is a good estimate of the 5th percentile of the actual connection. The confidence interval reduction is counterbalanced by the upward factoring for twin ended testing. The 5th percentile is reduced to a normal load duration by the factor 0.80. The design capacity is then the following, using the CSA-086 adjustment factors (K factors):

$$Pr = \phi * P_{0.05} * K_D * K_{SF} * K_T \qquad [2.22]$$

Where,

$P_{0.05}$ *is the* 5^{th} *percentile strength from testing*

The following factors are from CSA-086 for bolted connections:

K_D *is the load duration factor*

K_{SF} *is the service condition factor*

K_T *is the treatment factor*

2.6 DISCUSSION

This above equation holds for the C.O.V. range of 10-20% typical in parallam connections. If the coefficient is much higher, then I would recommend re-evaluating the impact of twin-ended testing. Also If one is interested in the upper-percentiles, such as the 95% values, then the effect of twin-ended testing is severe and requires attention. However for the testing program contained in Section 4.0 and 5.0, the 5^{th} percentile strength is unaffected by the usage of twin-ended specimens.

3.0 ANALYSIS OF PROPOSED STRUCTURAL SYSTEM

Arena Stage in Washington DC is a collection of public theatres in the heart of the capital of the Unites States. The project involves retrofitting 3 theatres and the design of a large space-truss roof that encloses all 3 theatres. Structurecraft is involved in this project to construct the glazing facade system for this shelter. The heavy timber support system for the glass façade is large and complicated in geometry. Although Washington DC is not known for being vulnerable to hurricanes, strong wind loads with design speeds of 80 Miles per hour dominate the threat to the structure. These high winds cause a net suction of 40psf over the window mullion system equivalent to the weight of over 3 inches of concrete hanging sideways.

3.1 STRUCTURAL SYSTEM

The window mullion system proposed by the architect is an expanded version of the original window mullion system for Surrey City Centre. The columns in the Surrey Façade system were 24 feet (7.3m) on centres whereas the proposed system will be 36 feet (11m) on centres. The muntin support beams retain their original length of 12 feet (3.7m). To facilitate the larger span, each span consists of 3 muntin beams, two of which cantilever past the supporting arms to accept a "drop-in" muntin beam in the middle. The structural system is unstable without the inherent rotational rigidity of the spring-pin connections. The spring-pins are used for all connections of the wind resisting system. The weight of the glass is supported by the muntin beams which are in turn supported by cables hung from the roof (See Figure 3.1).

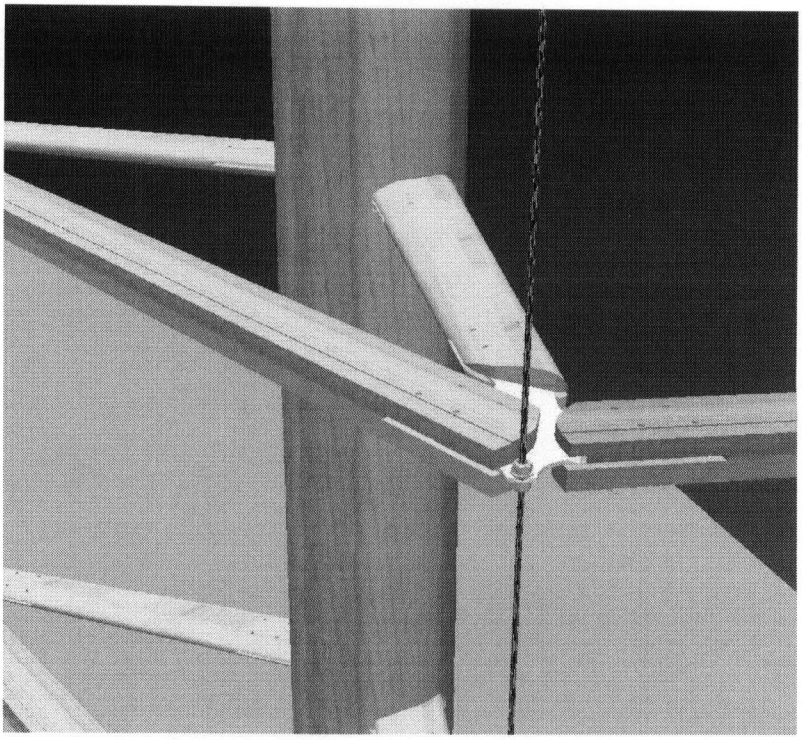

Figure 3.1 *Detail of Cable Hanger Connection*

3.2 WIND PRESSURES: RWDI RESEARCH

RWDI consulting in Ontario has a division that studies wind problems on buildings using a wind tunnel. For Arena stage a flexible model was created of the entire roof and façade and tested in the wind tunnel. The reason for this testing was to study the vibration stability of the flying cantilever roof under wind loads. A by-product of this research was to assess pressure coefficients for window mullions. It is these pressure coefficients that are used for the wind loads on the window mullion system. On average the coefficients are similar to that prescribed by code for a standard building, but have local regions where the pressures would be less than that of the code.

3.3 RELATIONSHIP BETWEEN CONNECTION RIGIDITY AND LOADS

The structure was analyzed using S-Frame and Sap2000 to confirm the results. The first pass at the structure was a linear-elastic solution with no attempt to model the stiffness of the connections. Due to the curved geometry of the structure, significant centenary tension or compression action along the curve of the window support allowed very light beams to be used to span the 36 feet between the columns. Only about 30-40% of the structural response was attributed to the flexure in the muntin beams. These bending moments are distributed in the beam such that there is minimal bending at the connection splices, even under unbalanced wind loading. There is significant bending, however, in the arms reaching out from the columns. The moment in the connection can reach as high as 5.9KN-m, more than the capacity of reasonable bolted connection. This is because the centenary action through the muntin beams pulls on the arms resulting in double curvature of the arms (See Figure 3.2 and 3.3)

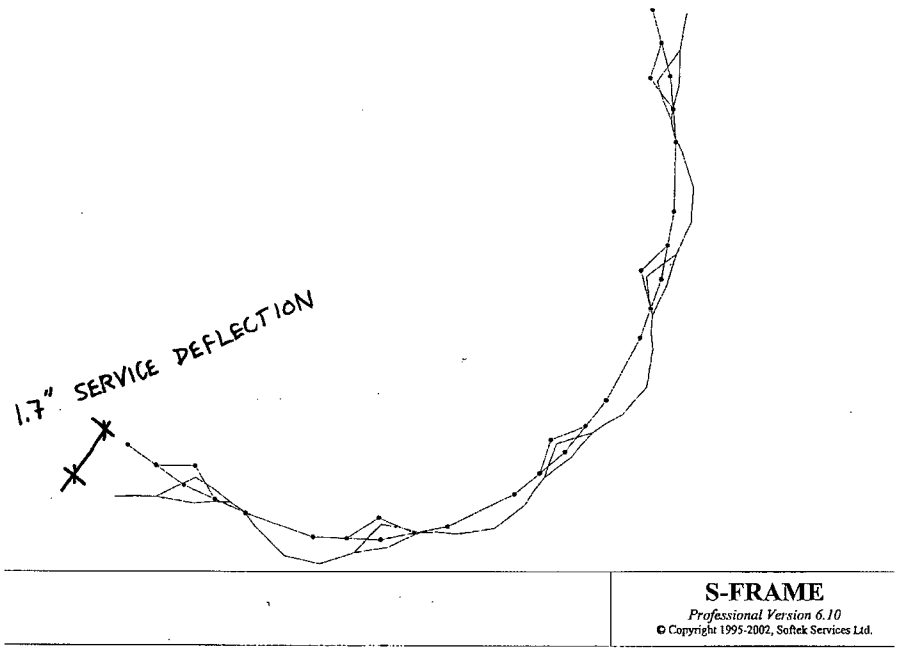

Figure 3.2 *S-Frame prediction of deflected shape of façade structure*

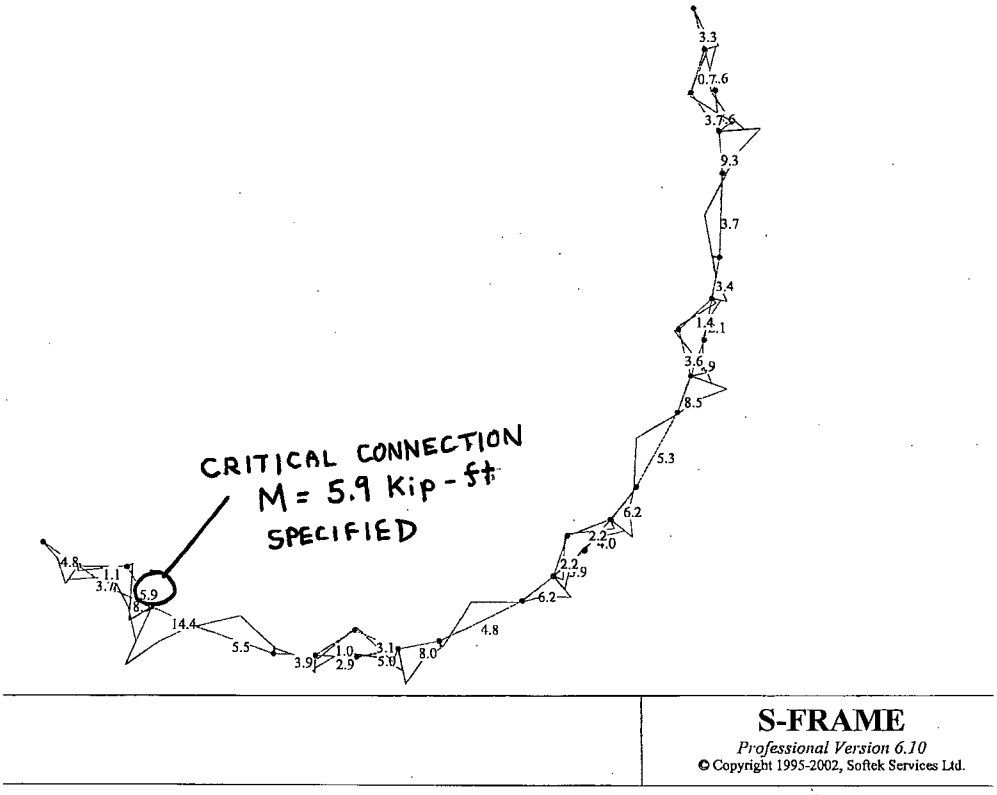

Figure 3.3 *S-frame prediction of bending moment demands*

Designing the arm connections to resist the un-factored moment of 5.9Kip-ft would be costly if not impossible. If the connections are modelled with purely pinned connections at the arms, the structural system is still inherently stable and the moments do not transfer to other connections. Rather, the moments are distributed to the hogging moment of the PSL beam where it would be desirable. In steel, these connections could be discounted as attracting moment and designed as carrying axial forces only because the connection will deform plastically to accept the imposed rotations. Unfortunately this cannot be done with wood connections due to the potential for brittle failure. The axial capacity of the connection is compromised by the imposed rotations of the structural system.

The graph below is a graph of bending moment demand vs. rotation on the connection. If the connection pin modelled the rotation is 0.7 degrees. If the connection is fixed the connection moment is 7.3 Kip-ft (9.9KN-m). Because the analysis is linear-elastic, a straight line in between would represent the bending moment demand for a given rotational stiffness of the connection. If the rotational stiffness of the connection is super-imposed on this graph, the design point for determining the bending moment demands on the connection can be determined (See Figure 3.4).

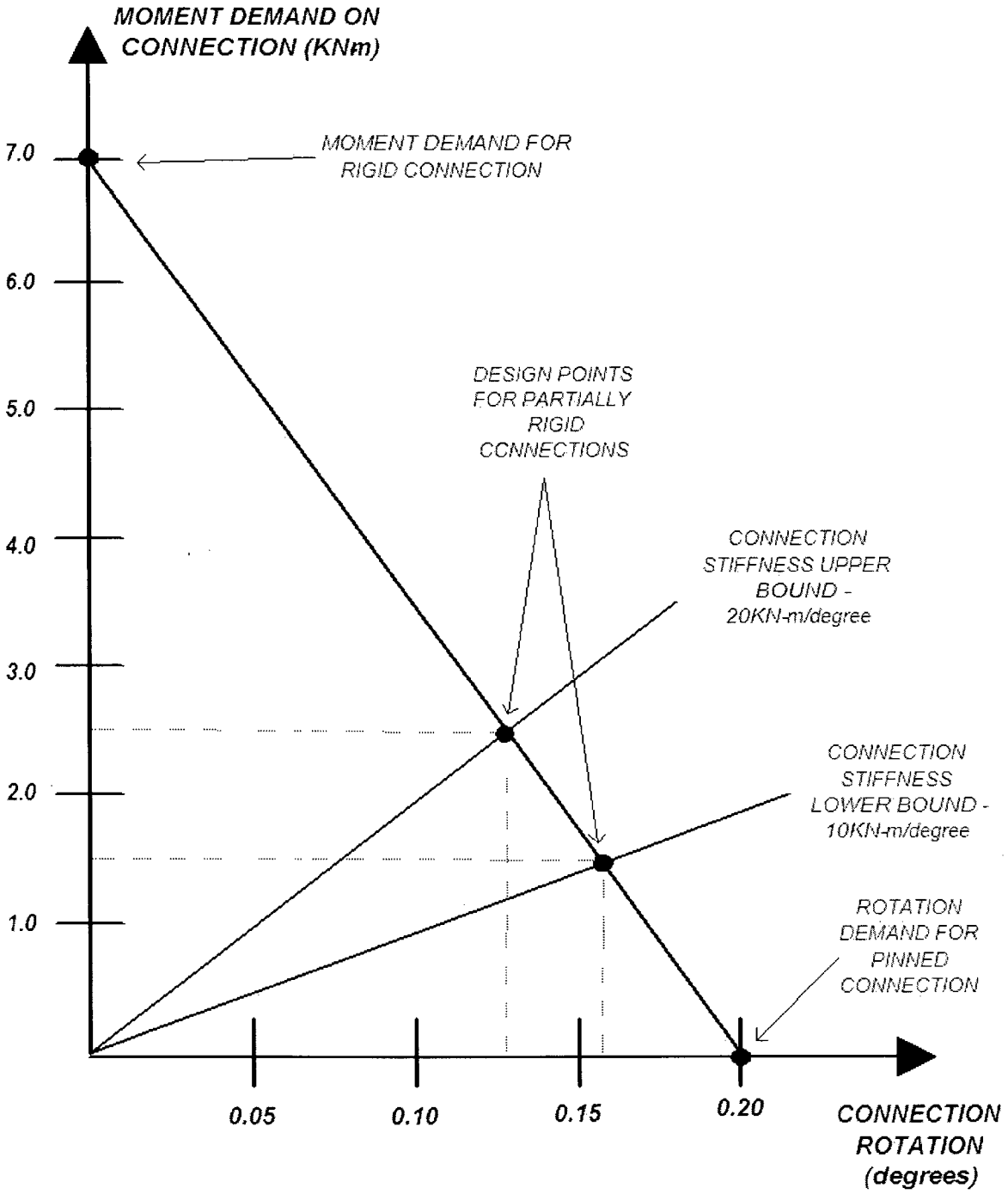

FIGURE 3.4 *MOMENT DEMANDS AS A FUNCTION OF CONNECTION STIFFNESS*

To confirm the reliability of this design curve, the structure was modelled with flexible connections. The structural models confirmed the design moments from the simplified method, and also showed that the moment demands did not become significant in the beam splice connections.

The connection was modelled by introducing a soft link that is the approximate length of the connection itself. The stiffness of the soft link was selected such that there is equivalency to a rotational stiffness of 10kip-ft/degree. Then the nodes on either side of the soft link were slaved so that they have the same translational degrees of freedom.

The model was refined further by acknowledging that the round parallam columns are quite large, 32" in diameter. The 16" from the centreline of the column to the connection was modelled as a rigid link. This had the effect of stiffening the structural system, but unfortunately this also distributed more bending moment to the arm connection. This refinement is shown schematically in Figure 3.5.

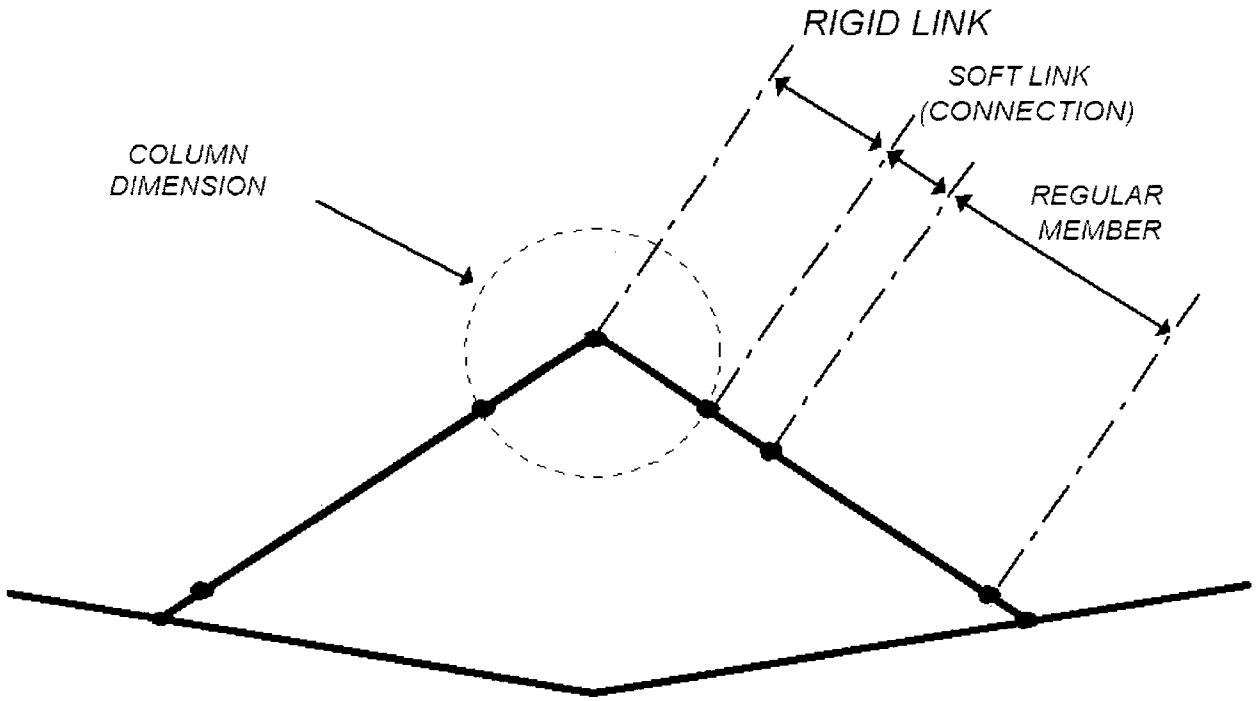

Figure 3.5 *Structural Model of the façade member. The model includes a rigid link to represent the column thickness. The connection is reprented by a soft link 6" long which is the length of the connection itself. The soft member was sized such that the soft link represents a connection with a rotational stiffness of 10KN-m /degree.*

The results of the refined analysis were felt to be a more reasonable representation of the structural system. The bending moment demands on the arm were relaxed, but the stiffness of the structural system was improved by modelling the thickness of the 32" diameter columns. See the deflections in Figure 3.6.

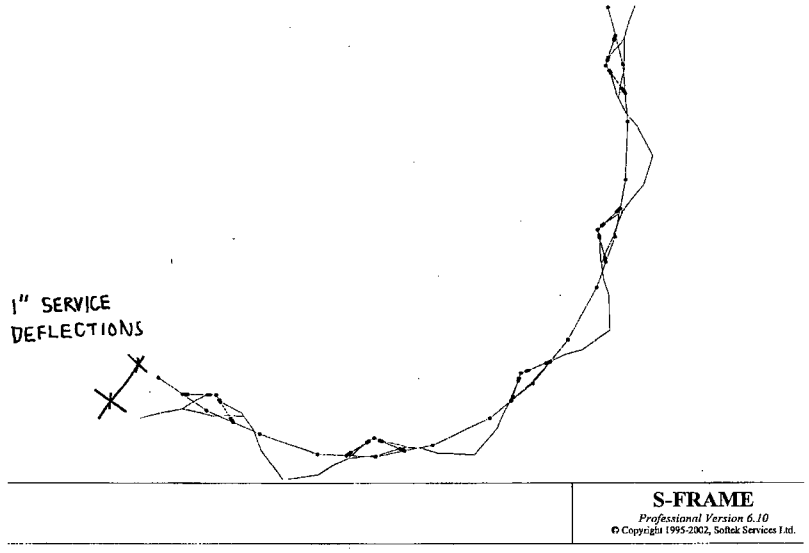

Figure 3.6 *Deflection predictions from refined structural analysis*

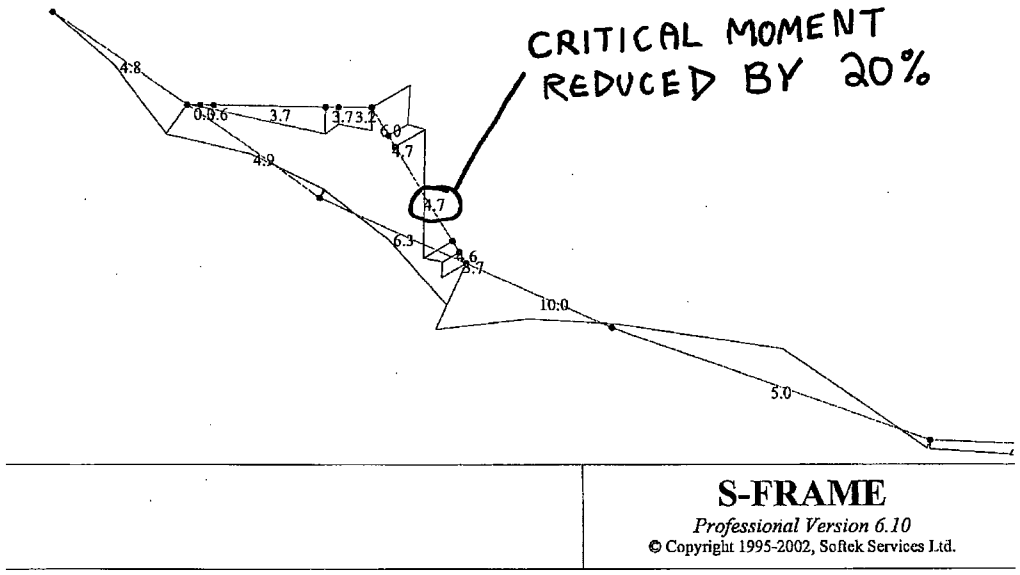

Figure 3.7 *Bending moment predictions from refined structural analysis*

3.4 FULL MODEL

Once the basic structural behaviour of the small 2-dimensional section was understood, the full 3-dimensional façade structure with all its complexities was modelled piece by piece. This model captures the behaviour of the façade structure under the wind load that varies in elevation. It also identifies localized problems associated with the entrances that interrupt the façade at several locations. Differential deflections between the stiffer entrances and the façade structure were a potential threat to the panes of glass.

The returns, perpendicular jogs in the façade, were of particular interest. These returns caused a severe interruption of the natural centenary behaviour of the façade structure causing increased deflections and bending moments in the spring-pin connections. The returns themselves are 4' wide panes of glass stacked on top of each other from floor to ceiling. Thin rubber bearing pads at the joints between the glass panes carry the self-weight of the glass panes into two cables hung from the roof.

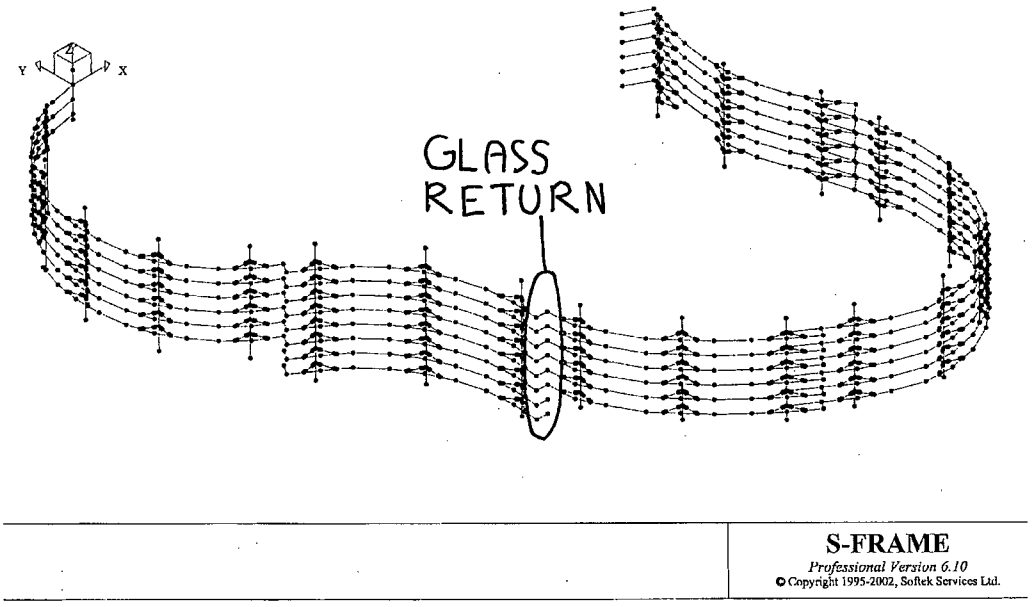

Figure 3.8 *Image of full model, the returns seen here are a significant challenge to the engineers*

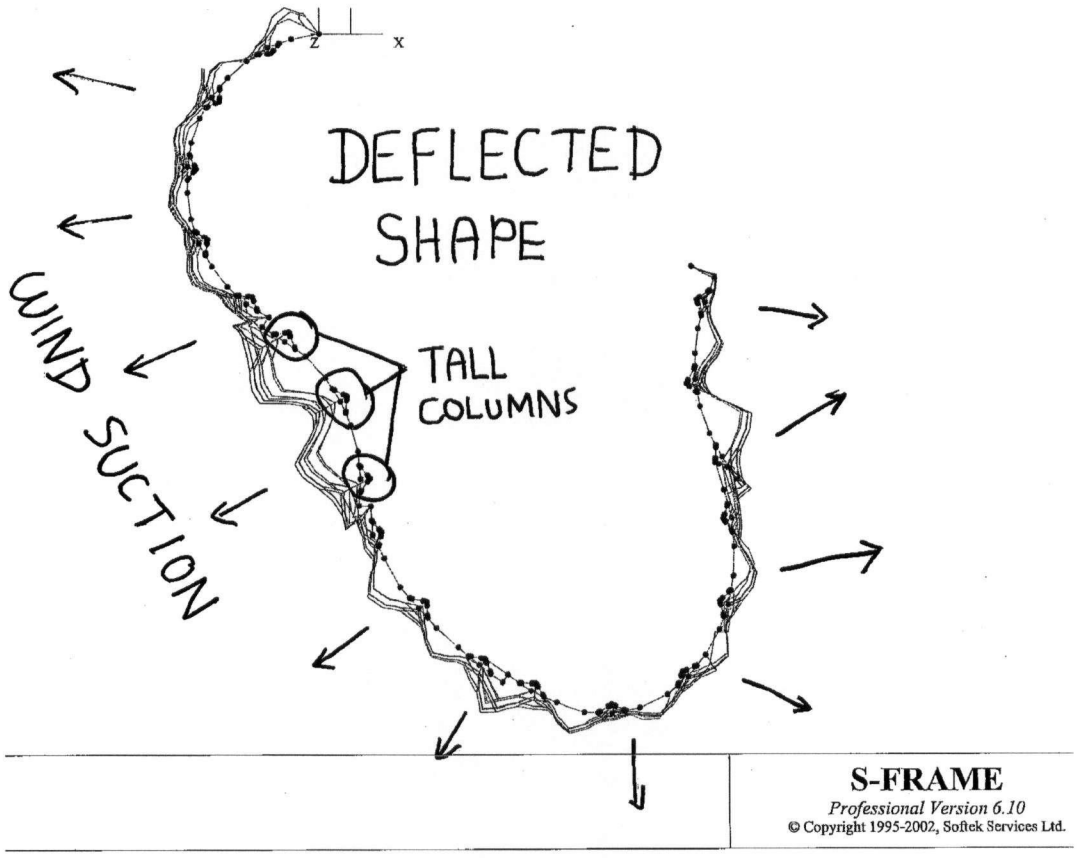

Figure 3.9 *The deflected shape of the 3-dimensional model. The overall deflections are within required limits, however the localized deflections are a concern.*

3.5 MODELLING UNCERTAINTIES AND DEVIATIONS FROM CONVENTION

Conventional structural analysis does not consider the semi-rigid contribution from a moment connection. In the case of the Arena Stage façade structure, the system would be unstable unless moment connections are present. The connections with a significant moment contribution were modelled as semi-rigid connections so as to capture the reduced stiffness of the structural system. With the connections modelled as such, the structural system maintains it's structural integrity and is stiff enough to meet

the deflection criteria required for the glazing. Increasing the stiffness of the connections will lead to overloading the connections, whereas decreasing the stiffness will result in a structural system that is too soft to function safely as a glazing system. This is a careful balance that is highly sensitive to the rotational stiffness of the spring-pin connection. Physical testing is needed to determine the rotational stiffness parameter for the structural model.

4.0 SINGLE FASTENER RESPONSE

Single fastener response to load has been well established and documented for any bolt or dowel in traditional sawn lumber. The spring-pin connection in parallam is a variation of a traditional dowelled connection. Bolts in Parallam have been tested and values can be found in the 2001, CSA-086 timber design code. However, there are some distinct differences in behaviour between sawn lumber connections and engineered timber such as parallam. A further motivation for single pin testing is to understand the hinging capabilities of the spring-pin dowel and to ensure that it fails in a desirable manner. Finally, as will be revealed in later sections, the non-linear stiffness of the single fastener will be used directly as a variable in an analytical model for the response of the multiple pin connections. The characteristic behaviour of a single pin is a building block to predicting the behaviour of multiple pin connections subjected to both axial load and moment and must be well understood before proceeding further.

4.1 BEARING CAPACITY

The bearing failure according to practice is when there is a "significant flattening" of the load displacement curve due to the local yielding of the material around the fastener under high compression stress. In many cases this flattening is quite gradual and it is difficult to decide at what point the connection has failed. ASTM D-5764-97 suggests a procedure for determining this "yield point" called the 5% offset method. This method involves taking a slope 5% offset from the initial stiffness curve. Where this curve meets the test curve is the definition of bearing capacity.

Another approach suggested by Borg Madsen(2000) acknowledges that the curve is highly non-linear with no defined yield plateau. The connection is declared to have failed when the measured slip has reached 4mm at which point the connection would probably re-distribute load to other elements in an actual structure.

4.2 SPRING-PIN HINGING CHARACTERISTICS

The spring-pins are hollow resulting in a reduction of the plastic section modulus compared to a bolt of the same diameter. However, spring-pins use relatively high strength steel. The steel properties are as follows for AISI 6150:

AISI 6150

Fy = 59,750 ksi (500 Mpa)

Fu = 96,750 ksi (800 Mpa)

elongation = 23%

Impact Strength = 20.2 ft-lb

Hardness = 197 Bbn

4.3 EFFECT OF ALUMINUM SIDE PLATES

The material of the knife plate used in most of the tests is a ¼" steel plate. Structurecraft typically uses a 3/8" aluminium plate for the connection plate. To study how this difference between test specimen and industry connection might affect the results I looked at the bearing resistance of the steel knife.

$\beta r = \phi * 3 * d * t * Fy$ **[4.1]**

= 75 KN (17 Kips) *for a ½" spring-pin.*

The steel has a bearing capacity far in excess of the ½" spring-pin wood bearing capacity. However this formula allows considerable yielding of the steel around the spring-pin before the capacity is reached. It is possible that the onset of yielding would occur at or before 1/3 of the capacity has been reached.

$\beta y = d * t * Fy$ **[4.2]**

= 27 KN

The average bearing strength of the test specimens was 38 KN with a 5^{th} percentile of 28KN for the single-pins. The majority of the test specimens caused yielding in the knife-plate material. Therefore the selection of the material may have an effect on the results. I felt justified in allowing this yielding to occur because in reality there is a strong likelihood that the steel plate will be equivalent to a ¼" steel plate or smaller in practice. Also, the yield marks on the plate were visible after the tests were conducted giving an indication of the load distribution (See Figure 4.1 below).

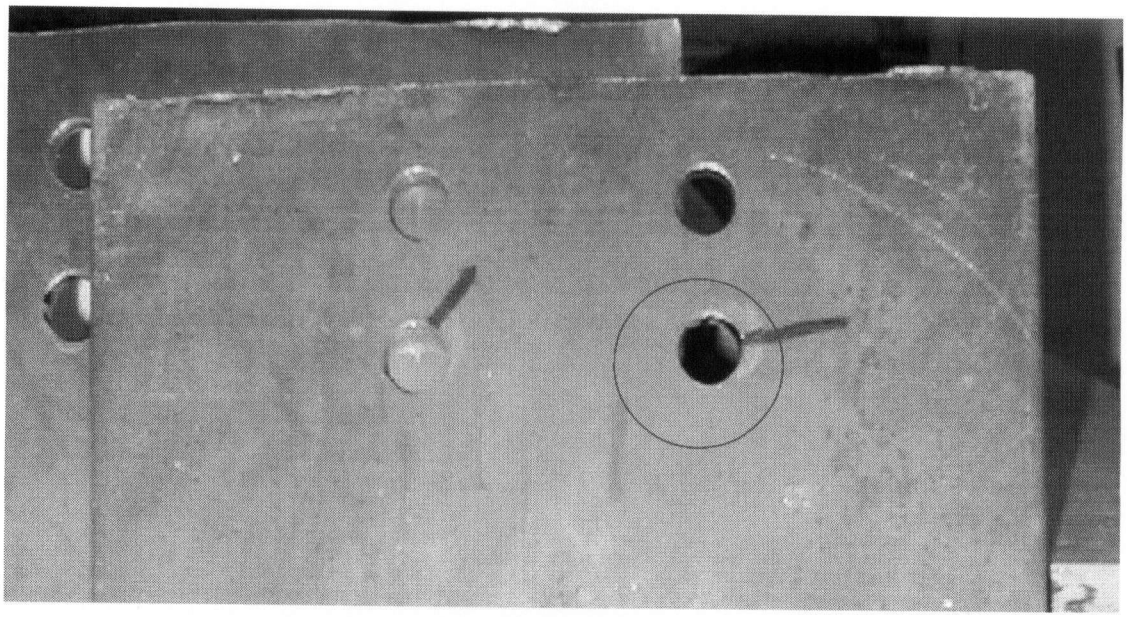

Figure 4.1 *Yield patterns can tell something about the force level in the pins during the load test. The lines in this moment connection show the direction of load in the pins at failure.*

4.4 TESTING SETUP AND PROCEDURES

The specimens were tested in accordance with ASTM D5652-97 for bolted timber connections. Testing duration was 5 minutes to reach peak load. Displacements were increased past ultimate capacity to capture the post failure behaviour. Two LVDT devices, for measuring displacement, devices were used for each sample. Only 4 samples were tested for each configuration since strength values were only of use for planning the larger multiple fastener connections. There were four variations of the single dowel specimens:

1) Tension Parallel to Grain
2) Tension Perpendicular to Grain
3) Compression Perpendicular to Grain
4) Compression Parallel to Grain

The specimens were tested in that order. The first two specimens were fabricated specifically for testing, whereas the latter two were fabricated from recycled material from some of the 4-pin specimens that were tested at the same time as the single pin tension tests.

4.4.1 Parallel to Grain Tests

The specimens are twin-ended specimens that were tested by pulling on opposing ends until one or the other failed. Section 2.0 discusses what this means statistically for the results. The opposing connections were spaced 6" apart center-to-center of the spring-pin/bolt. Both bolts and spring-pins were tested 4 specimens of each for the purpose of comparing bolts to spring-pins in parallam. The geometry specifications for one end of the specimen are shown below in Figure 4.2. The loaded end distance of 8 diameters was used in all subsequent connections. CSA-086 timber Code recommends an end distance of 7 diameters, but gives a significant strength increase for multiple bolt connections for larger loaded end distances up to 10 diameters.

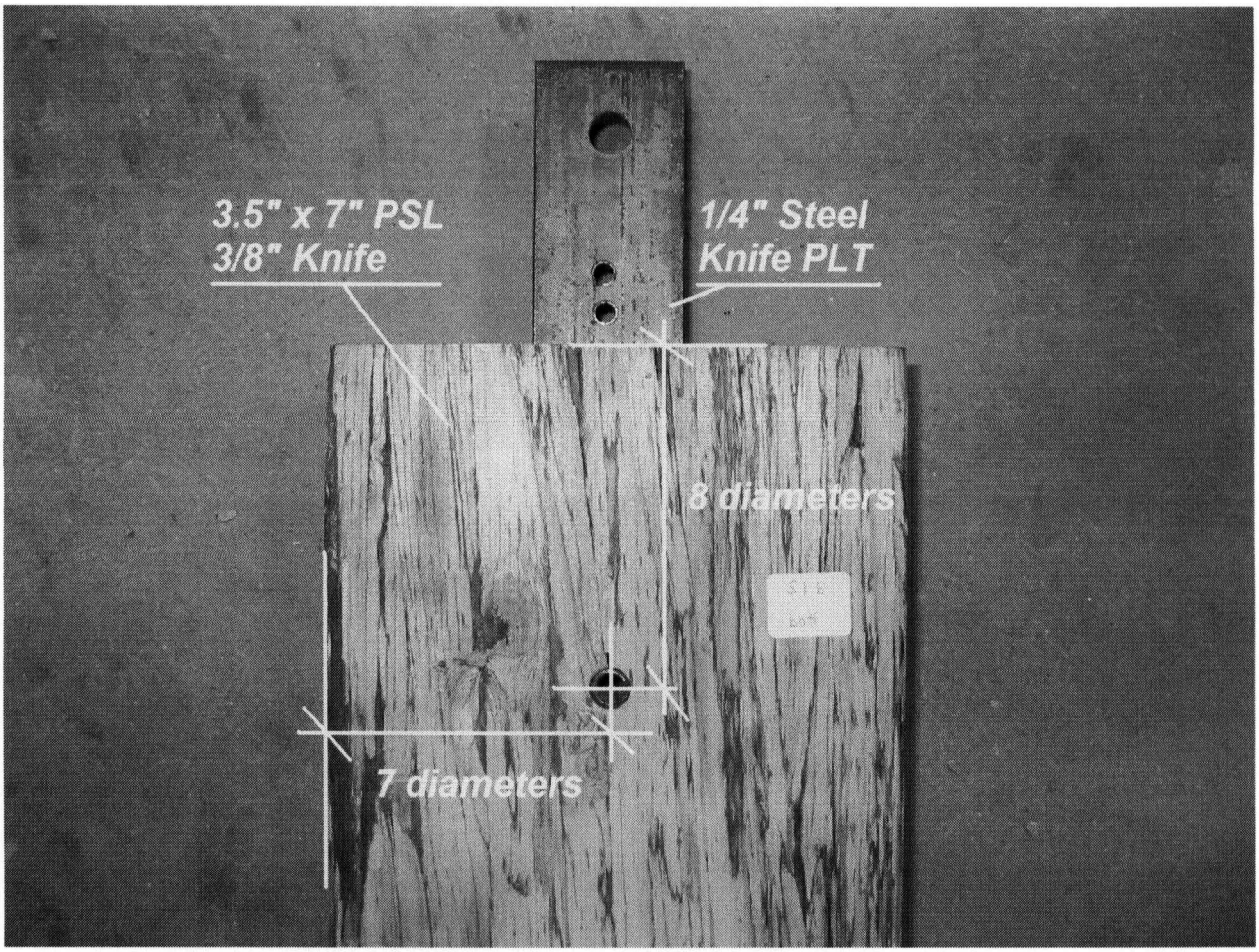

Figure 4.2 *Typical Tension Parallel-to-Grain Specimen*

4.4.2 Tension Perpendicular to Grain Tests

Since the main objective of this research is to create a moment connection, it was necessary to study the response of a single pin to perpendicular to grain loading. 3 specimens were designed with different widths to test the specimens. Unfortunately, all 3 specimens failed in the same manner with no observed bearing failure or non-linear response of any sort. Geometry specifications were typical for all 3 specimens except the width (See Figure 4.3).

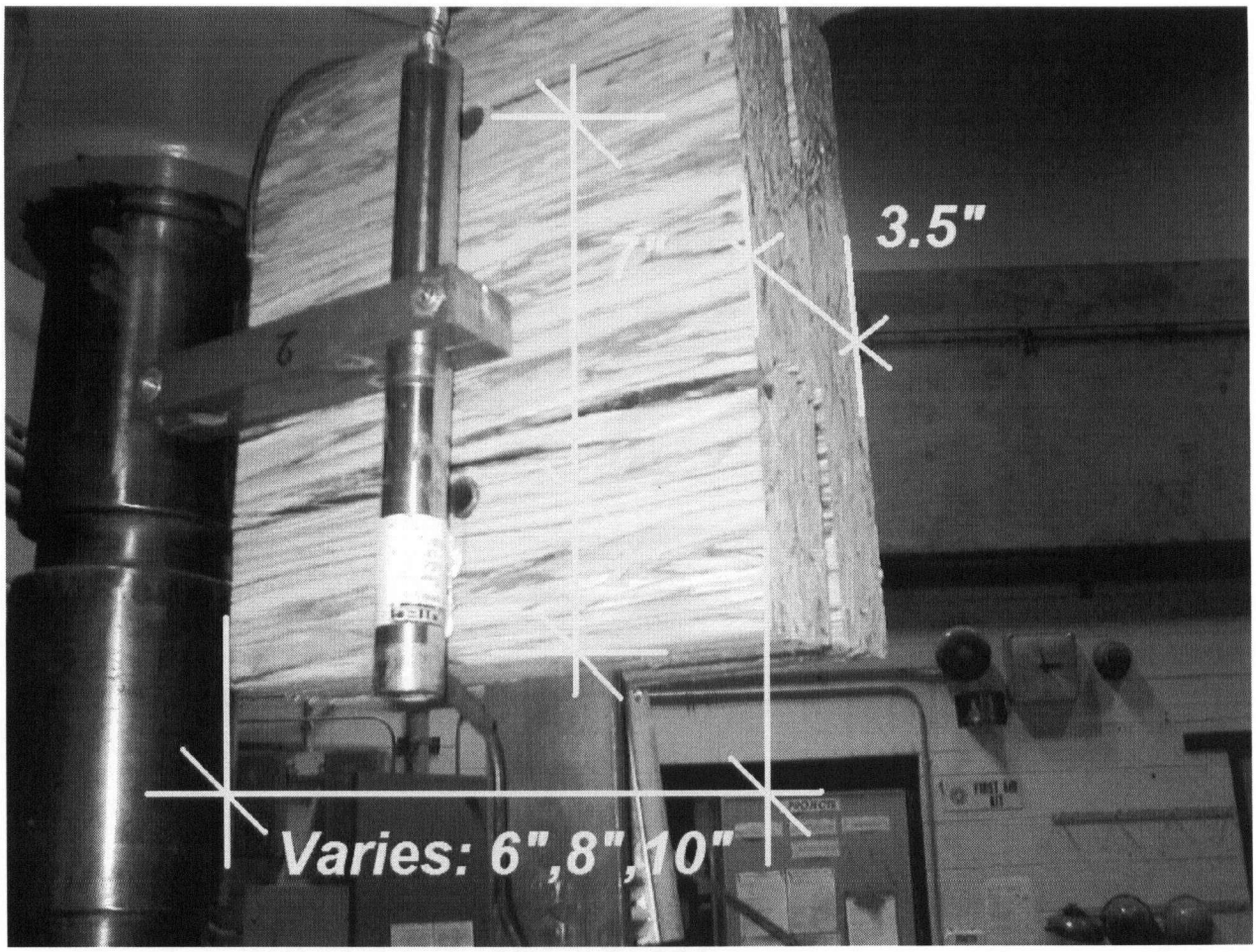

Figure 4.3 *Geometry of Tension Perpendicular to grain Test Specimens*

4.4.3 Compression Tests Parallel and Perpendicular to Grain

Since testing in tension perpendicular to grain did not produce any non-linear bearing failure response, it was necessary to develop a test that would ensure a bearing failure perpendicular to grain. The simplest way to do this was with a compression test in which there is no shear or tension perp. Stress in the wood. The samples were fabricated from recycled pieces of wood and steel from previously tested specimens that were not yet damaged.

The samples were simple in setup, a knife-plate was inserted into a chunk of wood and extended so that it was roughly an inch proud of the surface of the wood. The testing machine would then compress this piece of steel into the wood until the testing machine approached the surface of the wood after travelling almost an inch. A photo can be seen in Figure 4.4 of the test specimens, post testing, where the steel plate is now only slightly proud of the surface of the wood.

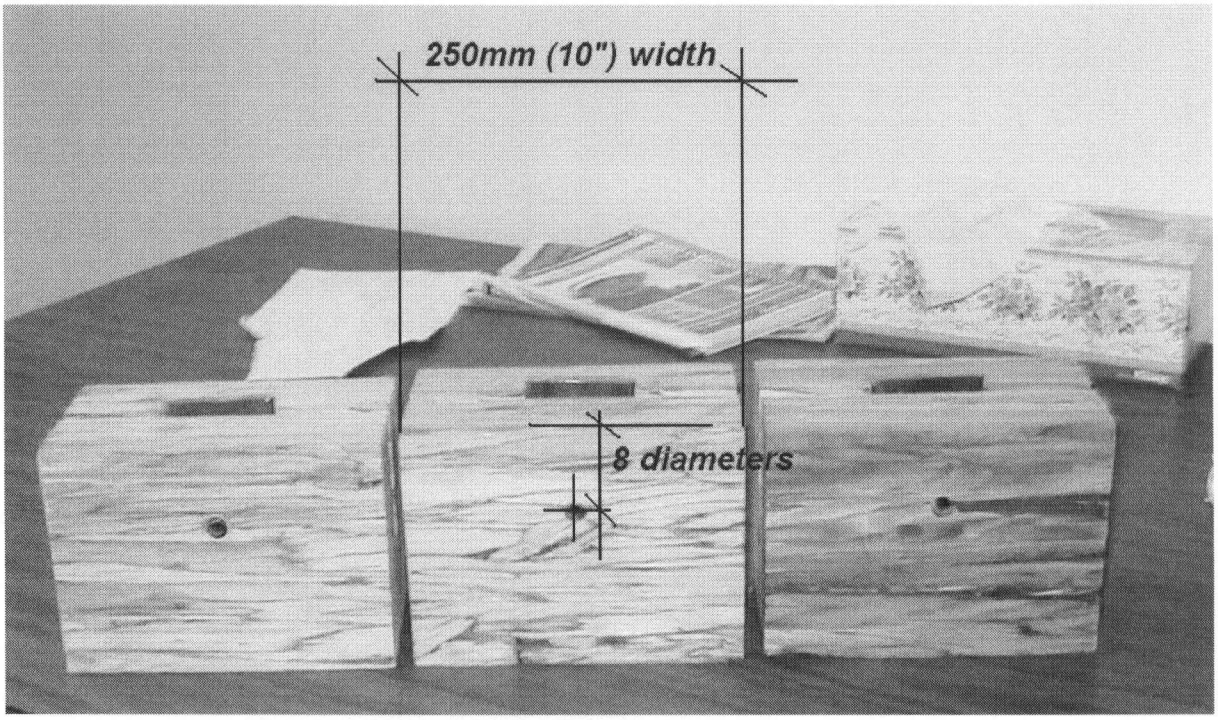

Figure 4.4 *Compression perpendicular-to-grain test specimens after loading*

Compression Parallel to Grain Specimens were the same configuration as the perpendicular-to-grain specimens but the un-loaded end distance on one of the specimens was only 4d and caused splitting before attainment of the theoretical "yield-point". Subsequent compression parallel to grain specimens have the 8 diameter

unloaded end distance as shown above in the perpendicular to grain specimens (See Figure 4.5).

Figure 4.5 *Compression Parallel to Grain Specimens After Loading*

4.5 RESULTS AND DISCUSSION

Any observations during load testing were recorded with associated load levels attained for the observation. Using these notes in combination with the load-displacement curves the failure modes could be understood.

It is important to note that the first two batches of test specimens in tension used faulty load LVDT measuring setups. Figure 4.6 shows this faulty LVDT setup in which the LVDT is screwed into the wood and the stopper is bolted to an arm extending from the knife-plate.

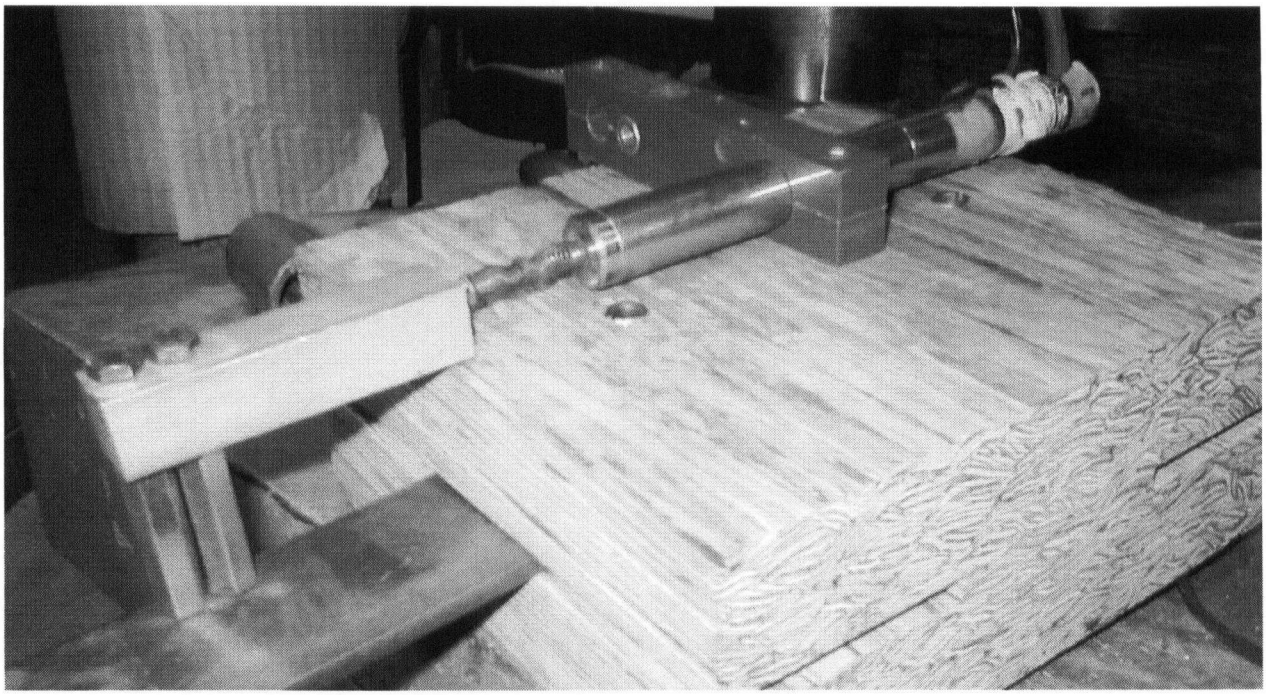

Figure 4.6 *Faulty LVDT setup used for parallel to grain loading and perpendicular to grain loading.*

The LVDT stopper is highly sensitive to any rotational movement of the knife-plate leading to strange recordings during the critical first 1-2mm of displacement. This was not detrimental in all cases, but some of the displacement recordings were not reliable.

4.5.1 Parallel to Grain Tests

The specimens tested in tension were observed to split during testing. It is the authors opinion that the end and edge distance are sufficient enough not to contribute significantly to this failure mode. It is simply the nature of the dowel stiffness and the material properties of parallam that ensure a splitting failure. Out of the 8 specimens

tested parallel to grain, 2 of them formed significant hinges occurring in conjunction with splitting.

The spring-pins were observed to develop plastic hinges in the same manner as bolts. Figure 4.7 and 4.8 show the bolts and spring-pins salvaged from the failed parallel to grain connections respectively. The similarity in the behaviour of the two dowels leads me to believe that a ½" spring-pin is roughly equivalent to a ½" A307 bolt in static behaviour.

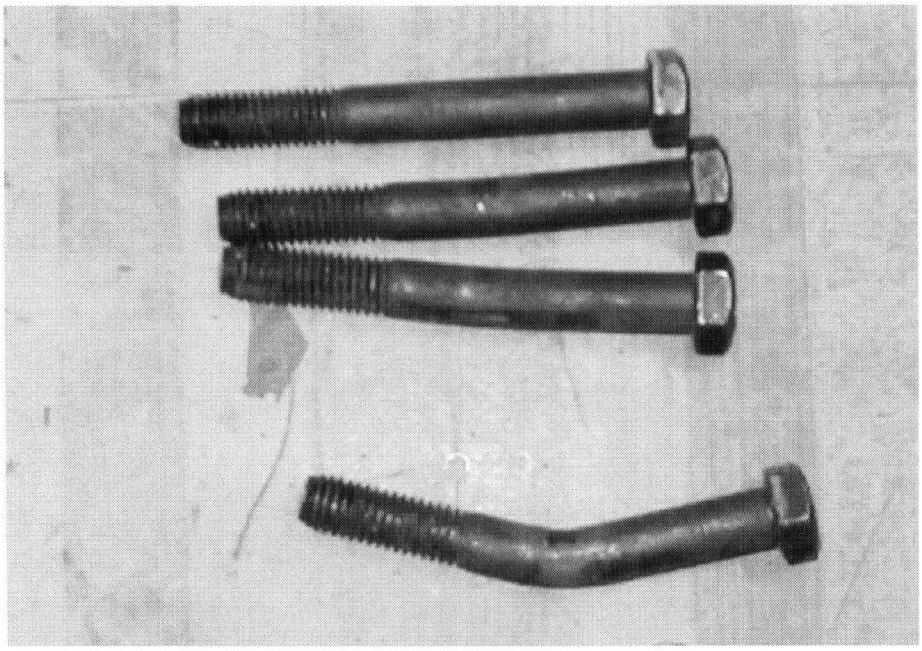

Figure 4.7 *Bent bolts from single fastener test*

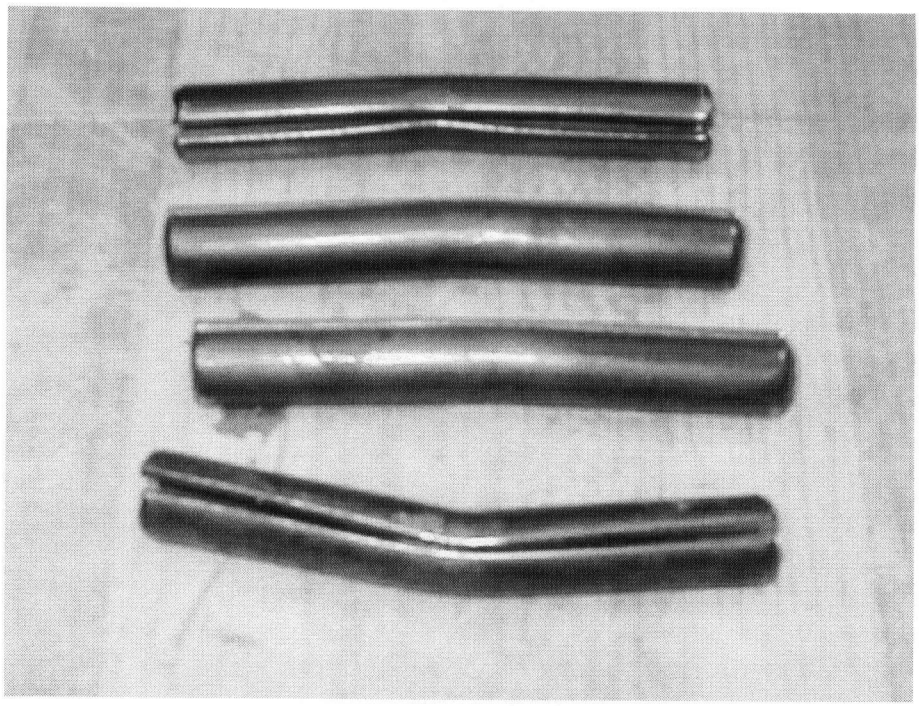

Figure 4.8 *Bent Spring-Pins from single fastener test*

The spring-pin dowels experienced some additional distortions when compared to the bolts, typically the split in the pins were pinched closed by the localized force of the knife-plate Figure 4.8. However, this behaviour made no observable difference to the performance of the connection.

4.5.2 Tension perpendicular to Grain Tests

The behaviour of these connections regardless of width was to respond linearly until tensile fracture occurred. The failure was sometimes a net section (throught the bolt), but sometimes a weaker path occurred above or below the dowel. The failure location and relative strength could be predicted by observing the defects in the

parallam material. Voids or pockets of discoloured material indicated weak zones, and failure always occurred around these areas.

The linear stiffness was observed to be significantly softer than the parallel to grain loading. At first it was assumed that this was due to the perpendicular to grain bearing stiffness, however the compression tests perpendicular to grain showed similar stiffness to the parallel to grain bearing stiffness as discussed in section 4.5.3.

4.5.3 Compression Tests

Specimens tested in compression parallel to grain were had similar load displacement curves to those tested perpendicular to grain. However, the observed failure modes were not the same. In parallel to grain loading the specimens failed in splitting. 3 out of 4 failed after reaching the "yield point" as recommended by ASTM. The specimen that failed before attaining a yield plateau did not have adequate end distance. Subsequent specimens used a larger unloaded end distance of 4 diameters as opposed to the 2 diameters in the first trial.

The difference between the load displacement curve perpendicular and parallel to grain is surprisingly quite subtle. The initial stiffness is very similar when comparing the two parameters. Beyond 2mm of slip, the perpendicular to grain specimens lose tend to lose stiffness in a gentle curve as the fastener hinges. The parallel to grain specimens retain their stiffness until about 3mm whereupon the load displacement curve flattens out much more rapidly due to splitting combined with fastener hinging. Figure 4.6 superimposes the load displacement curves for compression specimens in both parallel and perpendicular to grain loading.

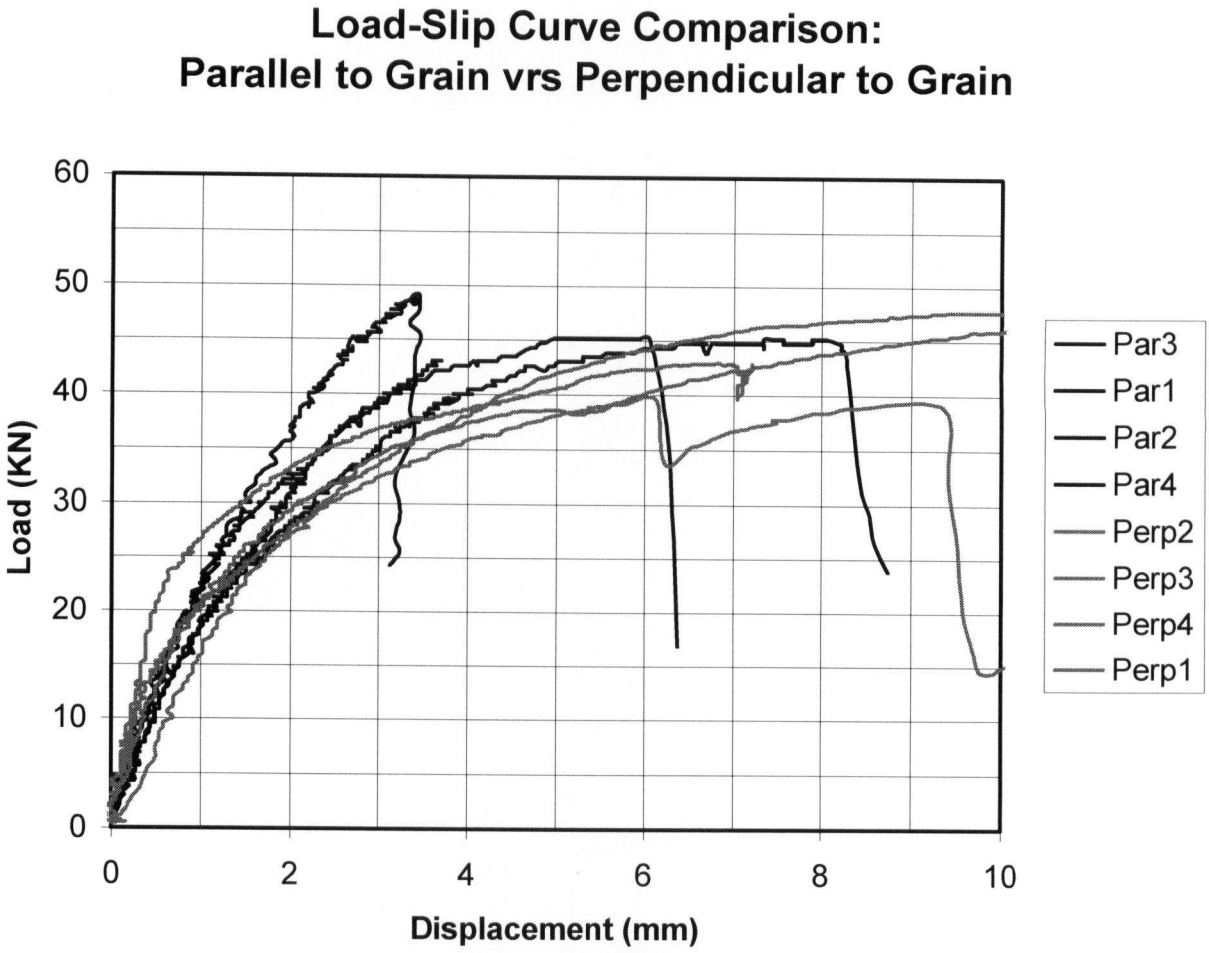

Figure 4.9 *Comparison of single fastener curves parallel and perpendicular to grain (in red).*

4.5.4 Bearing Capacity of PSL

Research has been done at U.B.C. by Helmut Prion to relate the bearing strength of dowels tested in sawn timber to PSL. The bearing strength in PSL is given by CSA 086 as:

*f = 63*G(1-0.1d)*

where G, the specific gravity has been found to be G = 0.628 (Moss et al.1998)

The results of the tension parallel to grain tests results in a 5th percentile strength of 30KN. Using G = 0.628 in the CSA-086 calculation for single pin strength, the 5th percentile is estimated as 26KN, 85% of that found through testing.

4.5.5 Foschi Load-Slip Parameters

The Foschi equation, developed by Ricardo Foschi at the University of British Columbia, was developed to predict the non-linear response of nails in wood. Fundamentally it is a 3-parameter curve that load-displacement data is fit to. This equation is generally applicable and fits a curve to test data with three parameters, initial stiffness, a intercept vertical intercept of the tangent to the curve, and a secondary stiffness.

P(Δ) = (K+ K2*Δ)*(1-e^(-K1*Δ/K)) Foschi(1974)

The parameters for the Foschi equation were found from testing spring pins in compression parallel and perpendicular to grain. The parameters were selected such that the Foschi curve matched the test curve as best as possible. The Foschi parameters determined from testing are as follows:

TABLE 4.1 *Stiffness values found through testing*

PARALLEL TO GRAIN COMPRESSION TEST

Parameter	Mean Value	C.O.V.	Std.Dev.	Units
K	50	12%	7.5	KN
K1	26	15%	14.7	KN/mm
K2	0	N/A	N/A	KN/mm

PERPENDICULAR TO GRAIN COMPRESSION TEST

Parameter	Mean Value	C.O.V.	Std.Dev.	Units
K	32	20%	7.5	KN
K1	37	40%	14.7	KN/mm
K2	1.7	45%	0.8	KN/mm

PERPENDICULAR TO GRAIN TENSION TEST

Parameter	Mean Value	C.O.V.	Std.Dev.	Units
K	9.5	20%	N/A	KN/mm

5.0 MULTIPLE FASTENER RESPONSE

The spring-pin connections were invented with the intent to reduce or possibly eliminate group effects. The results from the original tests conducted by Structurecraft on the 4 – spring-pin configuration connection showed a strength that was much higher than code predicted. In fact it was almost 4 times higher than the single-pin strength. The engineers assumed that the tight-fit of the spring-pin had in fact eliminated the group effects. But was this in fact the case? A comparison of bolted connections to spring-pin connections in parallam suggested that there is very little difference between the two. Perhaps the difference between the spring-pin connections and the Canadian code were due to other factors, or simply an overly conservative code prediction. In order to come to a definitive conclusion I decided it was necessary to study what causes group factors and what parameters most affect them.

Until relatively recently very little research has been done to investigate the strength of a large number of connectors in a single connection. In steel botled connections, the bolts are somewhat similar in stiffness, there are no bolthole tolerances, and the steel side-plates can be quite stiff relative to the connection movement. In wood connections, the fastener stiffness' have a large coefficient of variation (40-50%), bolt connections have up to 2mm tolerances (By Canadian Standards), and the there is the potential for a large differential in stiffness between the wood and steel side plates. This can cause a much larger difference in the distribution of forces amongst the fasteners leading ultimately to a group effect if there is a brittle failure of the wood.

The brittle failure mode is always affected by the tension perpendicular to grain strength. This is regardless of whether the connection is in tension, shear or sometimes even in compression. Tension perpendicular to grain strength is difficult to predict and strongly influenced by Weibuls weakest link theory (size effects). Therefore, for larger connections, it is reasonable to believe that a large portion of the wood connection group effect can be attributed to size effects in the connection region. Research is being done to find a rational method to deal with brittle connection failure modes in wood. Some are empirical and are not generally applicable. Some researchers utilize analytical methods that are more general in nature, but unfortunately these methods are plagued with a large number of variables of which little information is known and applying these variables to failure criteria that has a large amount of uncertainty.

5.1 BACKGROUND

Borg Madsen (2000) has done some significant research in to the history of the wood connections and their manifestation in the design codes. Much of the following literature review is taken from his work and merely comment on what this means for spring-pin connections.

5.1.1 Original Code On Bolted Connections Circa. 1950s

The concept of the wood bolted connection was presumably based on that of the bolted connection in steel. The bearing capacity of a single bolt was determined, as discussed found experimentally in section 4.0, and then the connection geometry

(end/edge distance and row/fastener spacing) is determined to ensure that the full bearing strength can be achieved.

Unfortunately, the connection geometry only holds for a limited number of bolts. In North America, it was normal to assume that n bolts in a row had the same carrying capacity as n x single fastener capacity. Anyone who built a connection with anything more than 4 bolts might be in for a surprise with the prescribed fastener spacings.

5.1.2 Group Modification Factor Circa. 1960s

Researchers Dr.Andre Jorissen and Mr.H.Fahlbusch in Europe proposed an alarming finding depicting strength reductions for bolts in a row. Their approach was to determine the effective number of fasteners that are acting in a connection resulting in the formulae below:

$$N_{ef} = 4n/(n+3) \qquad [5.1]$$

After reviewing the implications of this formula on the heavy timber construction industry, the European code committee chose to change the row spacing, edge and end distance to manage the premature fracture observed in the testing. This research led to what is still being used in Europe today.

$$Nef = 6 + 2n/3 \qquad [5.2]$$

Note that for n < 7 there are no group factors present.

In North America, however, research into group effects diverged from that done in Europe. The North American timber construction industry favoured a fewer number of large diameter fasteners with tight end/edge and row spacing distances. Research done by Lantos in the 1960s looked at the effect of fastener spacing, s, and slenderness ratio of the bolts (t/d) relative to the wood side-plate thickness. The work done by Lantos was highly analytical, and involves the relative elastic stiffness of the side-plates. The resulting equation is as follows:

$$\mathbf{Nef = 0.33K_m(t/d)\text{^}0.5(s/d)\text{^}0.2n\text{^}-0.3} \qquad \mathbf{[5.3]}$$

Where K_m is the row factor,

K_m = 1 for 1 row

K_m = 0.8 for 2 rows

K_m = 0.6 for 3 rows

It is sad to note that the row factor was based on an unfortunately small row spacing of 2d in which a group tear-out failure is ensured. The euro-code utilizes a row spacing of 4d that reduces the necessity for this reduction.

An attempt was made to postpone the brittle failure by increasing the loaded end distance from the minimum 7d to 10d resulting in more confinement for the group tear-out failure mode, but is generally not applicable to failure modes other than group tear-

out. This resulted in considerably higher carrying capacity. The results of this research leads to the group factors that were relinquished in the CSA-1989.

$$Jf = Jl*Jr*Jg \qquad [5.4]$$

Where,

$$Jg = 0.33*(L/d)^0.5*(s/d)^0.2*N^-0.3$$

$$Jl = 1.0 \text{ (for 10d) or } 0.75 \text{ (for 7d)}$$

$$Jr = 0.8 \text{ for 2 rows, and } 0.6 \text{ for 3 rows}$$

These equations are not perfect, but are conservative in estimating the strength of bolted connections. When using the minimum specifications for end, edge, and row spacing, these formulas provide a safe estimation of connection capacity.

5.1.3 EuroCode versus CSA-086

The specifications for the Eurocode and the Canadian code diverged sometime back in the 1960s where the Canadian construction industry favoured tight end/edge distances, whereas the European community preferred connections that failed in a ductile manner according to the Johanson model. Table 5.1 is a comparison of the specifications for the code carrying bodies.

TABLE 5.1 *Comparing minimum fastener geometry of EuroCode to CSA-086*

CODE	EuroCode 5	CSA-086
Bolt Tolerance	< 1mm larger than dia.	< 2mm lager than dia., but greater than 1mm
Fastener spacing (a1)	7d	4d
Row spacing (a2)	4d	2d
End distance (a3)	7d	7d
Edge distance (a4)	3d	1.5d

d = diameter of the bolt

To put these specifications into perspective Figure 5.1 illustrates the difference between the two codes for a 6 pin - ½" bolted connection.

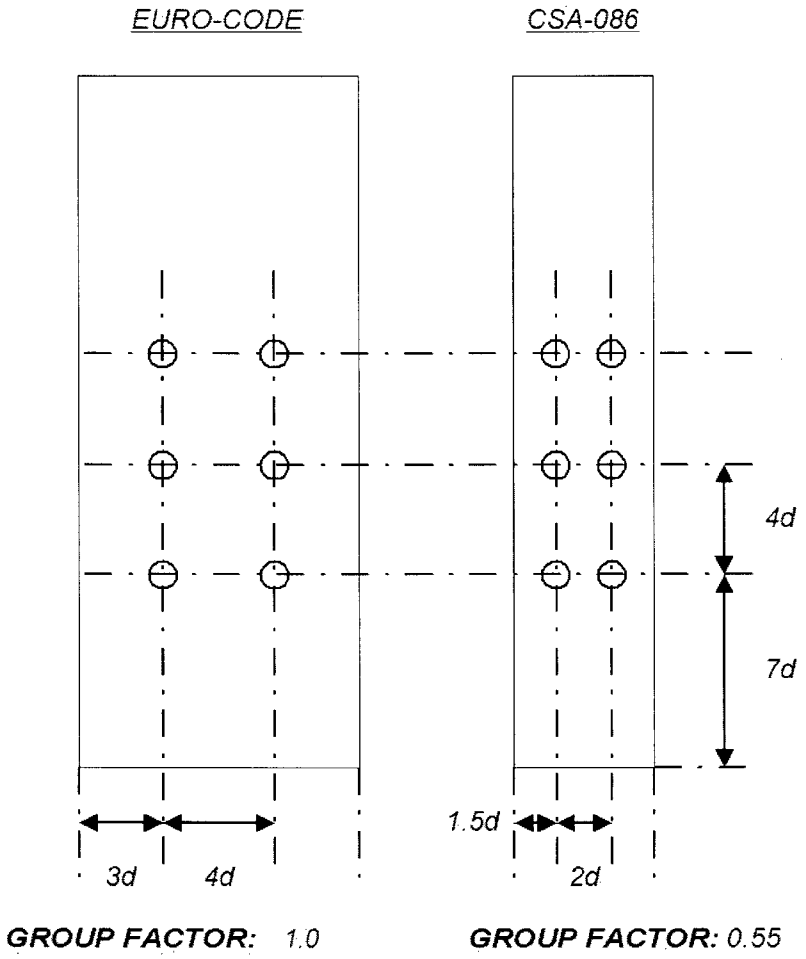

FIGURE 5.1 *Visual Comparison, drawn to scale, of Wood Connection meeting the minimum spacing specifications of the EuroCode and that of the CSA-089*

The connection designed by the Euro-Code recommends twice the capacity as the connection outlined by CSA-086. Supposing that both codes represent the connection capacities accurately, then a row of bolts could be removed from the Canadian connection without affecting the carrying capacity significantly. It seems this might also have the added benefit of resulting in a ductile failure mode rather than the brittle failure mode that is predicted by the presence of a 55% group factor. The large

difference between these 2 codes demonstrates the need for more research on doweled connections, and perhaps, an adoption of larger edge distance for CSA-086.

5.1.4 Contemporary Research

An extensive research project was carried out at the Delft University of Technology in the years 1994 to 1998. During this time, 950 tests on timber connections loaded parallel to grain were carried out in conjunction with analytical modelling of the load distribution on fasteners and the brittle failure modes. Borg Madsen wrote a chapter summarizing this research called, "the strength of bolts in a row". The specifications for the tests are as shown below:

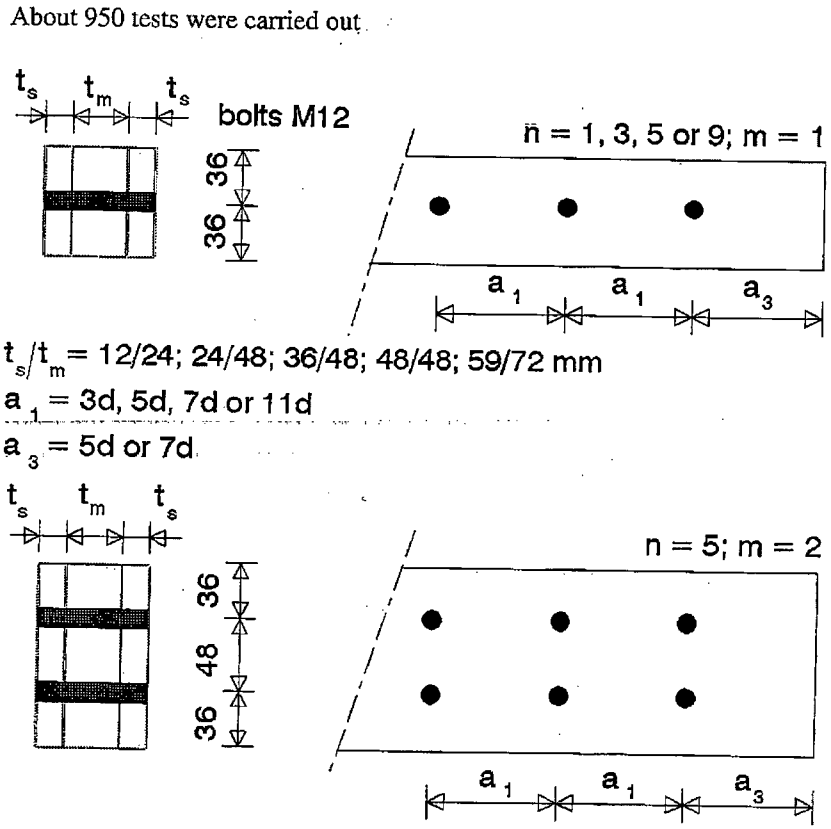

Figure 5.2 *The test specimen specifications for the tests conducted by Borg Madsen. In all cases the edge distance was 3-diameters.*

The variables studied and their effects on group factors are as follows:

1. Hole Clearance
2. Number of bolts in a row (N)
3. Spacing in the loaded direction (a1)
4. Number of rows (m)
5. Slenderness ratio (λ)
6. Loaded end distance (a3)

It was found that the spacing of the bolts in the loaded direction had the largest influence on the results. All other variables were of less importance. The Hole clearance was demonstrated to affect the stiffness of the connection, but since most connections deflected more than 3mm, the ductility of the Johanson failure mode ensured re-distribution of load to all the fasteners. Unfortunately the spacing of the rows and the edge distance were not a part of this study. Interestingly enough, the group factor did not change significantly when the number of fasteners in a row went up from 3 to 5 to 9 all spaced at 11d.

5.1.5 Contemporary Studies of Tight-Fitting Pins

It remains to be known whether the equations developed are also applicable to tight-fitting dowels. There are 3 sources of literature that talk directly on the impact of tight-fit for timber connections with multiple fasteners including that of Borg Madsen mentioned above.

1. Borg Madsen, Behavior of Timber Connections. Borg discusses research conducted in the Netherlands in which 61 test specimens were used to study the effect of hole-clearances on multiple fastener capacity. The study involved fabricating one set of specimens with precision drilling in order to eliminate hole-clearances, and comparing the results to specimens fabricated according to "typical construction" practices. The results demonstrate that the connection capacity is unaffected by hole clearances unless connection slip was less than

3mm. It is interesting to note that the amount of bolt tolerance was carefully recorded in this study.

2. Borg Madsen, Behavior of Timber Connections. Research done at UBC compares bolted connections with and without glue injection in the holes. The test involved comparing 3 configurations of bolted connection... single bolt, 4 bolt group, and a 6 bolt group. The results show that reinforcing the holes with glue results in an increase in strength of 30-40% for the single fasteners, and 10-20% for the 4 and 6 bolt group connections. The connection slip for these tests was recorded as being about 5-8mm.

3. Research was conducted in Zurich Switzerland demonstrating that the precision of drilling has an effect on the strength of multiple fastener connections when a brittle failure mode occurs. This effect can be as much as a 40% reduction in strength when comparing a hole clearance of 2mm to 0.05mm. When the failure mode is ductile it is observed that the hole clearances no longer play a significant role in the connection due to re-distribution of forces.

4. Research at UBC by Mischler, A., Prion H., Lam F., concluding that tolerances only affect timber connections when a non-ductile failure occurs. This research controlled the hole tolerances in each direction. The tolerance in the direction perpendicular was shown to have the most significant effect on the strength.

5.1.6 Premature Brittle Fracture

Without premature brittle fracture there would be no group factors. A connection failing in a ductile bearing failure mode will average out the capacities resulting in no group factors. Certainly brittle failures are the most important factor contributing to group effects. Unfortunately, it is also the most difficult to predict, avoid, and observe.

The body of knowledge on numerical modelling of brittle failures in timber connections is quite extensive, however there is still much that remains to be done. Fracture mechanics are typically used to determine failure-criteria for stress in wood. Complications arise in connections due to the difficulty in establishing criteria for combined stresses. This process is complicated by the random nature of both the strength and stiffness of the material in all directions. There is also the problem of the stability and stiffness assumptions inherent in any numerical finite element.

D.M Moses (2000) conducted an investigation of using 3-D non-linear finite element modelling to capture the behaviour of composite lumber in the connection zone. The modelling was highly rigorous and attempted to capture all physical aspects of a wood connection. The model included the bearing contact mechanics modelling the friction and contact stiffness of the bolt wood interface. The complex failure criterion was checked against 3-dimensional stress state. All the parameters were carefully measured or taken from existing literature.

The predicted capacity under-stated the test behaviour by a factor of 0.5 – 0.7. The ultimate deflection was typically half of that observed in the test program. The results, although not quantitatively accurate, did give insight into the stresses that occur in and

around the connection zone. I used these results to help gain a qualitative understanding of the connection behaviour.

5.1.7 Connection Zone Stresses

The stresses in the Connection Zone in Timber are fundamentally the same as the stresses in a steel connection. The main differences are due to the large difference in *stiffness* between the parallel and perpendicular to grain directions in wood. The basic mechanics involve the transfer of the bearing stress in compression into the eventual uniform tension stress over the member cross-section. In both steel and timber, the compressive bearing stresses must spread-out in order to be "picked-up" by the lines of tensile stress. This spreading-out of the load happens at different angles in steel and timber. In steel this angle is close to 45 degrees. In Timber this angle is probably as high as 10 degrees due to the large difference in stiffness parallel and perpendicular to grain. A simple strut and tie model of the connection stresses can give qualitative insight into the behaviour of bearing type connection.

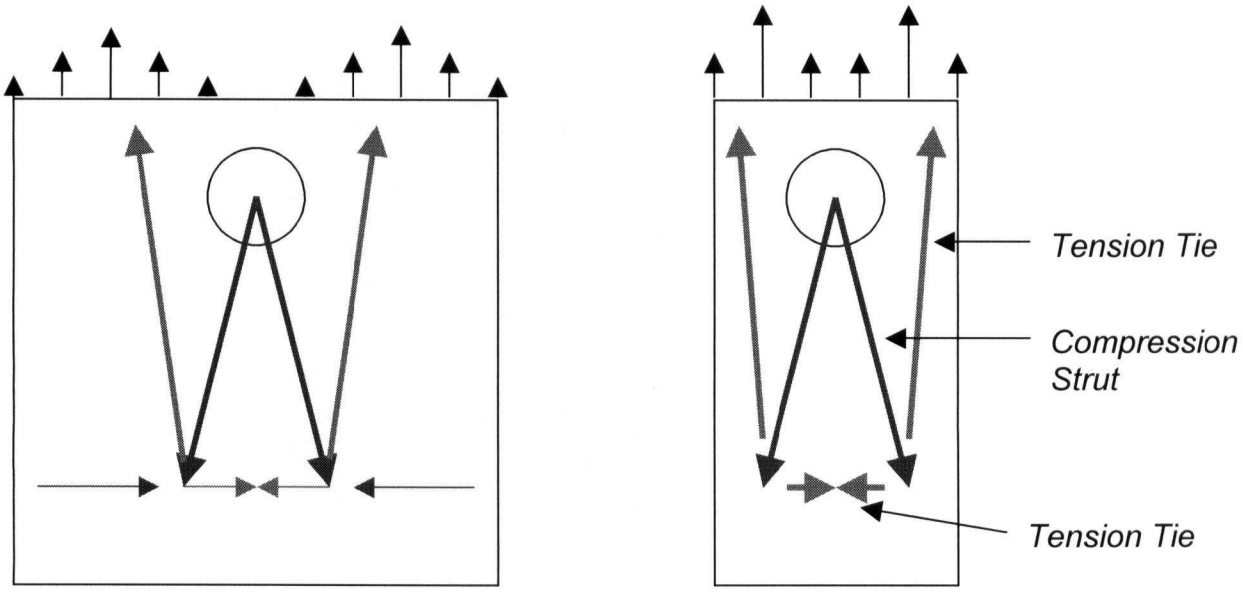

Figure 5.3 *A strut and tie model with the tension-perp strands acting as a tie. Struts(Compression)) are in blue and ties(tension) are in red.*

A) Large edge distance; the compression struts that spread out from the fastener are restrained by stiff side material.

B) B) Small edge distance; the side material is not as stiff resulting in more load shared by the tension-perp tie.

In case 'A' (Figure 5.3), the confining forces are actually transferring shear forces. These shear forces get carried out through theoretical cantilever beams that reach out from the middle of the member either side of the bolt. With increasing edge distance, the clamping stiffness of the theoretical cantilevering beams increases. This not only delays the onset of splitting, but also provides more ductility after failure.

5.1.8 Tension Perpendicular to Grain Properties

The dreaded tension perpendicular to grain strength is the property of wood that governs a large number of failure modes yet has received very little attention by the engineering profession. Dowels in wood transfer their load mainly in compression, however a percentage of this load acts perpendicular to grain as the dowel tries to wedge apart the material. It is difficult to understand tension perp stresses because the strength is not a constant value. The strength is highly dependant on the volume of material exposed to a given stress according to Weibuls weakest link theory. Not only this, but there are shrinkage stress vectors that can be present and potentially lead to fracture before any load is applied to the connection. There are several factors in a connection that affect the distribution of stress component perpendicular to grain.

1. The spacing of fasteners in a row
2. The edge distance of the connection
3. The end distance of the connection
4. The diameter of the fastener
5. The spacing of the rows

The spacing of the fasteners in a row has been shown to significantly affect the carrying connection of wood connections when increased beyond minimum spacing. Borg Madsen has shown that beyond 11d fastener spacing, the strength remains the same.

The edge distance is very important for reducing tension perp stresses. The larger the amount of wood surrounding the fastener, the stiffer the confinement or clamping action is. The effect of the confinement is illustrated above in Figure 5.3

The end distance is required to be quite large in order to reduce the tension perp. Stresses. In steel, an isotropic material, the end distance is only 2d. However, because of the weak tension perp. Strength in wood, this distance must be 4 to 5 times larger to prevent premature splitting at 7d – 10d. Also, shear plugs are also highly sensitive to end distance which is a particular problem for Parallam. The larger the fastener diameter, the bigger the wedging forces are under load. For PSL, CSA-086 recommends using less than ¾" bolts because of this.

The spacing of the rows is important when considering stresses due to shrinkage. Spacing the rows extremely far apart can result in premature cracking. The material confined between the rows may attempt to shrink, but will be restrained by the bolts. The stresses that develop are proportional to how much material is confined between the rows. If the rows are to close together, the connection will be in danger of group tear-out.

5.1.9 Shear Plug Properties of Parallam

Parallam is quite vulnerable to shear plug failures due to the nature of the material. Parallam is created by compressing wood shavings together. The failure occurs by the dowel pushing individual or groups of shavings out of the end of the specimen. The interface between the wood shavings has failed in shear. These failures usually occur when there are a lot of voids between shavings in the vicinity of the connection.

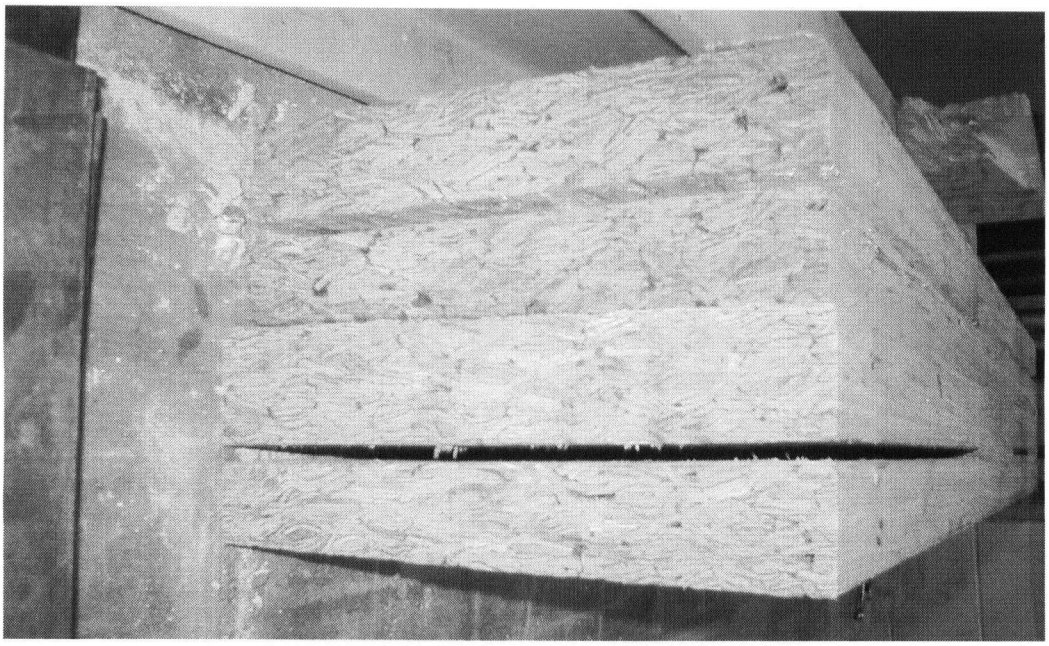

Figure 5.4 *End grain of parallam. The voids can reach large sizes and splitting or shear plug failure always occur around voids.*

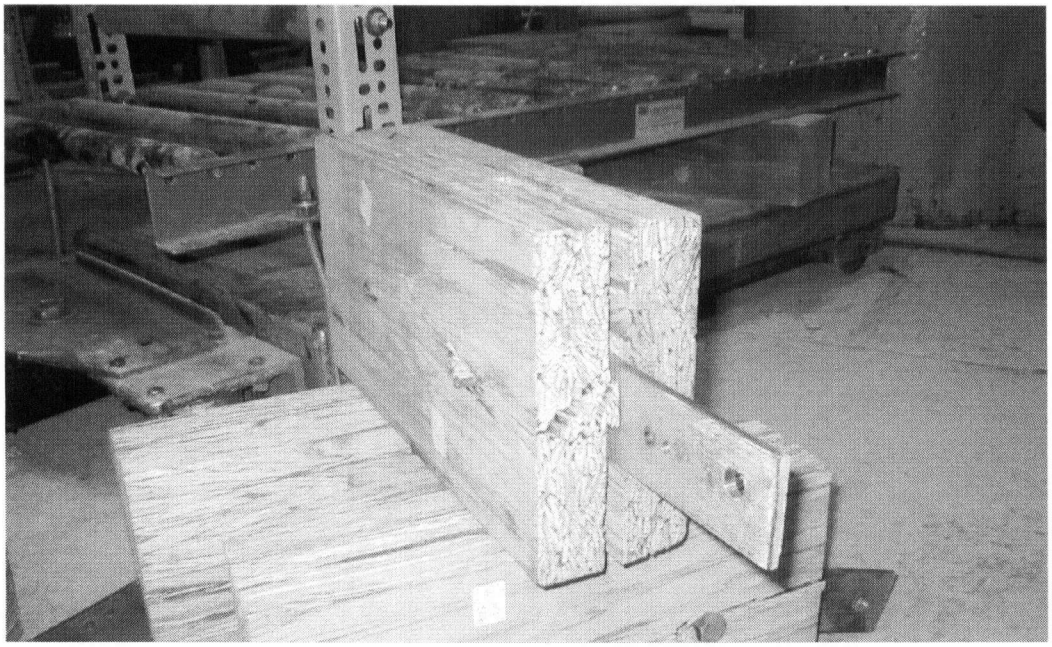

Figure 5.5. *Shear plug failure in Parallam*

To avoid shear plug failures in a Parallam connection, a large end distance should be used such that there is enough interface surface area to resist the shear stresses along the wood shavings.

5.2 ANALYTICAL INVESTIGATION

There are two main factors contributing to group effects.

1. Non-uniform load distribution amongst fasteners
2. Premature Brittle Fracture of the surrounding wood

My analytical model focused on the load distribution on the fasteners because I felt that a quantitative investigation of brittle fracture required a some sort of solid model. The problem is that Parallam is a fairly recent material of which the constitutive parameters are not well known. Conducting tests and developing a reliable constitutive model for Parallam would be a separate thesis unto itself and well beyond the scope of my own.

5.2.1 Probabilistic Load Distribution

To gain an understanding of how tight fitting pins and bolts take up their load differently I developed a simple spring model to investigate the difference based on Isyumov (1967). The model studies the load take-up and distribution on the pins as the displacement of the connection is advanced. The model is based on summing up the contributions of several fasteners with non-linear springs. My personal twist to this

model is that I added a stochastic aspect to it. The non-linear springs are represented by three variables. I created a monte-carlo simulation to randomly vary these three variables in each individual spring according to their mean and standard deviation. A schematic diagram of a timber connection is shown below illustrating the logic behind the load distribution model.

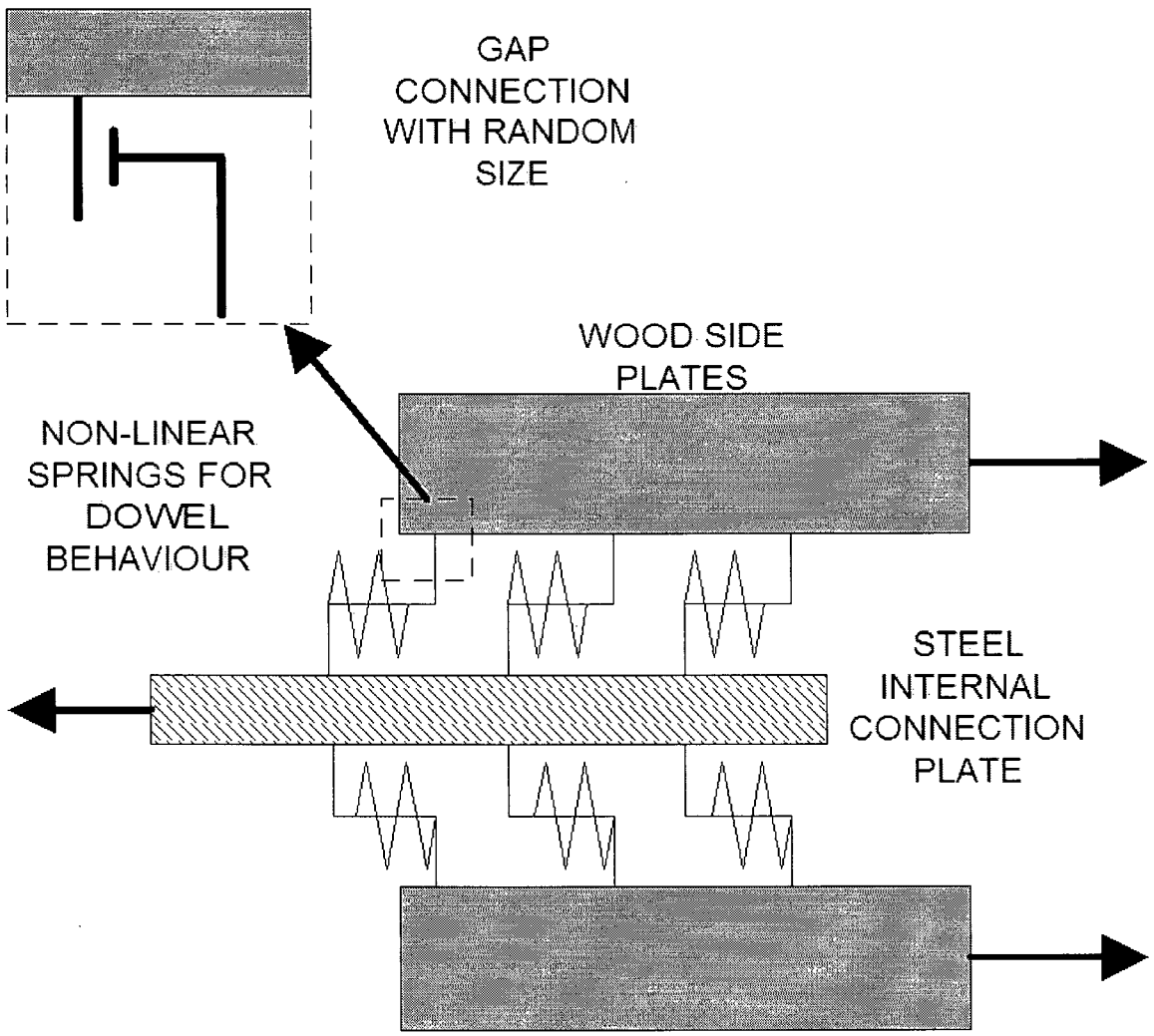

Figure 5.6 *Schematic diagram of the load distribution model. The fastener spring-stiffness dominates the behaviour of this model.*

The assumption that the side-plates are rigid is not strictly correct. Axial displacements can be up to as much as 0.2mm at the point of failure. However, the displacements of the steel knife-plt are the same as the displacements of the wood side-plts. These two displacements cancel each other out and result in even load distribution of all the pins. This is only a special case, however, and may be violated under some cases. Even if the side-plate stiffness does affect the connection, it is relatively small for the size of the connections I am studying.

5.2.2 Implementation of Foschi Equation

In section 4.0 the properties of the load displacement behaviour of the single pins was studied and quantified. The average and the statistical spread of the fastener stiffness was determined see Table 5.2 below.

Table 5.2 *Stochastic parameters for the Foschi Load Slip Equation.*

Parameter	**Mean Value**	**C.O.V.**	**Std.Dev.**	**Units**
Kp	50	12%	7.5	KN
K1p	26	15%	14.7	KN/mm
K2p	0	N/A	N/A	KN/mm

A spreadsheet program was created that randomly varies each foschi load-slip parameter according assuming a normal distribution for the random variable. The

spreadsheet then creates a synthetic load slip curve for each fastener in the connection. The force in the connection at any given displacement is the sum of all the individual fastener forces. This can be seen graphically below. The dark line is the sum of all the 6 individual fasteners.

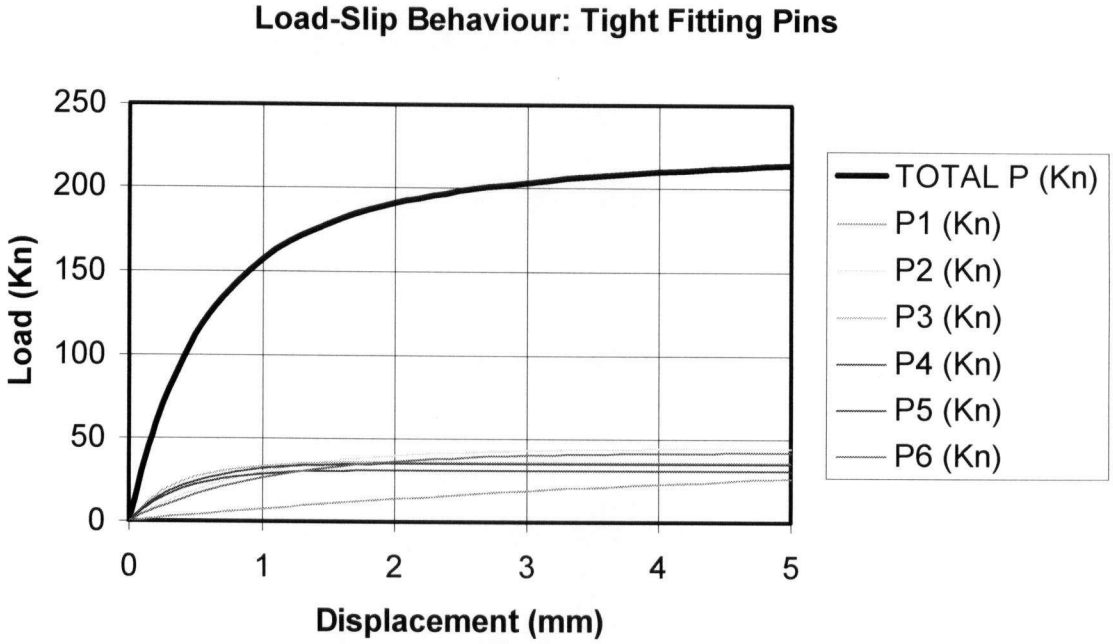

Figure 5.7 *Randomly generated foschi load slip curves for single pins. The dark line is simply the sum of the load of each single pin.*

As the displacement increases the fastener forces converge such that the total load is the average of all the component capacities. If this is done several times the average of the connection strength can be determined for various load slips.

This was also done for bolted connections to compare them to tight-fitting pins. To model the bolthole tolerance another random variable was created. The bolthole

random variable had an absolute minimum of 0 and a maximum of 2mm. This bolthole tolerance was randomly generated for each individual pin. The variability of the bolthole tolerance was based on two distributions.

- Geometric probability distribution. The bolt has an equal probability of occurring anywhere within the tolerances. This by definition has the probability distribution of a circle.
- Workmanship probability distribution. The probability of the bolt occurring in the centre is weighted heavier than the perimeter. This is to reflect that the average workman would try and put the bolt in the centre of the hole. This was modelled using a sign curve for simplicity and is not based on any relevant data. The difference between the geometric probability and the workmanship probability is not significant enough to warrant further refinement.

Below is an example of the bolt load slip curve with the workmanship distribution used for the bolthole tolerance random variable.

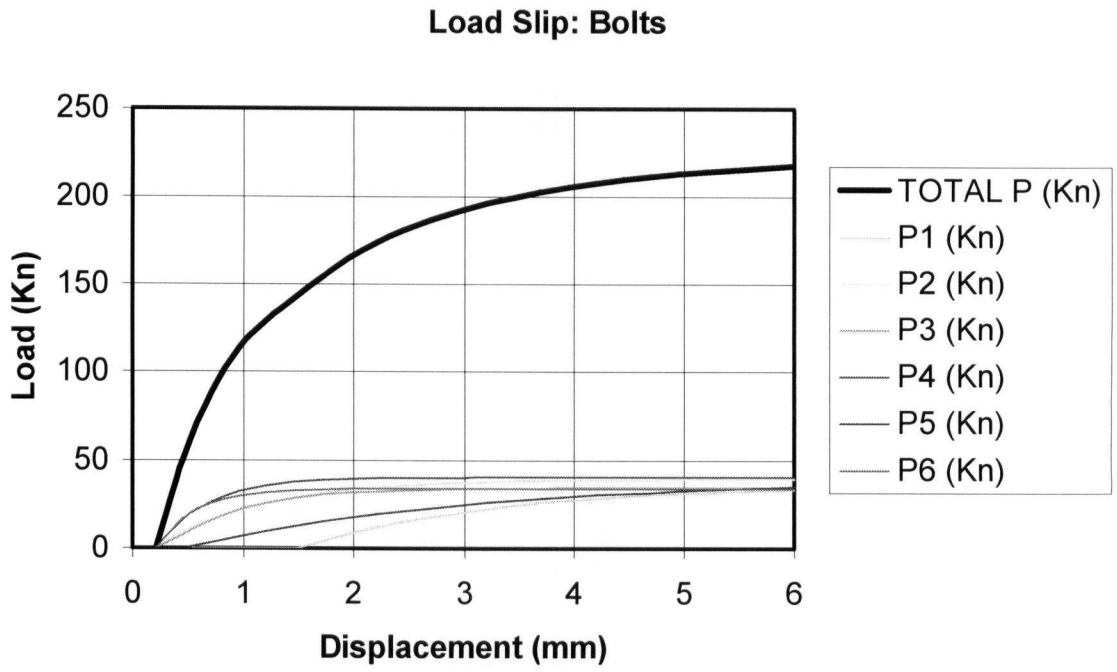

Figure 5.8 *Randomly Generated load slip curve for multiple loose bolts.*

Both bolted connections and tight-fitting connections will ultimately have similar average strength at large displacements, we can produce a curve that shows what percentage of this ideal full capacity is attained for a given displacement. This graph is shown below. The graph removes the initial slop of the bolted connection and only includes "loaded displacement"

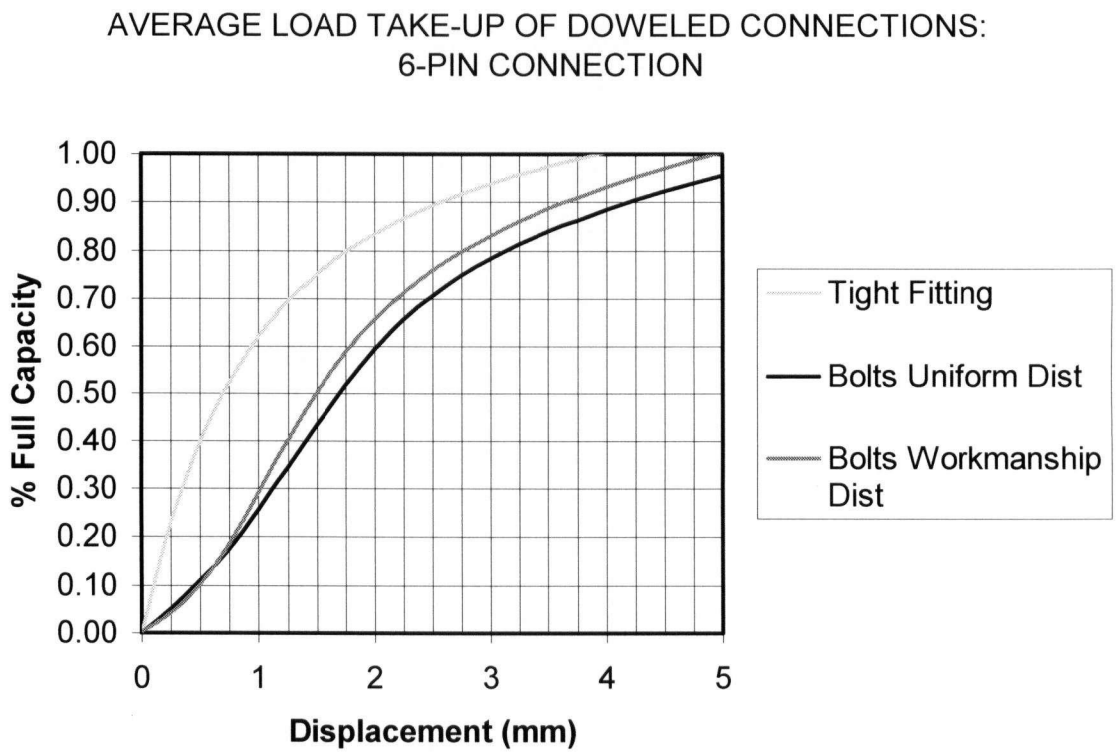

Figure 5.9 *The comparison of the average 6-pin, tight-fitting pin response to equivalent bolts with a bolthole tolerance up to 2mm.*

This graph shows that if the connection fails after displacing 1mm, the tight-fitting pins will, on average, carry 80% of the full capacity whereas the bolted connection will only carry 40%. For the bolted connection, only the loaded displacement in considered, the initial slip before load take-up is not part of the displacement above. The displacement above is "loaded displacement".

Beyond 3mm of connection slip there is little difference between the two curves as was observed by Borg Madsen. This curve also confirms the research done in Zurich that there could be a 40% difference between the two connections if a highly brittle

failure mode occurs. There is indeed a 40% difference between the two curves if the ultimate displacement is between 1.75mm and 2.0mm.

5.3 TESTING SETUP AND PROCEDURES

The testing was done on the "Baldwing" testing machine in the U.B.C. Structural Engineering Lab (SEL). The machine is a hydraulic machine capable of tension or compression loading. The load rate is manually controlled and was conducted at a rate that reaches the ultimate capacity of the connection in approximately 10 minutes, no less than 5 and no more than 20 minutes, in accordance with ASTM D-5652.

The LVDT displacement measuring devices were placed near the end of the wood specimen away from where splitting is likely to occur. The LVDT stoppers were installed, wrench tight, on the steel plate. By installing the LVDT to the steel plate, the measurement is the relative displacement between the steel plate and the end of the wood specimen, defined as the connection slip. Two LVDT devices were installed at each end in order to average out rotational motion of the steel plate and to capture the displacement behaviour were one of the devices to fail.

Testing was conducted past ultimate load to capture the post-failure behaviour of the test specimens. The amount of displacement imposed after failure was arbitrarily selected during testing, but typically when the capacity of the specimen was reduced to half of ultimate at large displacements.

- Four ½" pins in Tension
- Four ½" pins in Tension with a staggered arrangement
- Six ½" pins in Tension with a staggered arrangement

It was decided that if a connection requires more than 6 pins that a high capacity timber connection would be used instead such as glulam rivets.

5.3.1 Four Pin Tests

The specifications for the 4-pin tension tests were the following:

- Wood side PLT thickness, L = 1-9/16" corresponding to L/D = 6.25
- Loaded End distance = 8d
- Edge distance = 5d
- Row Spacing = 8d
- Fastener Spacing in row = 8d

where d is the diameter of the spring-pin

5.3.2 Six Pin Tests

The 6-pin connection essentially had the same basic specifications, but staggered with the following geometry:

Figure 5.10 *Spacing specifications of the staggered 6-pin connection*

5.4 RESULTS AND DISCUSSION

The information obtained in these axial tests is being used for more than one purpose. Primarily to obtain the axial capacity of the spring-pin connection in a configuration for use by Structurecraft in further projects. The capacity is not generally applicable as with the CSA-086 code on bolted connections. The capacity here is limited to a conservative set of geometrical specifications.

The second motivation behind this testing program is to validate the analytical model that is used for determining the stiffness properties of the moment connection. If

any fundamental problems with the model are brought to light, then the validity of the model for the moment connections would be highly suspect.

Thirdly, validation of the analytical model may offer some intellectual contribution to the behaviour of tight-fitting dowels. The use of this model has the potential to relate tight-fitting dowels to loose bolts of any prescribed bolthole tolerance.

5.4.1 Engineering Properties

The main engineering property of interest is the load carrying capacity, which is best represented by the 5^{th} percentile strength.

Table 5.3 *4-Pin Test Summary*

No. Specimens	4
Average (KN)	128
Stnd. Deviation (KN)	16.3
C.O.V. (%)	13
5^{th} Percentile (KN)	101

The 5^{th} percentile calculated in the original tests by others was 102KN using 12 specimens. Therefore there is a total database of 16 connection specimens.

The 5^{th} percentile strength of a single fastener is 32KN. Four times this amount is 128KN. The observed group factor for the 4-pin connection is,

$$JF_4 = 102/128 = 0.80 \quad [5.5]$$

Table 5.4 *6-Pin Test Summary*

No. Specimens	8
Average (KN)	217
Stnd. Deviation (KN)	19.1
C.O.V. (%)	9
5^{th} Percentile (KN)	186

Six times the single pin capacity is 192 KN. The observed group factor for the 6-pin connection is,

$$JF_6 = 186/192 = 0.97 \quad [5.6]$$

The 6-pin connection was observed to have less severe group factor than the 4-pin connection that has a much smaller group. The difference between these connections can be attributed to the staggering of the pins. Borg Madsen observed that the main factor affecting the connection is fastener spacing in the row. By staggering the pins, the effective spacing is increased from 8 diameters to 16 diameters.

5.4.2 Load Carrying Behaviour

To validate the application of the analytical model the predicted average, 5^{th} percentile, and 95^{th} percentile load-displacement behaviour are super-imposed over the load displacement graphs from testing, see Figure 5.11.

The test data fits reasonably close to the prediction. The error bars on the prediction do not represent the predicted variation in the test specimens.

Both the test specimen A and B failed due to a split before 2mm of displacement was attained. The test notes state that a split was observed at 24kips (107KN), which is the point at which the behaviour of A & B depart from that of the prediction. Specimen A remained quite stiff after the observation of the first split and carried ultimately more load than B.

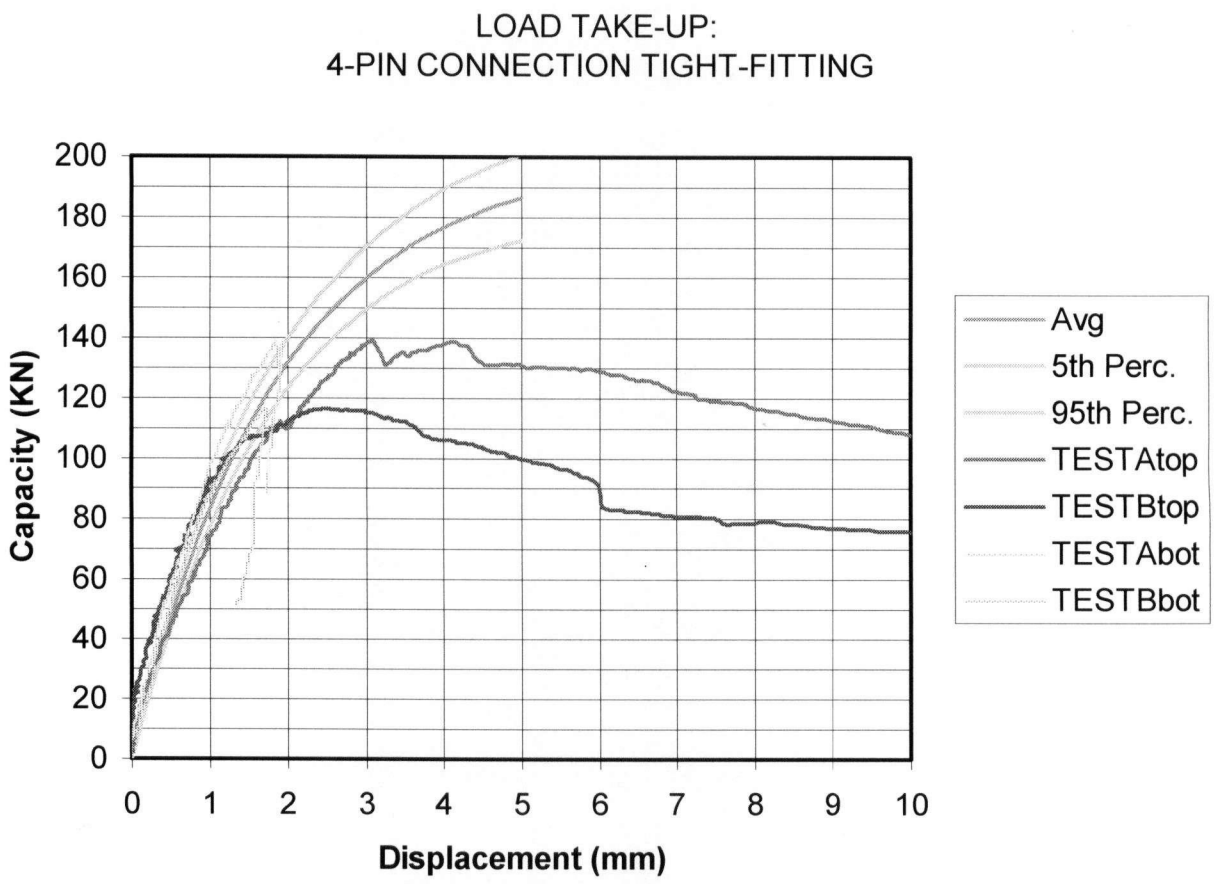

Figure 5.11 *The comparison of the load-displacement curves of the analytical model to 4-pin specimens*

The 4-pin connection is modelled reasonably well up until the first split. The 6-pin is equally well modelled, but a disturbing observation was made with respect to the LVDT setup. The second order effects due to the steel plate moving out-of-plane appear to be more pronounced in the 6-pin test specimens. Test specimen 'B', in particular, had a negative displacement for the first third of the load-slip curve. In other words the specimen was supposedly shrinking when it should be stretching. This is attributed to an inadequate LVDT test setup. This information was very important for further tests

where the rotational stiffness is a critical parameter that had to be obtained. The LVDT set-up was improved for these tests.

The testing notes for the 6-pin connection indicated that the specimens split at about 3mm. The 4-pin connection, as discussed before, was observed to split at a little under 2mm. Comparing Figure 5.12 to Figure 5.9, the capacity of a connection is fully attained at 4mm connection slip; The connection is 95% attained at 3mm slip, and is 80% attained at 1.75mm displacement. These numbers compare well to the group factors calculated in Equations 5.5 and 5.6. If a tight-fitting connection slips more than 4mm, one can be sure that there is no group factor present. Bolts, however, must reach 5mm of displacement before the same claim can be made.

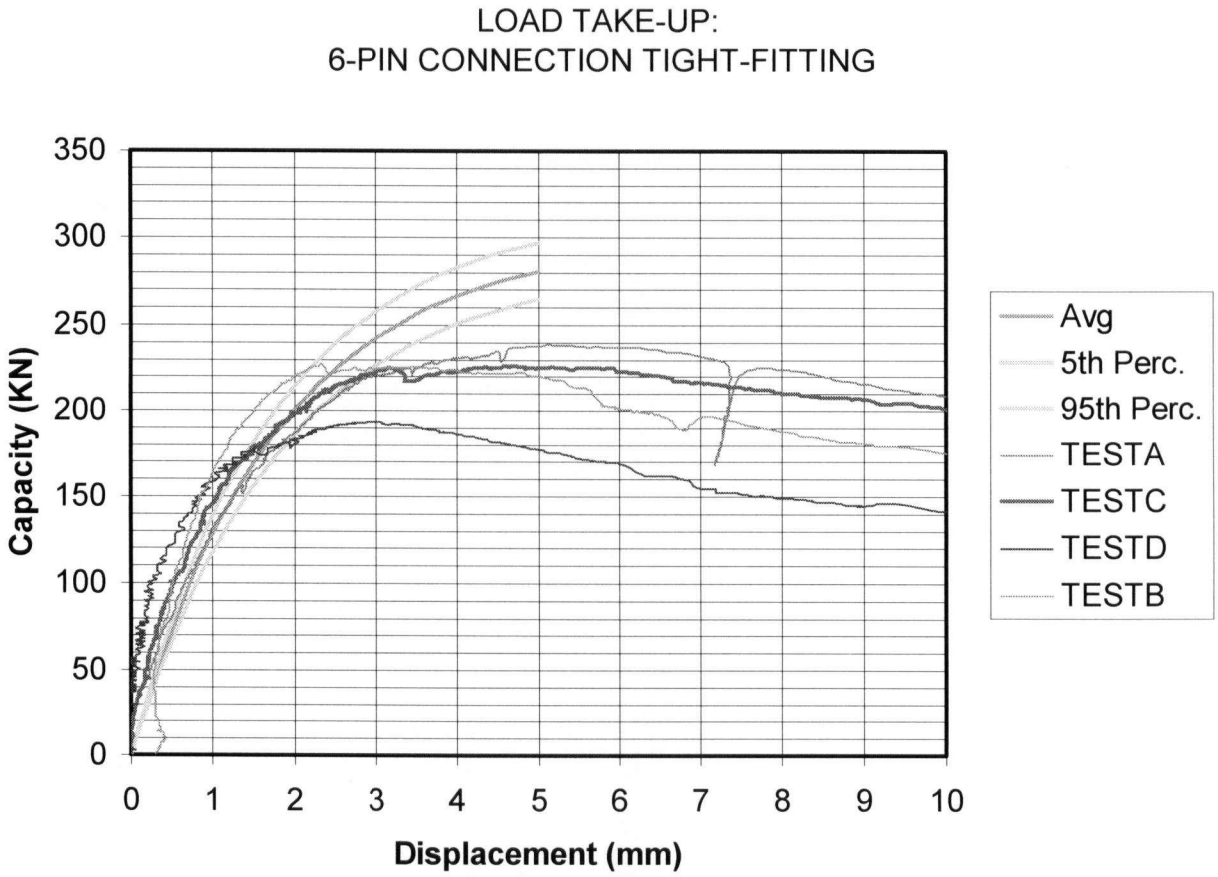

Figure 5.12 *Comparison of Load Displacement curve for the analytical model to 6-pin specimens*

5.4.3 Effect of Staggered Pins

Figure 5.13 and 5.14 show a connection of 4 spring-pins in the more conventional arrangement compared to a connection of 6 spring-pins in the staggered arrangement. Both pictures were taken after testing had taken place. The 6-pin connection had no group factors with an average load per pin of 8.1 Kips. The 4-pin connection had a group factor with an average load per pin of 7.2 Kips. Even though the 6-pin configuration had more pins, it had a less severe group factor because of the beneficial staggered configuration.

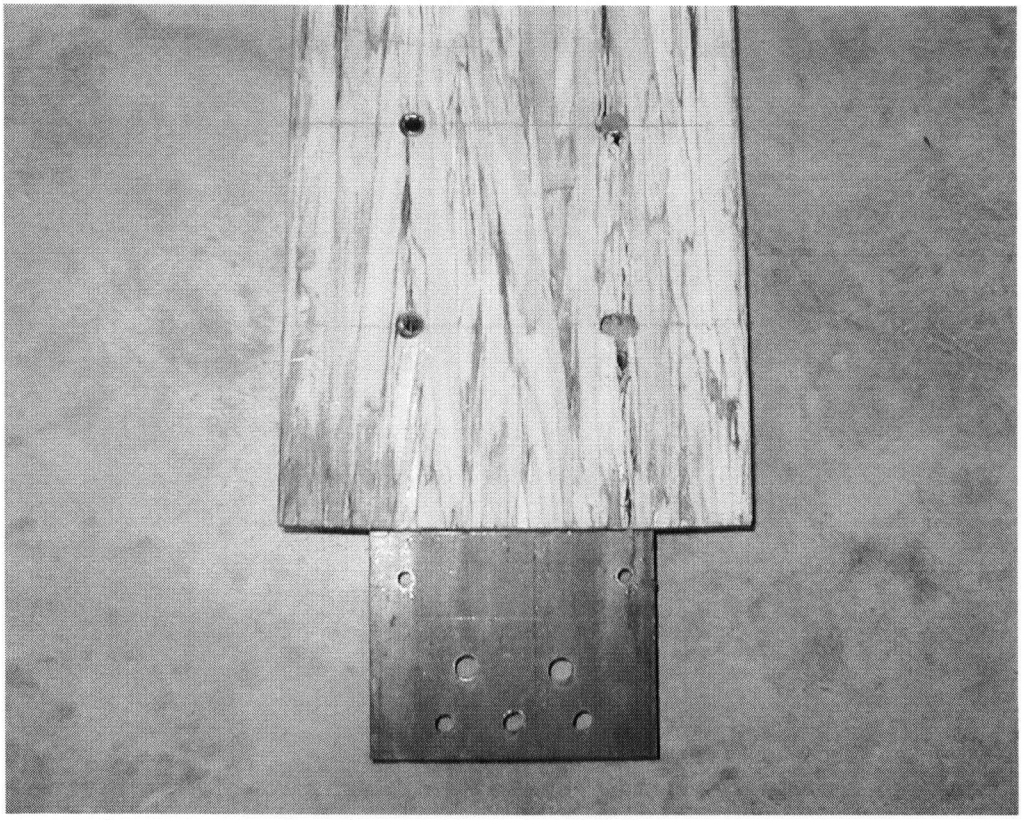

Figure 5.13 *Picture of failed connection with split along rows*

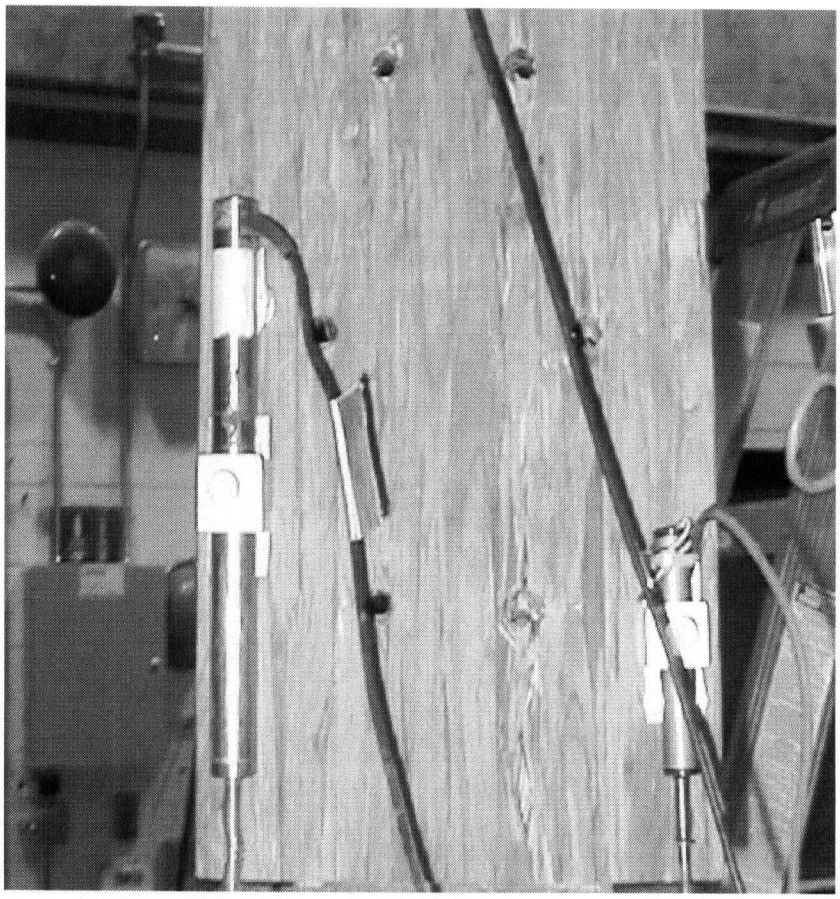

Figure 5.14 *In this connection the staggered pin is causes a split that does not interfere with the other connectors*

5.4.4 Sources of Error for Analytical Model

The analytical model is not a very robust model. One assumption that may lead to significant error is that displacement is axial only. In reality, the connection would rotate if loaded axially. This is because the connection would not be in equilibrium if the displacement is purely axial. The force distribution, not being even, would create an unbalanced moment and would rotate until equilibrium is preserved.

As discussed before, the displacement gauges can eliminate the inaccuracies due to rotation of the steel plate in its own plane. However, rotation out-of-plane is

possible with a knife-plate connection and is observed to cause inaccuracies. This information was valuable when testing the moment connections. Since, the rotational stiffness is a fundamental engineering property in the structural model it was important to change the LVDT setup to minimize this inaccuracy.

6.0 ECCENTRIC RESPONSE OF CONNECTION

Bending Strength of the spring-pin connection is not the only rotational performance characteristic of interest. As discussed in section 3.0, the structural system is highly sensitive to the rotational stiffness of the connection. If the connection is very stiff it will attract too much load and potentially fail in a brittle prematurely rather than distributing forces to other stronger elements in the system. If the connection is very flexible it will allow too much deflection in the structural system. It is very important that the response characteristics of this connection to eccentric loading are well understood.

Because the axial capacity of the connection was limited by a brittle failure mode, it follows that the brittle failure cannot be avoided during eccentric loading. To date there are no simple and generally applicable methods for determining a failure criterion for the brittle failure mode. This section does not involve the prediction of the capacity of the connection rather the stiffness and load distribution of the fasteners at failure. The approach to this problem is broken into an analytical portion for prediction of the stiffness/load distribution and a purely empirical portion for ultimately determining the eccentric load carrying capacity.

6.1 BACKGROUND

There are two main sources that were referenced with respect to eccentric/moment loading. Both are Masters dissertations from U.B.C. pertaining to the response of Glulam rivet connections. Karacabeylis thesis was submitted in 1986 and

Joel Hampson in 2003. Joel Hampson's thesis can be seen as an extension of Karacabeylis research.

6.1.1 Karacabeyli Model (1986)

Karacabeyli (1986) studied both the rivet yielding failure mode as well as the splitting failure mode in the wood. To study the non-linear response of the rivets, Karacabeyli made the following simplifying assumptions:

1. The steel rivet plate is assumed to be a rigid body with respect to the Glulam.
2. Non-linear load slip characteristics are modelled by the Foschi (1974) load slip equation
3. The Foschi parameters at an angle to grain are interpolated using the Hankinson's formula
4. The direction of the displacement is the same as the direction of load in the fastener

These assumptions reduce the problem to a non-linear system with 3 degrees-of-freedom. The 3 degrees of freedom also shown in Figure 6.1 are as follows:

1. Horizontal connection slip, Δx
2. Vertical connection slip, Δy
3. Rotational connection slip, θ

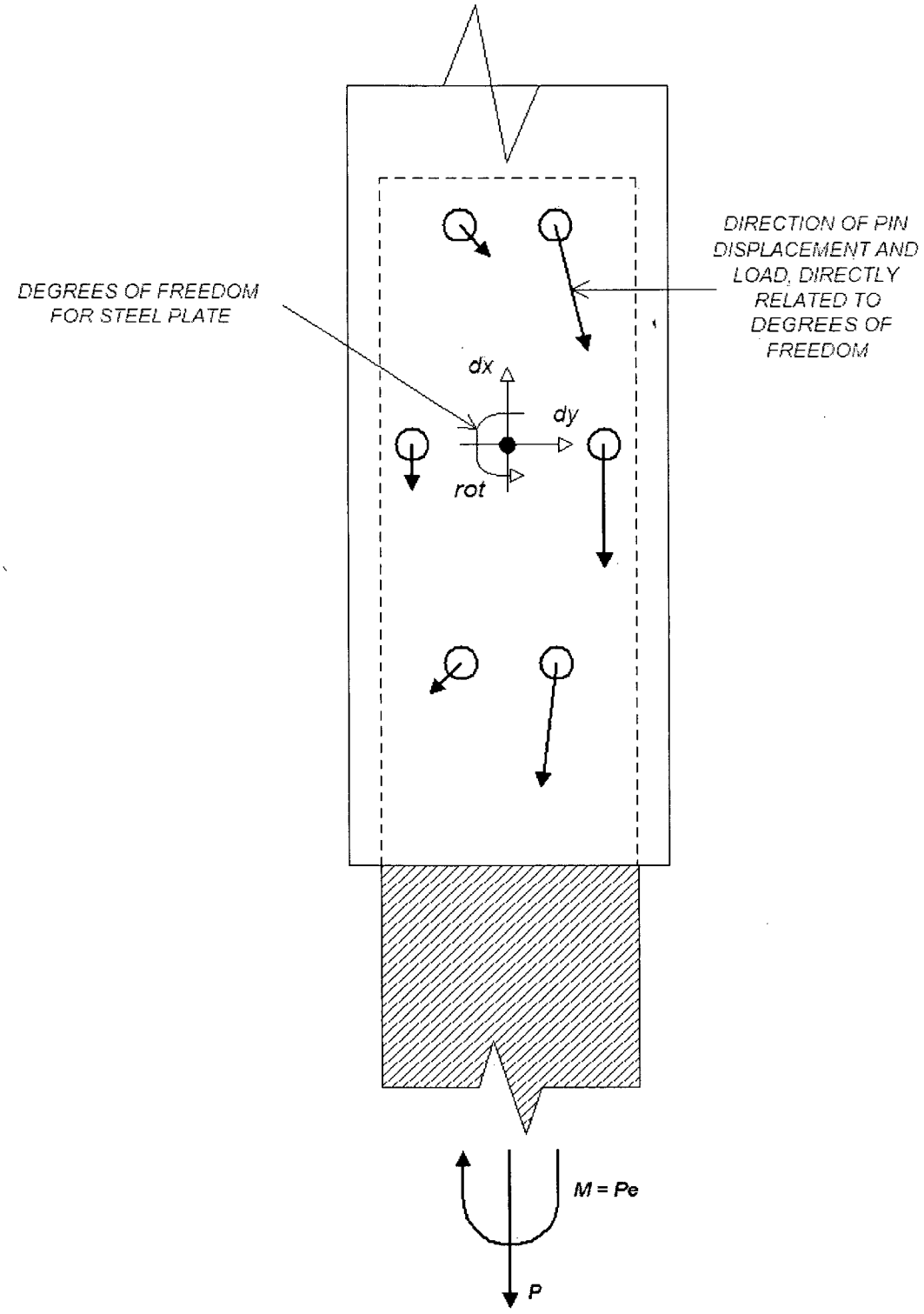

Figure 6.1 *Constitutive relationship between Degrees of Freedom and fastener displacements*

Karacabeyli's predictions strongly over-stated the initial stiffness, but had good agreement for ultimate rivet yielding capacity. The non-linear stiffness properties parallel and perpendicular to grain were taken from experiments done by Foschi (1974).

The brittle failure modes were predicted with a linear-elastic orthotropic 2-D model. The failure criterion was established by Foschi(1975). The criterion uses a 2-term weibull's weakest link model. The weibull's weakest link theory accounts for reduced strength for larger volumes of stress due to the higher likelihood of encountering a critical flaw. Three stress states were checked for failure:

- Tension Perpendicular to Grain
- Shear
- Combined Tension Perp. And Shear

The prediction of the brittle failure modes appeared to have excellent correlation to all but one of the test specimens. The one prediction that did not match up was for a rivet group in pure tension perpendicular to grain loading. It is important to note that there was only one test specimen for that particular configuration. Karacabeyli's conclusion on the brittle failure modes was to provide adequate spacing in order to avoid them. This is possible with rivets due to their high slenderness ratio.

6.1.2 Hampsen Implementation (2003)

Hampson (2003) revisited the Glulam rivet moment connection with the intention of using the results in practice. Hampson used Karacabeyli's recommendations on

connection geometry to avoid the brittle failure modes. The model is used to assess the capacity of the predictable ductile rivet yielding failure mode. Hampson used the same simplifying assumptions for his calculations. The only difference is that Hampson used different degrees of freedom. Kulak (1995) studied the non-linear response of a steel bolted connection to applied moment. The resulting design approach used the concept of an instantaneous centre of rotation, I.C.R.. The instantaneous centre of rotation, I.C.R., is the point on the steel plate that has no horizontal or vertical movement. This becomes the reference point for the displacements of the rest of the steel plate, since every other point on the plate rotates around this point. The three degrees of freedom become:

1. X-coordinate of the I.C.R
2. Y-coordinate of the I.C.R.
3. The rotation of the plate

These three degrees of freedom still have to be solved in order to determine the displacements at any point in the connection. In steel the I.C.R. can be solved by a simple equation. Unfortunately in wood the differences in stiffness perpendicular and parallel to grain complicate the simple expression. Hampson had to solve all three degrees of freedom using a stiffness matrix in the same manner as Karacabeyli. The one advantage of this format was that, during testing, Hampson could see where the I.C.R. was located and compare the location to his prediction.

Hampson's testing program involved using an actuator to load a lever arm that is attached eccentrically to the rivet plate in the Glulam specimen. The result is that the rivet plate is loaded with a large axial force and moment. All failure modes were indeed ductile. Unfortunately Hampson observed that on average the model under-stated the strength by 40%. Hampson's model uses an empirical correction factor of 1.4 to accurately predict the eccentric bearing failure mode. Hampson pointed out several potential sources of error leading to this correction factor.

1. The Hankinson's formula is known to under-predict the strength at an angle to grain by a factor of 1.3 in some cases(Moses, 2000).
2. The single fastener load-slip behaviour was determined by a test on 8 rivets. Perhaps this does not represent the single fastener response accurately
3. There were apparent discrepancies between the fit of the foschi load-slip curve to the test data for a single fastener
4. An assumption was made that the artificial lever arm and the radius to the instantaneous centre of rotation were co-linear

6.2 Load Distribution Model

The load distribution model used for this project is based on the previously mentioned work by Karacabeyli(1986) and Hampson(2003). Since Hampson's model overstated the stiffness of the moment connection, there was some concern as to the

usefulness of the model and careful attention was paid to the determination of the single fastener stiffness properties.

6.2.1 Single Fastener stiffness

The single fastener stiffness properties were found through experimental testing as discussed in section 4.0. The values are summarized again below in table 6.1.

Table 6.1 *Single pin stiffness for various directions to grain*

PARALLEL TO GRAIN COMPRESSION TEST

Parameter	Mean Value	C.O.V.	Std.Dev.	Units
K	50	12%	7.5	KN
K1	26	15%	14.7	KN/mm
K2	0	N/A	N/A	KN/mm

PERPENDICULAR TO GRAIN COMPRESSION TEST

Parameter	Mean Value	C.O.V.	Std.Dev.	Units
K	32	20%	7.5	KN
K1	37	40%	14.7	KN/mm
K2	1.7	45%	0.8	KN/mm

PERPENDICULAR TO GRAIN TENSION TEST

Parameter	Mean Value	C.O.V.	Std.Dev.	Units
K	9.5	20%	N/A	KN/mm

6.2.2 Hankinson's Formula: Stiffness at an Angle to Grain

The stiffness at an angle to grain is a function of both the perpendicular and parallel to grain stiffness. Hankinson's model was determined to interpolate between the perpendicular and parallel to grain strength to determine the bearing strength at an angle to grain. Bearing strength, however, is a state of non-linear stiffness. In steel, the yield point is quite defined and abrupt. In wood, the yield point is very gradual and is determined by "rules of thumb" to assure consistency. Therefore the Hankinson's formula can be seen as interpolating the stiffness at an angle to grain. The Hankinson's formula is modified as follows:

HANKINSON'S:

$$Nr(\theta) = \frac{\Pr Qr}{(\Pr Sin^2(\theta) + QrCos^2(\theta))} \qquad \textbf{[6.1]}$$

MODIFICATION:

$$K(\theta) = \frac{KpKq}{(KpSin^2(\theta) + KqCos^2(\theta))} \qquad \textbf{[6.2]}$$

Where,

Nr is the capacity at an angle to grain

Pr is the capacity parallel to grain

Qr is the capacity perpendicular to grain

Kp is the non-linear stiffness parallel to grain

Kq is the non-linear stiffness perpendicular to grain

Q is the angle of displacement and or load direction relative to grain

6.2.3 Spreadsheet Implementation

The Engineers at Fast + Epp favour formatted spreadsheets for calculations over dedicated programs such as MathCAD. The assumptions are made in such a manner that requires no complex integrals for calculating the constitutive model for the moment connection.

MOMENT CONNECTION ALGORITHM:

1. There are three degrees of freedom, Δx (mm), Δy (mm), and θ (radians), that are related by geometry to the direction and magnitude of displacement in each individual dowel, assuming a rigid steel connector plate (See Figure 6.1).
2. From the direction and magnitude of each fastener displacement, the force level is determined in the fastener using the Hankinson's formula.
3. Note that the perpendicular to grain stiffness is different in different directions. When the displacement is outward the tension perp. Stiffness is used, Kqt, then the displacement is inward the compression perp. Non-linear stiffness is used. The difference here is attributed to the bulging out of the wood side plate when load is applied outwards from the center of the connection.
4. Assuming that the force is in the same direction of the displacement, the internal forces of the connection are calculated by summing up the

individual fastener force components. Thus Ni (KN), Vi (KN), and Mi (KN-m) section forces are determined.

5. The user enters a set of external forces applied to the connection, Ne (KN), Ve (KN), Me (KN-m). A computer algorithm then adjusts Δx , Δy, and θ until the internal section forces are equal to the externally applied forces. The iterative algorithm employed is a Newton-rhapson search algorithm included in MS SOLVER. This program comes with every Excel program, but must be installed off the CD. The algorithm is robust and can handle non-linear problems. For a bi-linear material model the solution is insensitive to the initial inputs for this particular problem and typically results in a unique solution. If complicated load-displacement behaviour is used with multiple peaks and valleys, one might no longer expect a unique solution.

6.3 Testing Program

The intent of the testing program was to load the eccentric connections with loads that would replicate the worst case loading combination from the structural model for the façade system. Table 6.2 is a summary of the connection loading from the structural model, with the selection of 2 loading scenarios for testing.

Table 6.2 *Structural Design Loads for the connections in the arena stage facade with the highest loading demands. The location of the connection is denoted by the section of the façade and then the column or bay that it's located at.*

	MOMENT (K-ft)		AXIAL (Kips)		SHEAR (Kips)			
LOCATION	Specified	Factored	Specified	Factored	Specified	Factored	**No. Pins**	**Ecc. (in)**
Section 1: Col.4	2.1	3.2	3.8	5.7	0.9	1.4	6	6.8
Section 2: Col.1	3.2	4.8	4.6	7.0	1.2	1.8	6	8.3
Section 2: Col.1	3.9	5.9	3.9	5.9	0.8	1.3	6	12.0
Section 3: Col.2	2.3	3.5	5.0	7.5	0.6	0.8	6	5.5
Section 4: Col.1	3.6	5.4	9.6	14.4	1.4	2.1	6	4.5
Section 5: Col.1	3.7	5.6	5.6	8.4	1.3	2.0	6	7.9
Section1: Col.1	2.1	3.2	5.0	7.5	0.8	1.2	6	5.04
Section 2: Col.2	3.3	5.0	-7.3	-11.0	0.6	0.9	6	5.4
Section 3: Col.2	0.7	1.1	-2.0	-3.0	0.0	0.0	4	4.2
Section 4: Col.1	1.2	1.8	-3.2	-4.8	0.6	0.9	4	4.5
Section 5: Col.2	2.8	4.2	-5.0	-7.5	0.5	0.8	6	6.7
Section1: Bay 4	1.3	2.0	3.8	5.7	0.6	0.9	4	4.1
Section 2: Bay 2	3.0	4.5	-1.5	-2.3	1.1	1.7	6	24.0
Section 3: Bay 2	1.2	1.8	2.0	3.0	1.0	1.5	4	7.2
Section 4: Bay 2	1.2	1.8	7.5	11.3	1.6	2.4	4	1.9
Section 5: Bay 1	1.7	2.6	-1.3	-2.0	1.0	1.5	4	15.2

Critical Connections
Test Specimen Loading

6.3.1 Test Specimen Specifiations

The connection geometry chosen was staggered the same as that tested for the 6-pin axial test (See Figure 5.10). The 4-pin connection is also staggered, and has the same geometry as the 6-pin connection with the 2 fasteners farthest from the end of the member removed (see Figure 6.2 and Figure 6.3).

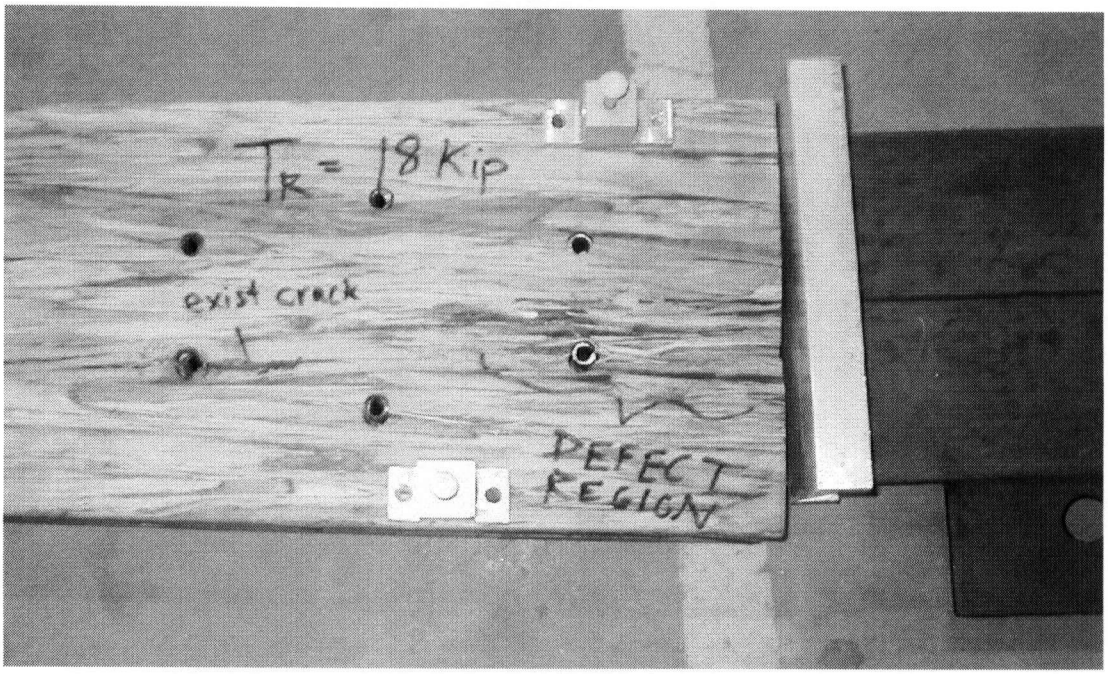

Figure 6.2 *Failed 6-pin specimen with 5" eccentricity*

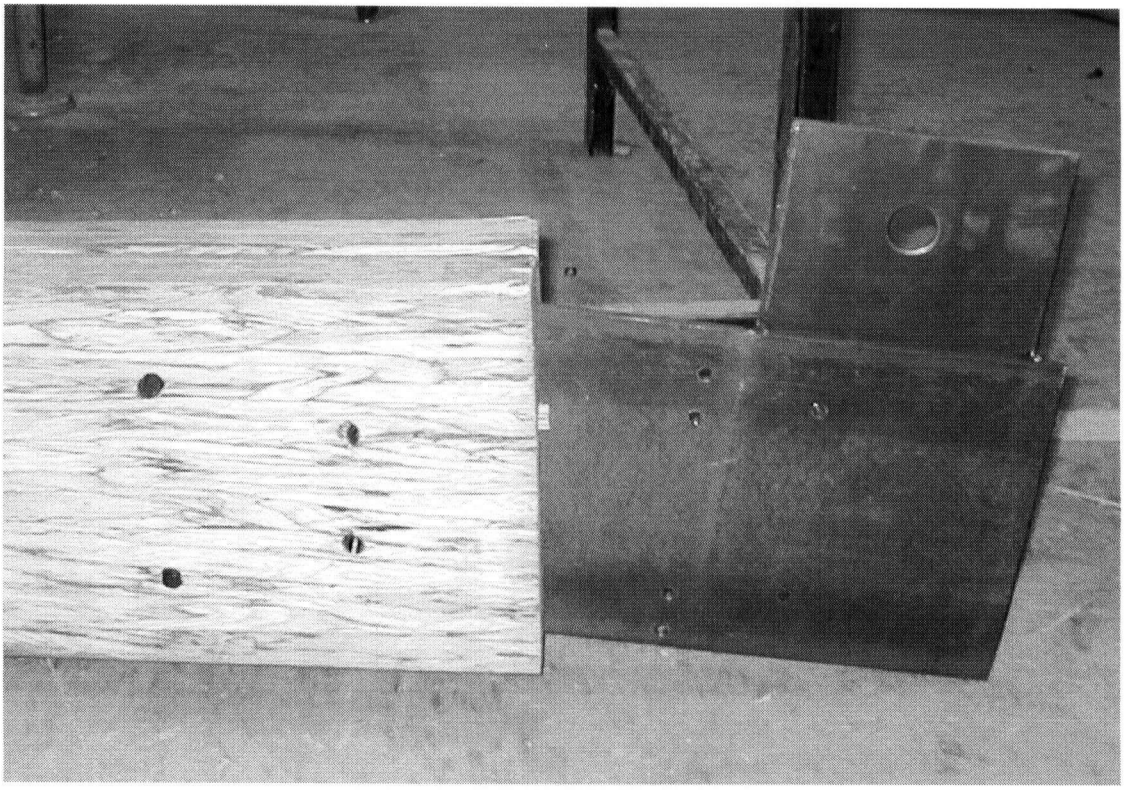

Figure 6.3 *Failed 4-pin Specimen with 8" eccentricity*

6.3.2 Test Setup and Procedure

The specimens were tested in a similar manner to the axial connections. The load rate was typically between 5 and 10 minutes until peak load occurs. The specimens were tested past peak load to study the post failure behaviour and ductility. Specimens were typically tested until the LVDT devices slipped off the gauge stoppers due to the visibly large rotations reached after failure.

The setup of the displacement gauges were altered after observing that a number of load-displacement curves did not make rational sense. The appendix of this report goes into detail on how the displacement gauges were setup and what caused the erroneous information.

6.4 RESULTS AND DISCUSSION

All specimens were observed to split at or slightly below their peak load. The dominant mode of failure was splitting with an occasional shear plug in combination with splitting. All specimens had a considerable post peak load response.

The information needed from the testing program is for three purposes. Strength or resistance to bending forces is of course needed. Of equal importance is the rotational stiffness of the connections. The stiffness at serviceability load levels and factored design load levels are equally important to the structural system.

Validation of the estimation of rotational behaviour is also of interest. The model is only adequate for estimating the capacity of moment connections that fail in an exclusively bearing failure. If splitting is present, as is expected to be the case with parallam connections, then the model can only be used to predict strength over a specific range of geometry.

6.4.1 Strength Properties

The strengths of the specimens are summarized in Table 6.3 and Table 6.4. The strength is characterized as the peak load carried by the connection, or the load at a rotation of 2 degrees (typically 4mm of displacement for a pin to achieve this rotation).

TABLE 6.3 Capacity of Eccentric Connection

Connection	Loading	Average (KN)	Std.Deviation (KN)	C.O.V. (%)	5^{th} Percentile (KN) $P_{0.05}$	$\phi*Kd*P_{0.05}$ (KN)
4-PIN	8" ecc.	45	8	18	31	20
6-PIN	5" ecc.	88	8.8	10	74	48
6-PIN	8" ecc.	53	6.2	11	45	28

The difference between studying an axial connection and a moment connection is that the *expected* load in each individual fastener is different. In an eccentric connection there is one fastener that carries the most force. To complicate things further, each fastener carries load at different angles to grain. The distribution of forces on the fasteners and the direction to grain is a function of the connection geometry, the eccentricity of the connection, and the relative stiffness of the fastener in different directions. To simplify the problem, the analytical model can determine the force level and angle to grain in the most critical fastener. A more fundamental description of strength can then be determined and with sound engineering judgement, be applied to different connection geometries with reasonably similar specifications. Figure 6.5 below graphically illustrates the level of forces present in the 6-pin test specimen subjected to a 5" eccentricity.

Comparing these forces to the typical failure mode of the 6-pin moment connection, it becomes apparent that the critical pin is causing a premature splitting due to the large angle to grain component of the critical pin force. Figure 6.4 shows the failure mode of the 6-pin moment connection subjected to a 5" eccentricity. Notice how splitting occurs adjacent to the most highly loaded pins.

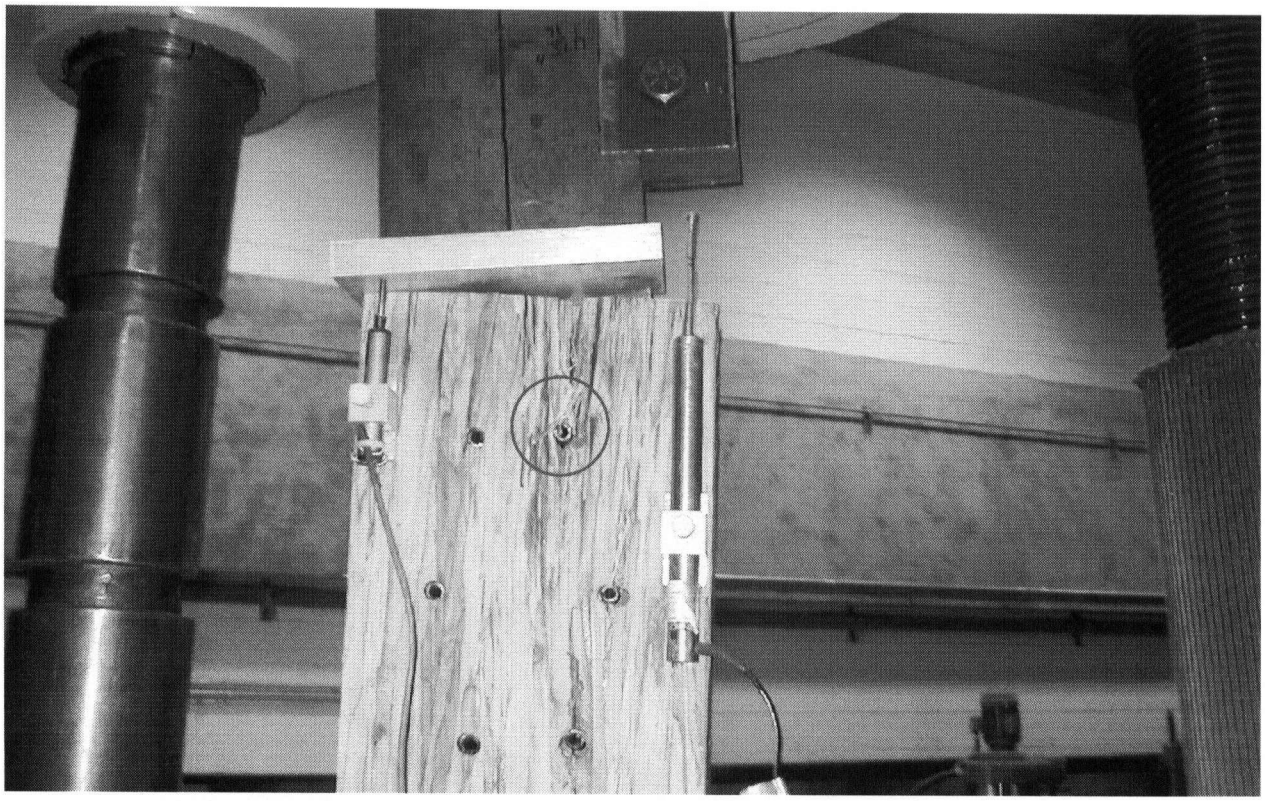

Figure 6.4 *6-pin 5" eccentric connection at failure*

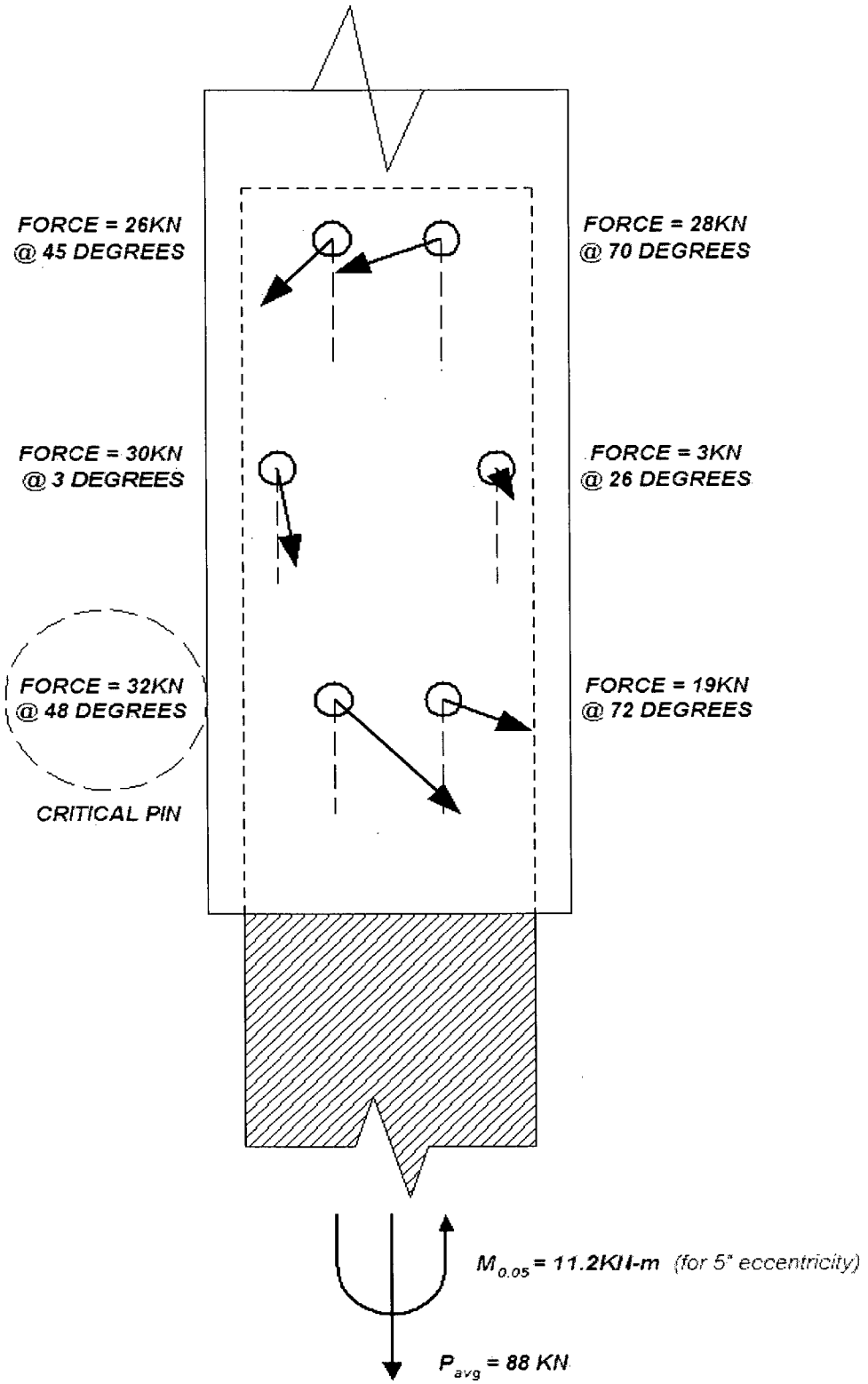

Figure 6.5 *Predicted peak fastener forces present in 6-pin test specimen with a 5" eccentricity. The force applied is the average capacity of the test specimen.*

The analytical model was used to estimate the state of force in the critical fastener of each type of test specimen, and the results are summarized in Table 6.4.

TABLE 6.4 *Highest Load level in the critical pin at failure.*

Connection	Loading	Average (KN)	5^{th} Percentile (KN) $P_{0.05}$	$\phi*Kd*P_{0.05}$ (KN)	Angle to Grain (degree)
4-PIN	8" ecc.	41	29	16	36
6-PIN	5" ecc.	32	27	15.2	45
6-PIN	8" ecc.	28	23	12.8	53

This number can be considered the resistance of a pin under moment loading conditions. Load demands on a pin are determined from the non-linear spreadsheet. A linear spreadsheet would give more severe load demands on the pin for the same combination of connection loads. The non-linearity has the effect of distributing the forces to the other pins when the critical pins approach capacity.

To put these numbers in perspective, the design resistance of a single pin in an axial connection (from Section 5.0) is 22 KN. Comparing this to the design resistance of a single pin in a moment connection, It is apparent that the single pin in the moment connection is reduced by between 10-30% depending on the configuration. The design resistance of a single pin drops significantly with increasing angle to grain of loading on the critical pin.

6.4.2 Simplified Design Approach

In consulting practice, structural systems will undergo several changes throughout the design process and an efficient approach is essential. A simplified design approach can be used in combination with good engineering judgement.

The mechanics inherent in the timber moment connection are similar to a single story building with a rigid diaphragm in which the shearwalls are the fasteners. If we make the following assumptions the calculation can be made with very little computational effort.

The axial force is distributed evenly amongst the fasteners.

$$f = \frac{N}{n_{fasteners}} \qquad \textbf{[6.3]}$$

The moment is distributed to the fastener couple reactions according to their stiffness. For the 6-pin moment connection, it can be assumed that there are two couple reactions, 1 parallel to grain and 1 perpendicular to grain.

$$f_{mi} = \frac{K_i d_i M}{\sum K_i d_i^{\,2}} \qquad \textbf{[6.4]}$$

The force in a given fastener is the vector addition of parallel to grain components and perpendicular to grain components

$$f_i = f_p + f_q \qquad \textbf{[6.5]}$$

And the angle to grain of the force is found from the angle between f_p and f_q

$$\vartheta = Tan^{-1}(f_q / f_p) \qquad \textbf{[6.6]}$$

For the 6-pin moment connections the critical pin is part of the perpendicular to grain couple. The perpendicular to grain couple is more than twice the stiffness of the parallel to grain couple due to the large leverage between the pairs of fasteners at the front and back of the specimen. As an example, the forces on the critical fastener can be approximated as,

$$f_n = 88KN/6 = 14.7KN$$

$$f_{mi} = \frac{11.2KN \cdot m \cdot 73\%}{0.2m} = 41KN \quad \textit{per pair of fasteners perpendicular to grain}$$

$$f_{mi} = \frac{11.2KN \cdot m \cdot 9\%}{0.064m} = 15.8KN \quad \textit{per pair parallel to grain}$$

$$f_p = 14.7 + 15.8/2 = 22.6KN$$

$$f_q = 41KN \cdot \frac{K_{qc}}{(K_{qc} + K_{qt})} = 26KN$$

where fqc and fqt are the perpendicular to grain stiffness inwards and outwards respectively. Adding the parallel and perpendicular to grain components together we get,

f_i = *35KN at an angle of 49 degrees to the grain*

The simplified approach results in a 10% higher force in the critical fastener than the non-linear analytical model. The difference can be attributed to the re-distribution of forces as the critical fastener loses stiffness as it approaches capacity. The simplified approach is not significantly different from the non-linear model suggesting that there is not much non-linear behaviour in the fasteners before splitting occurs.

The simplified approach is surprisingly close to predicting the behaviour of the connection and, if in error, it is a conservative method for determining fastener demands.

6.4.3 Load Carrying Behaviour

The moment vrs rotation curve for the eccentric specimens is similar to the force vrs displacement curves for the axial test specimens. The response is mildly non-linear until splitting occurs. For most specimens the load was still held, and sometimes increased after splitting. One of the 4-pin specimens held its load, and continued to increase in load carrying capacity up to about 8 degrees of rotation. A picture of the

deformation of this connection can be seen in Figure 6.3, and its associated load displacement graph is in Figure 6.4.

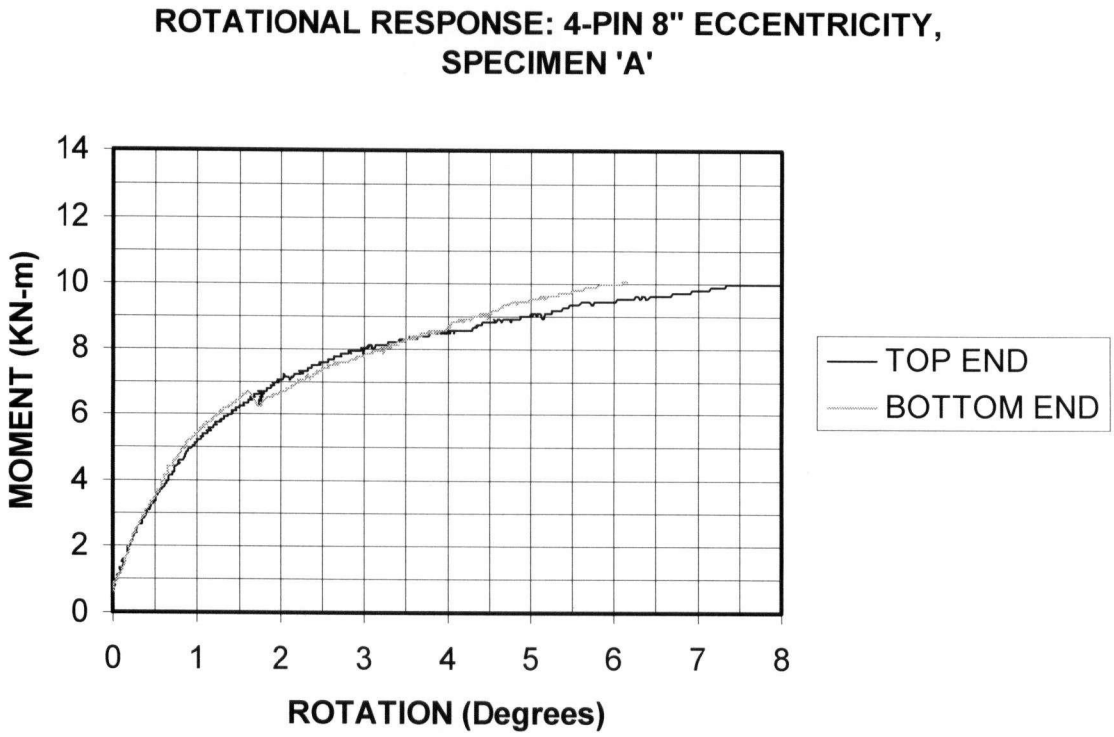

Figure 6.6 *Rotational response of 4-pin connection with an 8" eccentricity. Splitting was perceived at between 6 and 7 KN-m, but the load increased well beyond this value.*

The 4-pin connection specimens were generally more ductile than the 6-pin connections due to the less leverage causing tension perpendicular to grain stress, Figure 6.5 shows the large non-linear portion of the connection response. The added leverage to the 6-pin connection caused an increased stiffness and strength, but a more explosive failure mode. However, many of the fasteners in the 6-pin connection were bent. It is interesting to note that fewer fasteners were

bent in the pure axial tests. The fasteners tended to rotate about the knife plate at failure, whereas the fasteners were sometimes bent in the eccentric connections.

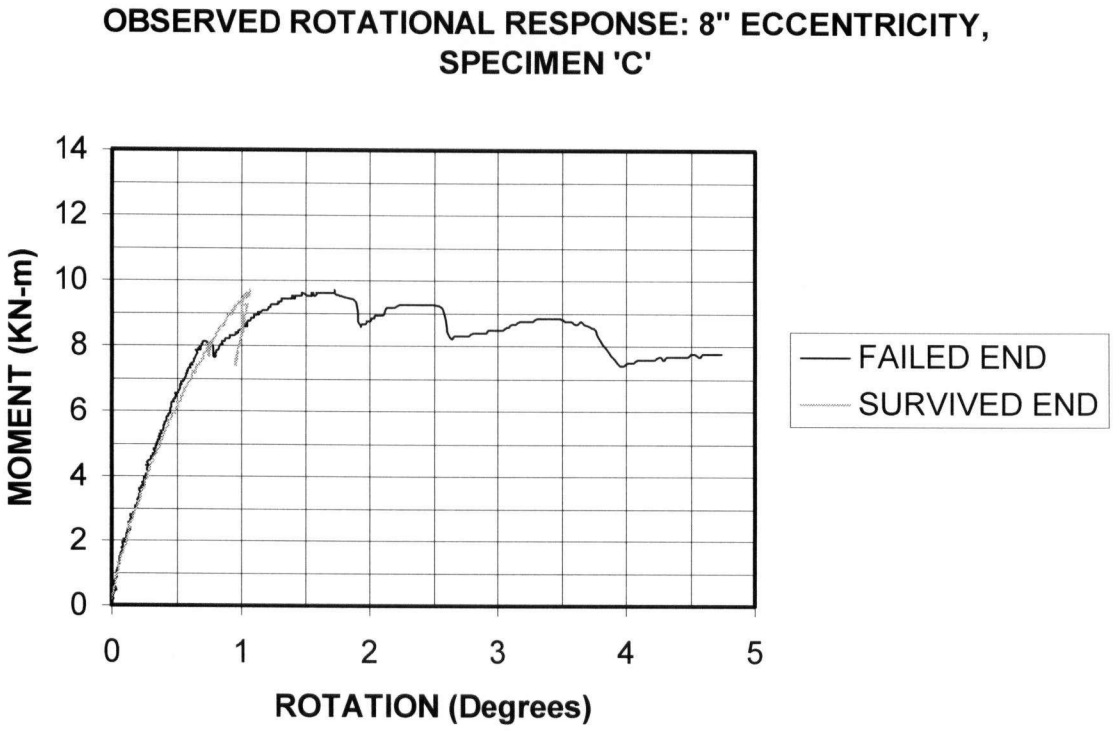

Figure 6.7 *Rotational response of 6-pin connection subjected to an 8" eccentricity*

Figure 6.7 shows a 6-pin connection curve. Note that only 1 side of the connection failed in this test, black. The red side depicts a connection that did not fail, and as the load backed off a portion of the unloading curve was produced. The failed end reached full capacity and then began to drop slowly as cracks were formed in the connection zone. The moment capacity is more than 70% of full capacity after 4 degrees of rotation. The arena stage façade will impose rotations of 0.5 degrees or less.

Figure 6.6 shows a 6-pin connection subjected to a 5" eccentricity. The 5" eccentricity resulted in a similar response as the 8" eccentricity. Failure due to splitting was observed at 12 KN-m of moment, connection holds it's load above 11KN-m for up to 5 degrees of rotation.

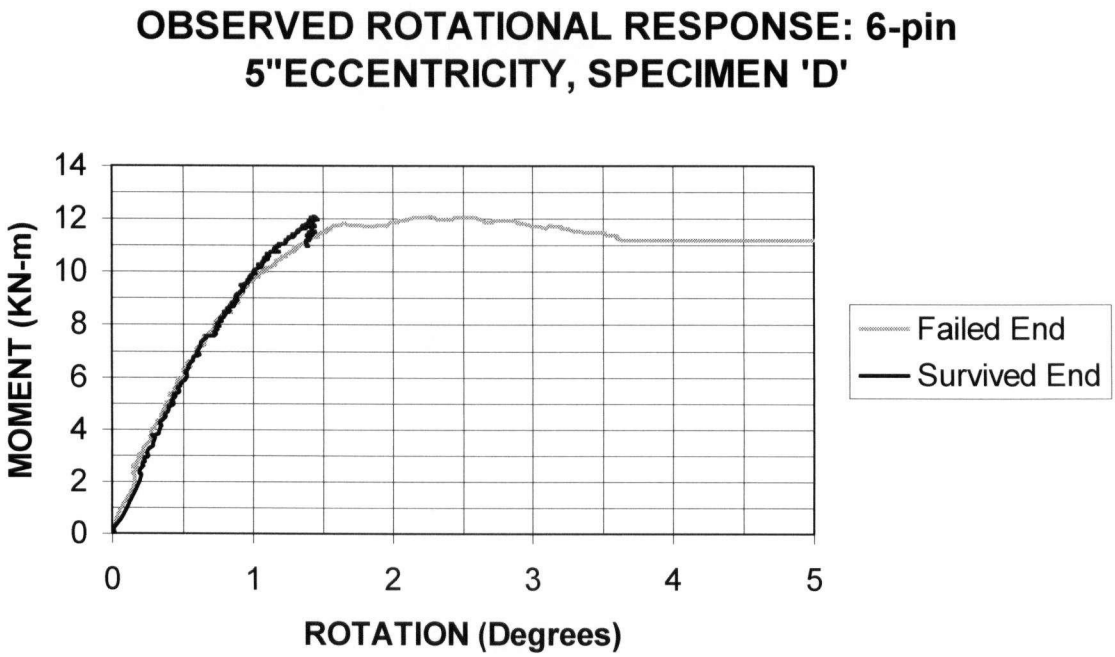

Figure 6.8 *Rotational response of 6-pin connection subjected to a 5" eccentricity. The connection forms a hinge while maintaining the loads imposed on it.*

6.4.4 Comparison to Analytical Model

The prediction of the moment-curvature response of the connection in general lost accuracy with increasing rotation. The model did not make any attempt to predict the onset or effect of splitting in the connection, and showed reasonable accuracy before splitting occurs.

Figure 6.9 compares the prediction to the response of the 4-pin subjected to an 8" eccentricity. The prediction is observed to be a lower bound for the initial stiffness of the connection. However, after about a ½ degree of rotation 2 specimens cross the prediction line and the prediction begins to overstate the stiffness.

The response curves for the 6-pin connections tell a similar story about the accuracy of the prediction (See Figure 6.10 and 6.11). However, the model begins to overstate the stiffness earlier on. At about ¼ degree of rotation, after that point the model is merely an upper bound to the connection response.

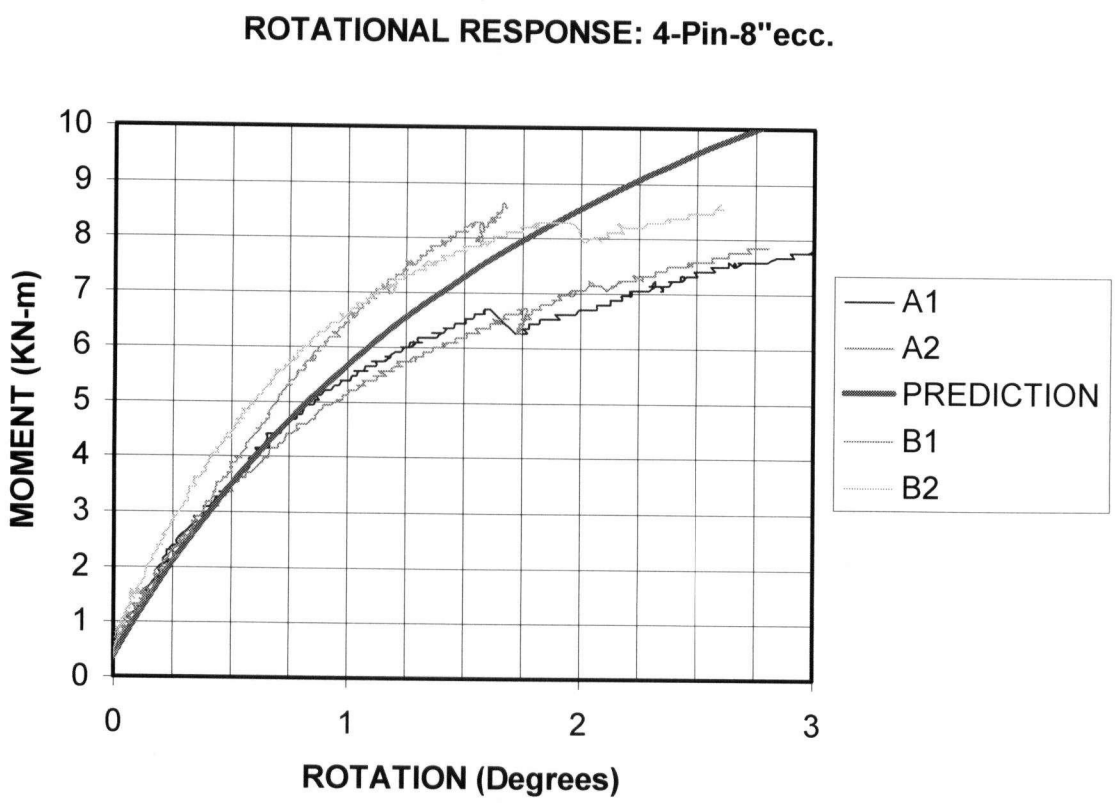

Figure 6.4 *Comparison of the prediction to the 4-pin test*

Note,

A1 is side 1 of specimen A

A2 is side 2 of specimen A

B1 is side 1 of specimen B

B2 is side 2 of specimen B

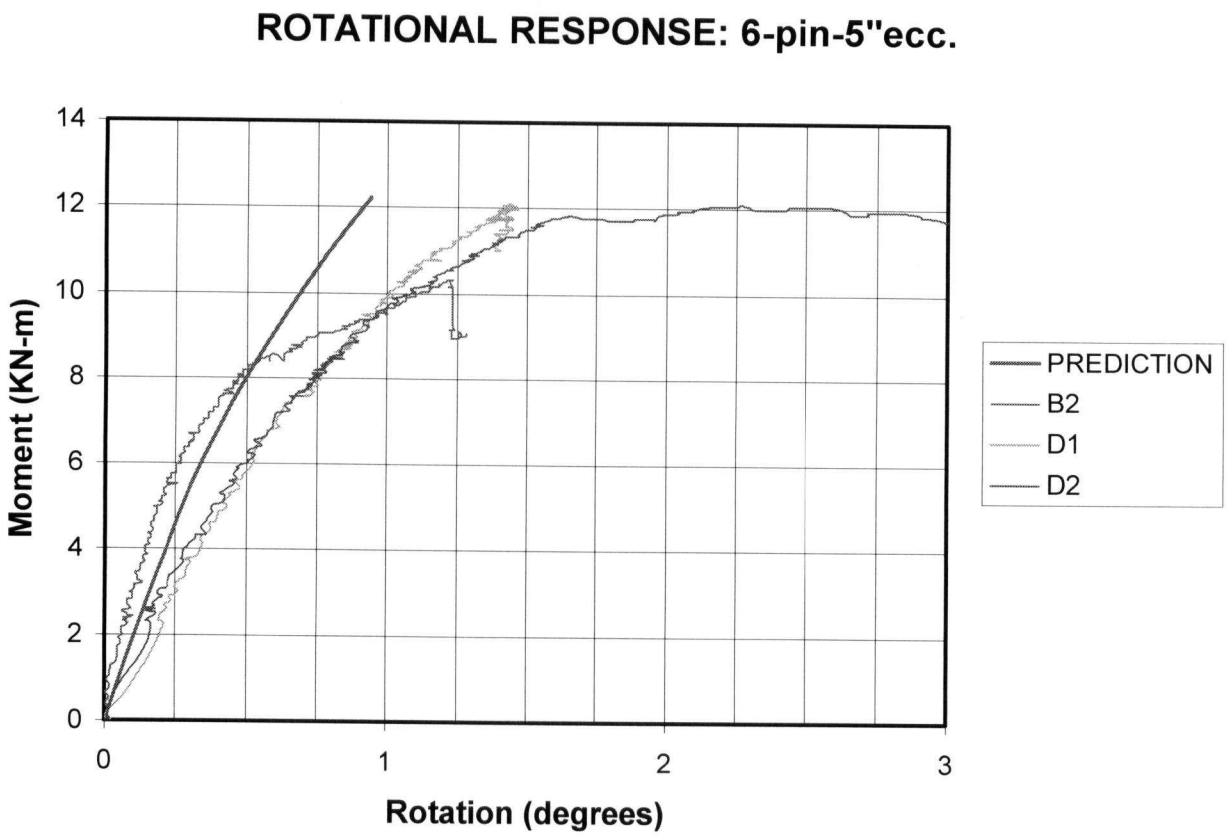

Figure 6.10 *Comparison of the prediction to the 6-pin test with 5" eccentricity*

B2 is side 2 of specimen B

D1 is side 1 of specimen D

D2 is side 2 of specimen D

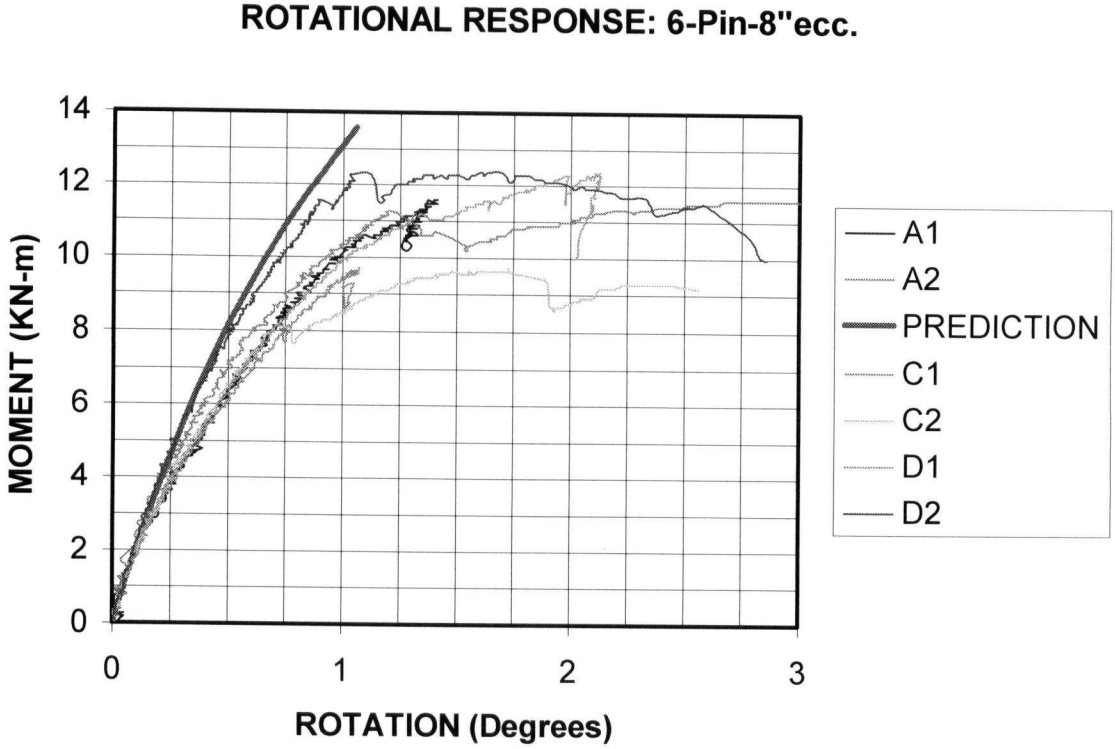

Figure 6.11 *Comparison of the prediction 6-pin test with 8" eccentricity*

A1 is side 1 of specimen A

A2 is side 2 of specimen A

C1 is side 1 of specimen C

C2 is side 2 of specimen C

D1 is side 1 of specimen D

D2 is side 2 of specimen D

6.4.5 Stiffness Properties

The average stiffness parameters for the 4-pin 8" eccentricity connection are as follows in Table 6.4. The initial stiffness is important for serviceability requirements, whereas the tangent stiffness may be important for determining the moment demands on connections in a structural system.

Table 6.5 *Rotation Stiffness Results*

Connection Configuration	**Initial Stiffness (KN-m/deg.)**	**Initial Stiffness (Kip-ft/deg.)**	**Stiffness at 1/2 deg. Rotation (KN-m/deg.)**	**Stiffness at 1/2 deg. Rotation (Kip-ft/deg.)**
4-pin 8" ecc.	9	6.6	7.5	5.5
6-pin 5" ecc.	17.5	12.9	13	9.6
6-pin 8" ecc.	16	11.8	12.5	9.2
6-pin avg.	16.75	12.3	12.75	9.4

It was observed that the stiffness parameter for the 6-pin connection was very similar whether the eccentricity was 5" or 8". Therefore the average of the two configurations is also presented as a stand alone estimation of the 6-pin connection rotational stiffness properties.

6.4.6 Sources of Error

There are several sources of error that are inherent in this type of model. The model is not robust enough to be generally applicable to all types of geometry let alone different dowel types or species of wood. The main sources of error in the model are summarized as follows:

1. The Hankinson's formula is known to under-state the bearing capacity at an angle to grain under certain conditions
2. The flexibility of the wood side plates was not studied sufficiently. The model takes in to account the flexibility of the wood side plates by testing the fastener in tension perpendicular to grain. This works for a specified edge distance, but for different edge distances the fastener stiffness is no longer correct in tension perpendicular to grain. The model also neglects the shear deformations of the wood side-plates. For long connections, such as the 6-pin connection, this effect would be more pronounced.
3. The direction of load is assumed to be in the same direction as the movement of the dowel through the wood, which is not the case if there is significant difference in stiffness perpendicular and parallel to grain as discussed in Figure 6.12.
4. The assumption that the wood side-plate and the steel connection plate are rigid results in error. The tension perpendicular to grain test shows that the stiffness is much less than in compression where there is limited distortion of the wood side plates. The incorporation of this reduced stiffness is crude and would

be better replaced and confirmed by a finite element solid model of the wood side-plate behaviour under load

5. The single fastener tests did not investigate the differences in stiffness due to the installation direction of the spring-pin. If loaded along the slit in the spring-pin, one would expect the stiffness to be less than the back of the spring-pin, which would act like a solid dowel. This is because the slit edges are the only bearing surface and would tend to "dig-in" until there is sufficient bearing area resulting in lower stiffness.

6. The measurement error of the test apparatus. Although there is some minor error in load measurement, the majority of error will come from the displacement measurement. The out-of-plane displacements inherent in a knife-plate connection have a serious impact on the measurement of displacements.

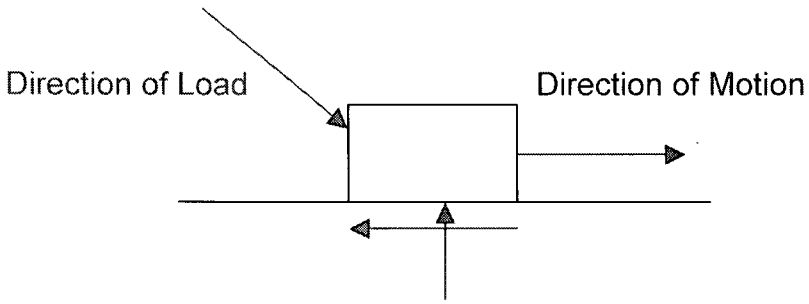

Figure 6.12 *Analogy of box sliding on a rigid surface. A dowel passing through timber with significantly different stiffness in different directions will not necessarily experience a force in the same direction.*

The implication of the assumption in Figure 6.12 for the calculation of a moment connection with timber rivets is that the force in a dowel is less than the dowel will actually experience for a given movement through the wood at an angle to grain. The direction of load will tend to be more along the parallel to grain direction and will thus be stiffer than if the load is assumed to be in the same direction as the displacement of the dowel. This is an under-statement of the force level for timber rivets because of the difference between perpendicular and parallel to grain stiffness. However, for spring-pins in Parallam, the difference in stiffness parallel and perpendicular to grain is not as severe over the initial stiffness range.

7.0 CONCLUSIONS

7.1 ARENA STAGE PROJECT

The main focus of this research into the spring-pin connections was to find the best possible solution for the proposed Arena Stage Project. The testing updated the modelling assumptions and proved that the structural system was sound. The structural system for the Arena Stage Façade is highly sensitive the rotational stiffness of the spring-pin connections. Assuming fixed connections would result in an un-conservative estimation of the façade deflections under wind loading. Assuming pinned connections would result in a structure that is inherently unstable and not possible to predict. Only in modelling the correct rotational stiffness of the connections, can a reasonable prediction of the loads and displacements of the structure be made.

7.2 AXIAL SPRING-PIN CONNECTIONS

The spring-pin connection in parallam is a consistent connection with predictable behaviour under load. The connection is not meant as a high capacity connection, such as timber rivets or other modern timber connections being merely an alternative to bolted connections. If more than 100KN of load is required, then timber rivets or other high capacity connections are considered more economic than large dowels.

7.2.1 Design Strength

The spring-pin fastener was typically 5% stronger than the prediction based on guidance from the CSA-086 design code for a single fastener, without consideration of group effects. As single fasteners, the spring-pins were virtually identical in behaviour to an A325 bolt of the same diameter. The recommendation for predicting the spring-pin connection strength would be to use the code for single fastener strength and ignore group factor as long as the guidelines for fastener geometry used are the same as the test specimens in this paper.

7.2.2 Effect of Tight Fit on Capacity

This issue was not the focus of this thesis and the test results do not offer a definitive answer. The analytical model for predicting axial connection response was useful for understanding the difference between tight-fitting dowels and loose bolts. The model appears to suggest that tight-fit will help if the connection is very brittle. Say for instance, the contractor installed the fasteners with smaller end distance than required. The tight-fit would ensure a more consistent load take-up amongst the fasteners before a wood failure occurs. The tight-fit can thereby be seen as an insurance against any unforeseen premature brittle failure mode.

7.2.3 Limitations

If more than 6 fasteners are used or if the proposed fastener geometry cannot be adhered to, or different wood materials are used then the strength values found in

Section 5.0 no longer apply. CSA-086 will provide a conservative method for predicting capacity if these requirements are not met.

7.3 ECCENTRIC CONNECTIONS

Spring-pins are a better choice of fastener than bolts for use as a moment connection, because bolt tolerances would result in significant rotations before any load is picked up. In general, timber moment connections are not a good idea because it is difficult to develop significant strength, and it is generally more economical to change the structural system altogether. For peculiar structural systems such as the arena stage façade where the moment loads are not very high, the spring-pins can be useful as a light-duty moment connection. The designer should be aware that the moment connection presented here is extremely soft and connection flexibility should be modelled when considering deflections and in most cases the load demands on the connection itself.

7.3.1 Design Strength

As mentioned before, the first step is to determine the structural moment demand on the connection. The rotational stiffness of the connection should be used in the structural model if the model as deflections will likely be a concern.

The load demands on a single fastener in a moment connection can be determined by a 3 degree-of-freedom system of equations, such as the one explored with the non-linear design spreadsheet. Alternatively the designer can predict the capacity of the moment connection with the simplified approach discussed in Section

6.0. A simplified approach will inherently result in a more conservative estimation due to the lack of non-linear load redistribution. Comparing the two approaches, it was found that a simple approach did not differ significantly from the non-linear approach.

It is also comforting to note that the eccentric connections in this study responded with a large amount of ductility and energy absorption. Even when entirely split apart, most connections held more than 80% of their peak capacity. When considering that the partial safety factor on wood connections in CSA-086 is 0.7, the connection has a large degree of redundancy and safety.

7.3.2 Recommended Rotational Stiffness

The rotational stiffness based on the spreadsheet provides a reasonable estimate of the true rotational stiffness. The stiffness at large deflections (over a degree of rotation) is overstated by the analytical model. For preliminary design the value of 10KN-m/degree for a six-pin connection should give reasonably accurate results.

7.3.3 Limitations

The strength of a single-pin in a moment connection can be estimated from table 6.4 in section 6.0. This paper did not explore connections in which the load demands on a single fastener are orientated more than 55 degrees to the grain direction. The potential for splitting is significant, not studied, and it is recommended that testing should be conducted to provide a reliable strength value.

7.4 TESTING PROCEDURES

The testing procedures used for this research departed from typical testing procedures because the specimens were twin ended as discussed in section 2.0. The use of twin ended specimens saved time during the testing phase and also saved some material fabrication. Section 2.0 rigorously determined the statistical implications of twin ended testing on the estimation of the 5^{th} percentile. The implication was only a 5% understatement of the 5^{th} percentile for specimens with a Coefficient of Variation (C.O.V.) of 10-20%. If the C.O.V. is significantly more than this, then perhaps the statistical implication is more severe.

7.4.1 Load Displacement Curve With Faulty LVDT Setup

Setting up LVDTs to measure displacements of timber knife-plate connections requires some special care and attention. Many of the load displacement curves developed for this paper were tarnished by the rotation of the knife-plate. Figure 7.1 below demonstrates the effect that these rotations had on some of the tests done for this paper.

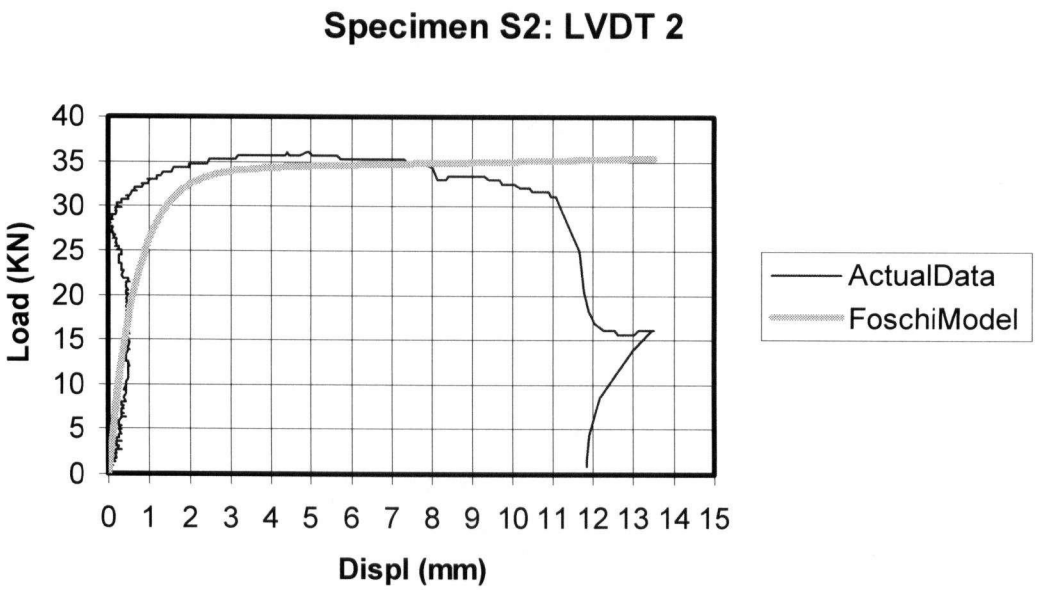

Figure 7.1 *The load displacement curve for an axial knife-plate specimen that rotated*

7.5 FURTHER RESEARCH IDEAS

There are a couple of research ideas that were not seen through to a rigorous conclusion during the course of writing this paper. With more time and budget it is possible to address the following two issues.

7.5.1 Relationship Between Tight-fit dowels and bolts

A by-product of this research was to produce a model that hints at the relationship between tight-fitting pins and loose fitting bolts. Using this simple model in conjunction with a model that also predicts the fracture behaviour of a bolted connection, perhaps it can be determined how the loose fit of a dowel affects the strength of timber connections with multiple fasteners. A paper recently published by

Quenneville, P (2006) proposes a 2-Dimensional finite element model that can predict the fracture behaviour of wood connections. This prediction also models the fastener stiffness as a spring and is therefore an ideal tool to understand the relationship of tight-fit in a timber connection.

7.5.2 Potential of high strength connection with spring-pins

Only light-duty spring-pin connections were studied in this paper. There may be a demand for higher capacity spring-pin connections with heavier timber members and more pins. A large connection with a well spaced and staggered connection may have the potential to become a less visible and costly alternative to other high capacity timber connections such as timber rivets.

Another way to increase the strength of the connection is to use multiple knife plates. This will increase the number of shear planes in the connection, so that a small diameter pin will have a reasonable L/d ratio when used in wide sections of timber. A single pin could possibly be two or three times stronger with the same ductility characteristics.

BIBLIOGRAPHY

Madsen Borg(2000), "Behaviour of Timber Connections", Timber Engineering Ltd., North Vancouver, BC, CANADA

Moses D.M., Prion H.G.L., (2000) "Constitutive and Analytical Models for Structural Composite Lumber With Applications to Bolted Connections", Ph.D. Thesis, University of British Columbia, Vancouver B.C.

Hockey Blake, Prion H.G.L.(2000)"Truss Plate Reinforced Bolted Connections in Parallel Strand Lumber", M.A.Sc. Thesis, University of British Columbia, Vancouver B.C.

Karikabeyli E., (1986)"Strength of Glulam Rivet Connections Under Eccentric Loading", M.A.Sc. Thesis, University of British Columbia, Vancouver B.C.

Hampson J., (2003), "Moment Resistant Connections Made with Timber Rivets in Wood Product Substrates", M.A.Sc. Thesis, University of British Columbia, Vancouver B.C.

Foschi, R.O. 1974. Load-Slip Characteristics of Nails. Wood Science, Vol.8, No.1, pp.69-76

Foschi, R.O. and Longworth, J. 1975. Analysis and Design of Griplam Nailed Connections. ASCE, J. Struct. Div. 101(ST12), pp.2537-2555.

Quenneville, J.H.P. and Mohammad, M. 2001. Bolted wood-steel and wood-steel-wood connections: verification of a new design approach. Canadian Journal of Civil Engineering. 28: pp.254-263

Quenneville, J.H.P and Mohammad, M. 2000. On the failure modes and strength of steel-wood-steel bolted timber connections loaded parallel to grain. Canadian Journal of Civil Engineering. 27: pp.761-773

Mischler, Adrian and Prion, Helmut and Lam, Frank. 2000. Load-carrying behaviour of steel-to-timber dowel connections. World Conference on Timber Engineering-Session 2. Whistler Resort, British Columbia, Canada.

ASTM. 1995 Standard Test Methods for Bolted Connections in Wood and Wood Based Products. Standard D5652-95

Canisius, T. 2001.Human error and quality control: Implications for design of timber structures. World Conference on Timber Engineering-Session 2. Whistler Resort, British Columbia, Canada.

Moss, Darren; McKay, Paul; Kuo, Andy; Hsu, Jack; Mui, Jeromy. 1998. The Behaviour of Multiple Bolt Connections in Parallel Strand Lumber with Claw Truss Plate Reinforcement. Unpublished Civil 321 Project Report, University of British Columbia, Dep. Of Civil Engineering, Vancouver, BC.

Mathys Levy, Mario Salvadori (1967), "Structural Design in Architecture", Prentice-Hall, Englewood Cliffs, N.J., USA

Benjamin, J. and A.Cornell, "Probability, Statistics and Decision for Civil Engineers," McGraw-Hill Inc., NY

Walpole, R., R. Myers, and S. Myers, "Probability and Statistics for Engineers and Scientists," Prentice Hall, New Jersey, 1998.

APPENDIX A

Summary of Single Pin/Bolt Tested Parallel to grain

SPECIMEN	Pu(KN)	P_4 (KN)
S1	39.4	40.5
S2	34.6	35.6
B3	37.5	37.9
B4	34.3	34.9
AVERAGE	36.5	37.2
STDEV	2.44	2.53
5th perc.	32.4	33.1
C.O.V.	7%	7%

Where Pu1 is the peak load. P4 is the load at 4mm of displacement.

Summary of Single 12.7mm dia. Pin Compression Tests Parallel to Grain

SPECIMEN	P_5(KN)
1	50
2	42
3	41
4	43
AVERAGE	44.0
STDEV	4.08
5th perc.	37.3
C.O.V.	9%

Where P5 is the load at 5mm of displacement

Summary of Single pins tested in compression perpendicular to grain
12.7mm (1/2") diameter pins

SPECIMEN	P_4(KN)
A	38
B	39.4
D	40.1
E	42.1
AVERAGE	39.9
STDEV	1.71
5th perc.	37.1
C.O.V.	4%

Where P4 is the load at 4mm displacement

Summary of Single Pin Perpendicular to Grain:
9.5mm(3/8") diameter pin

SPECIMEN	P_4(KN)
F	22.2
G	19.9
H	22.6
I	23.7
AVERAGE	22.1
STDEV	1.60
5th perc.	19.5
95th perc.	24.7
C.O.V.	7%

Where P4 is the load at 4mm of displacement

Summary of 4-Pin Tension Tests Parallel to Grain

SPEC.	Pu (KN)	Δu (mm)
A	139	3.1
B	116	2.5
avg	128	2.8
Stdev	16.3	0.4
C.O.V.	13%	15%
5th Perc.	101	2

Pu is the peak load, Δu is the displacement at peak load

Summary of 6-Pin tests parallel to grain

SPEC.	Pu (KN)	Δu (mm)
A	231	2.9
B	227	2.3
C	221	3.2
D	189	1.5
avg	217	2.5
Stdev	19.1	0.8
C.O.V.	9%	30%
5th Perc.	186	1

Pu is the peak load, Δu is the displacement at peak load

Summary of 4-pin tests with 8" eccentricity

SPEC.	P_u (Kips)
A	11.5
B	8.9
avg	10
Stdev	1.8
C.O.V.	18%
5th Perc.	7

Pu is the peak load

Summary of 6-pin connection with 8" eccentricity

SPEC.	P_u (KN)
A	58.7
B	49.4
C	46.7
D	57.9
avg	53.2
Stdev	6.0
C.O.V.	11%
5th Perc.	43

Where Pu is the peak load

Summary of 6-pin tests with 5" eccentricity

SPEC.	P_u (KN)
A	98.4
B	80.1
C	82
D	93
avg	88
Stdev	8.8
C.O.V.	10%
5th Perc.	74

Where Pu is the peak load

APPENDIX B

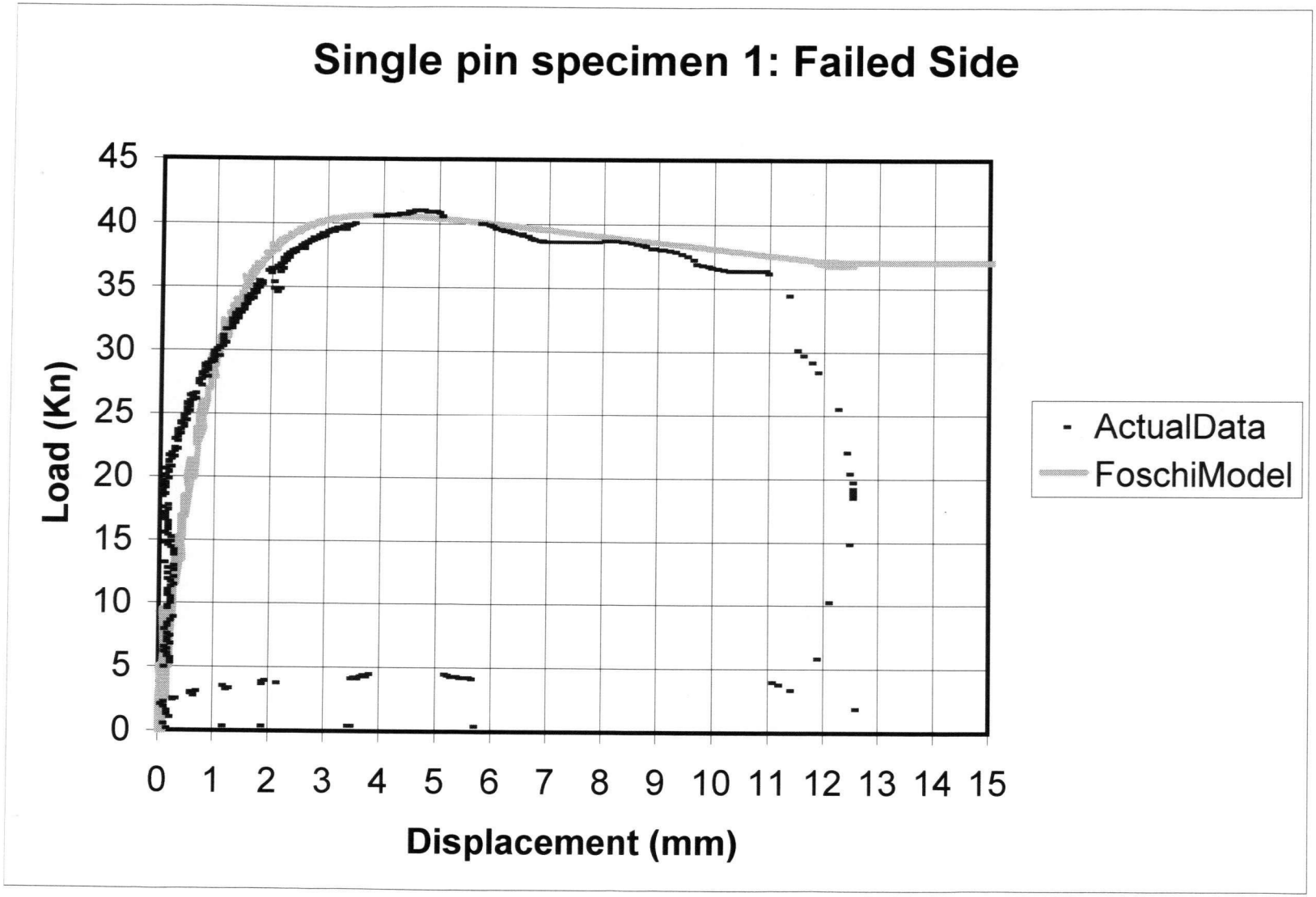
Single pin specimen 1: Failed Side
Load (Kn)
45
40
35
30
25
20
15
10
5
0
0 1 2 3 4 5 6 7 8 9 10 11 12 13 14 15
Displacement (mm)
ActualData
FoschiModel

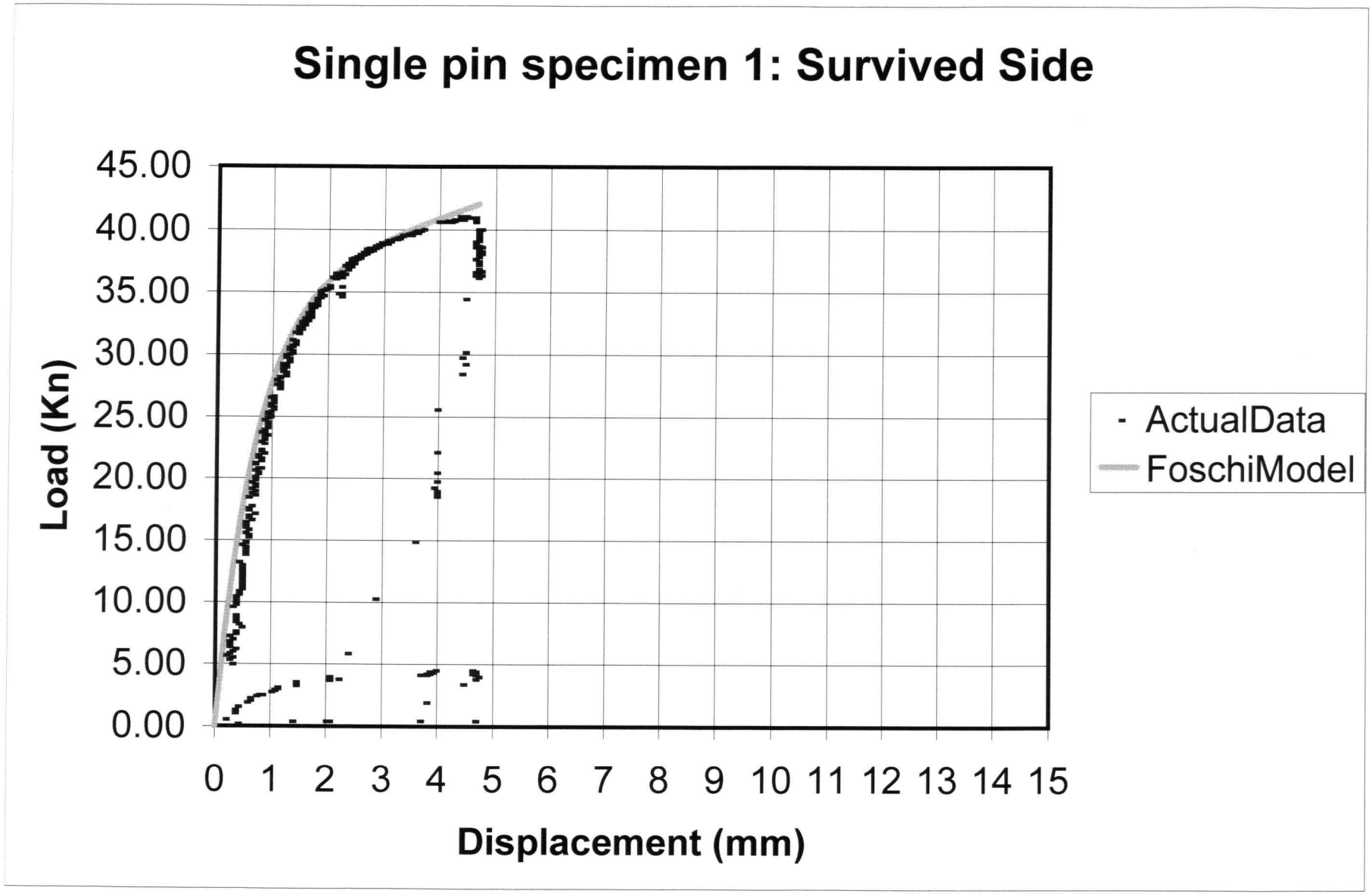
Single pin specimen 1: Survived Side
45.00
40.00
35.00
30.00
25.00
20.00
15.00
10.00
5.00
0.00
Load (Kn)
0 1 2 3 4 5 6 7 8 9 10 11 12 13 14 15
Displacement (mm)
ActualData
FoschiModel

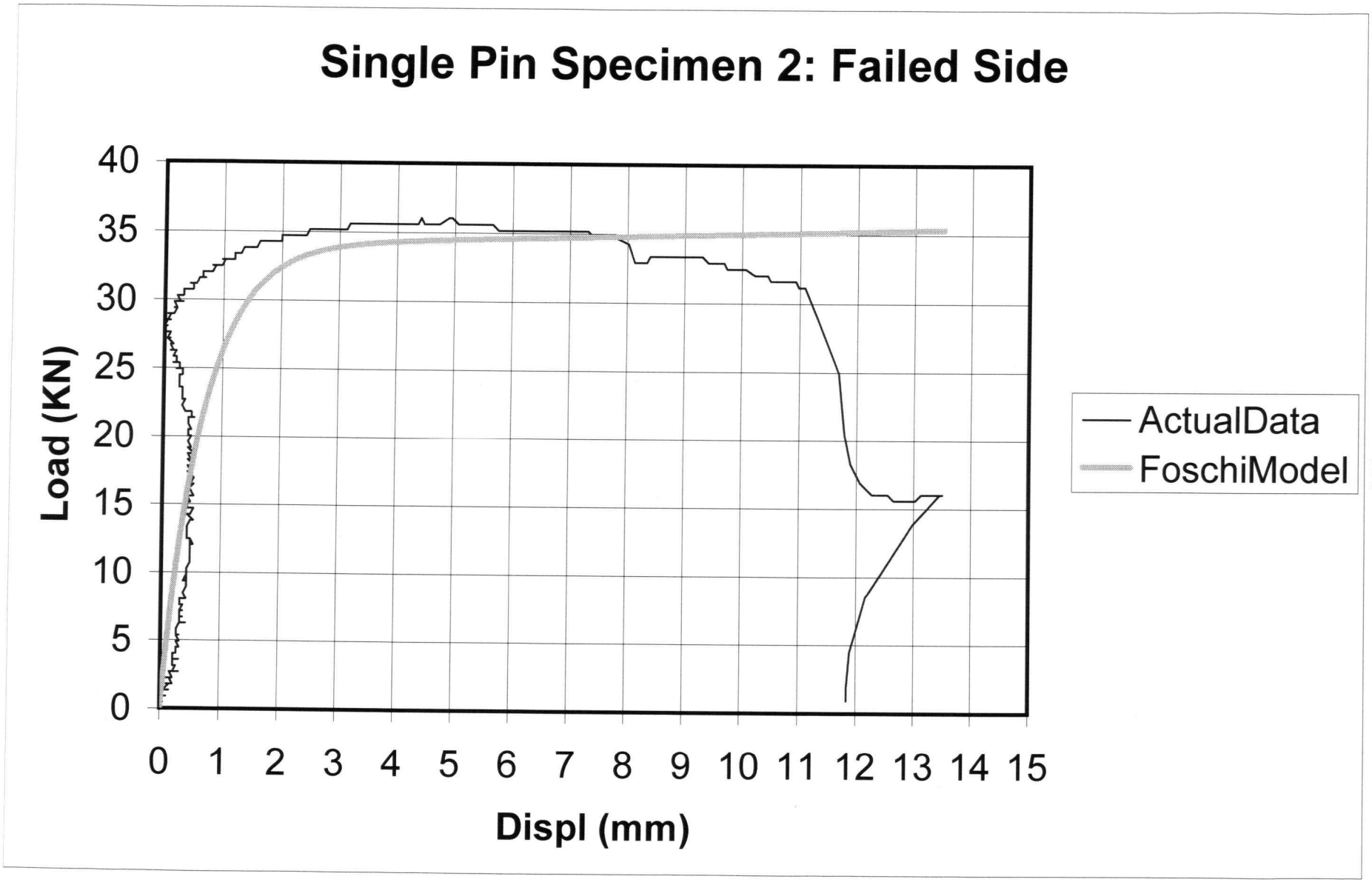
Single Pin Specimen 2: Failed Side
Load (KN)
40
35
30
25
20
15
10
5
0
0 1 2 3 4 5 6 7 8 9 10 11 12 13 14 15
Displ (mm)
ActualData
FoschiModel

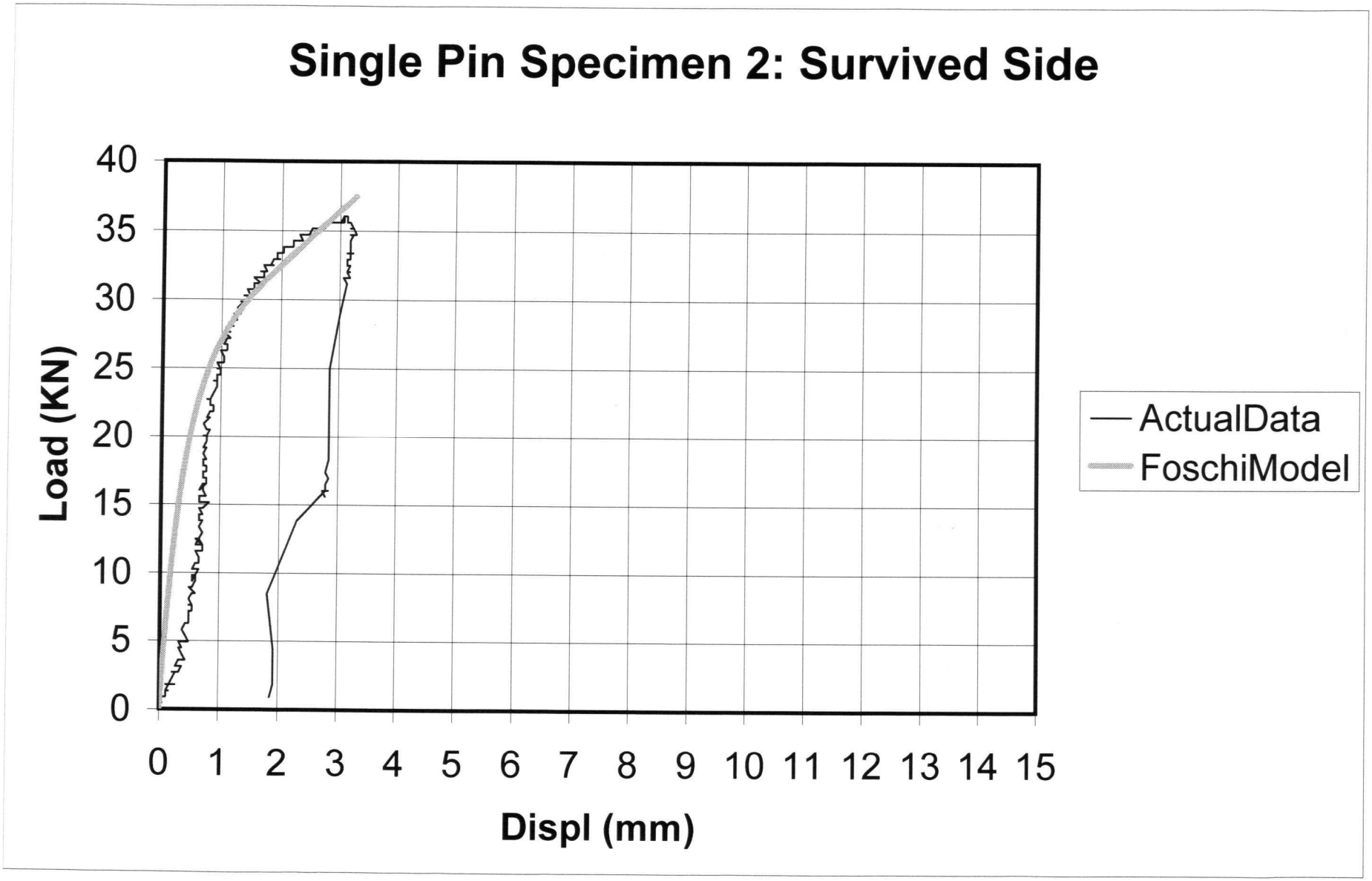
Single Pin Specimen 2: Survived Side
Load (KN)
40
35
30
25
20
15
10
5
0
0 1 2 3 4 5 6 7 8 9 10 11 12 13 14 15
Displ (mm)
ActualData
FoschiModel

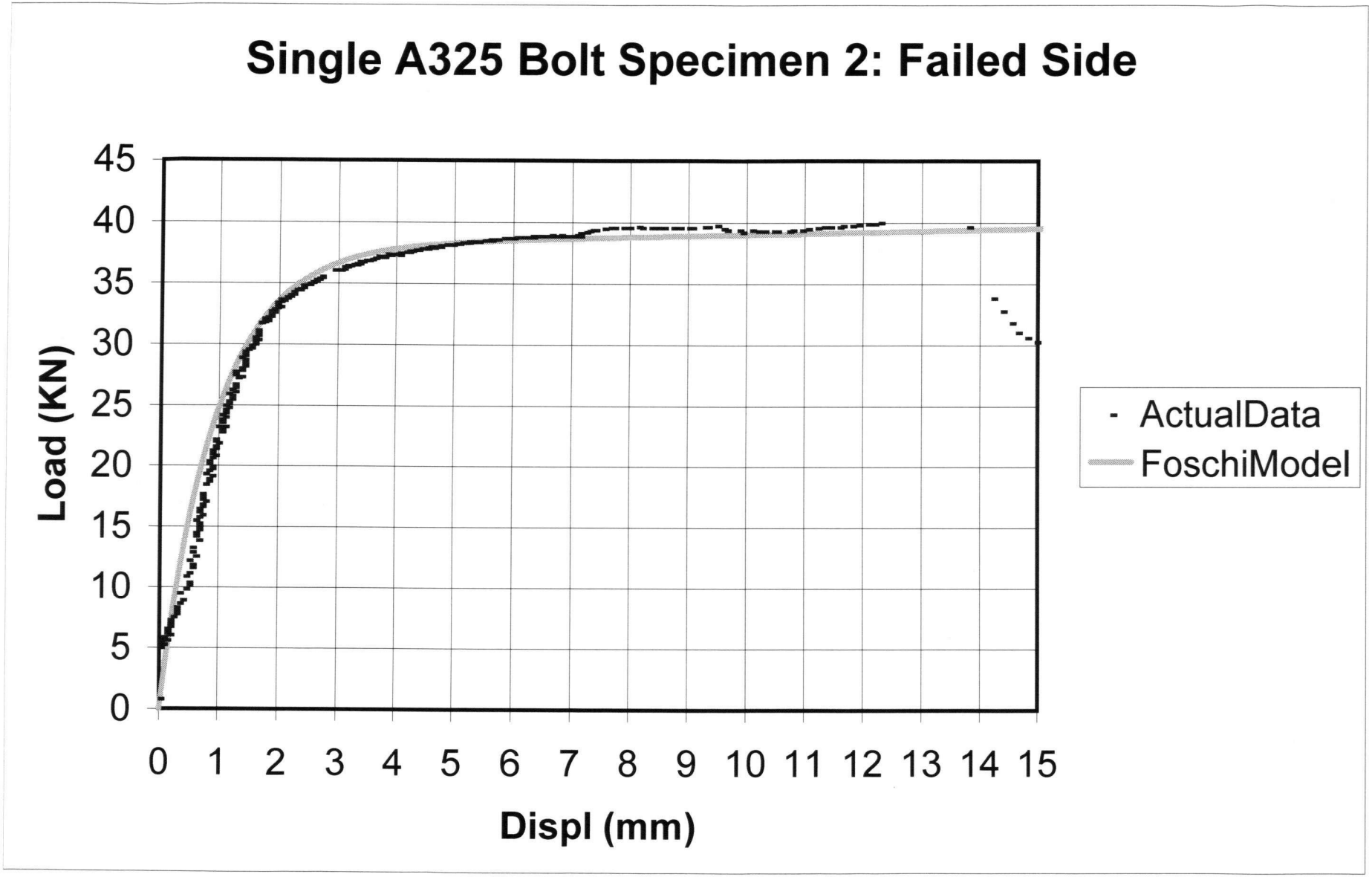
Single A325 Bolt Specimen 2: Failed Side
Load (KN)
45
40
35
30
25
20
15
10
5
0
0 1 2 3 4 5 6 7 8 9 10 11 12 13 14 15
Displ (mm)
ActualData
FoschiModel

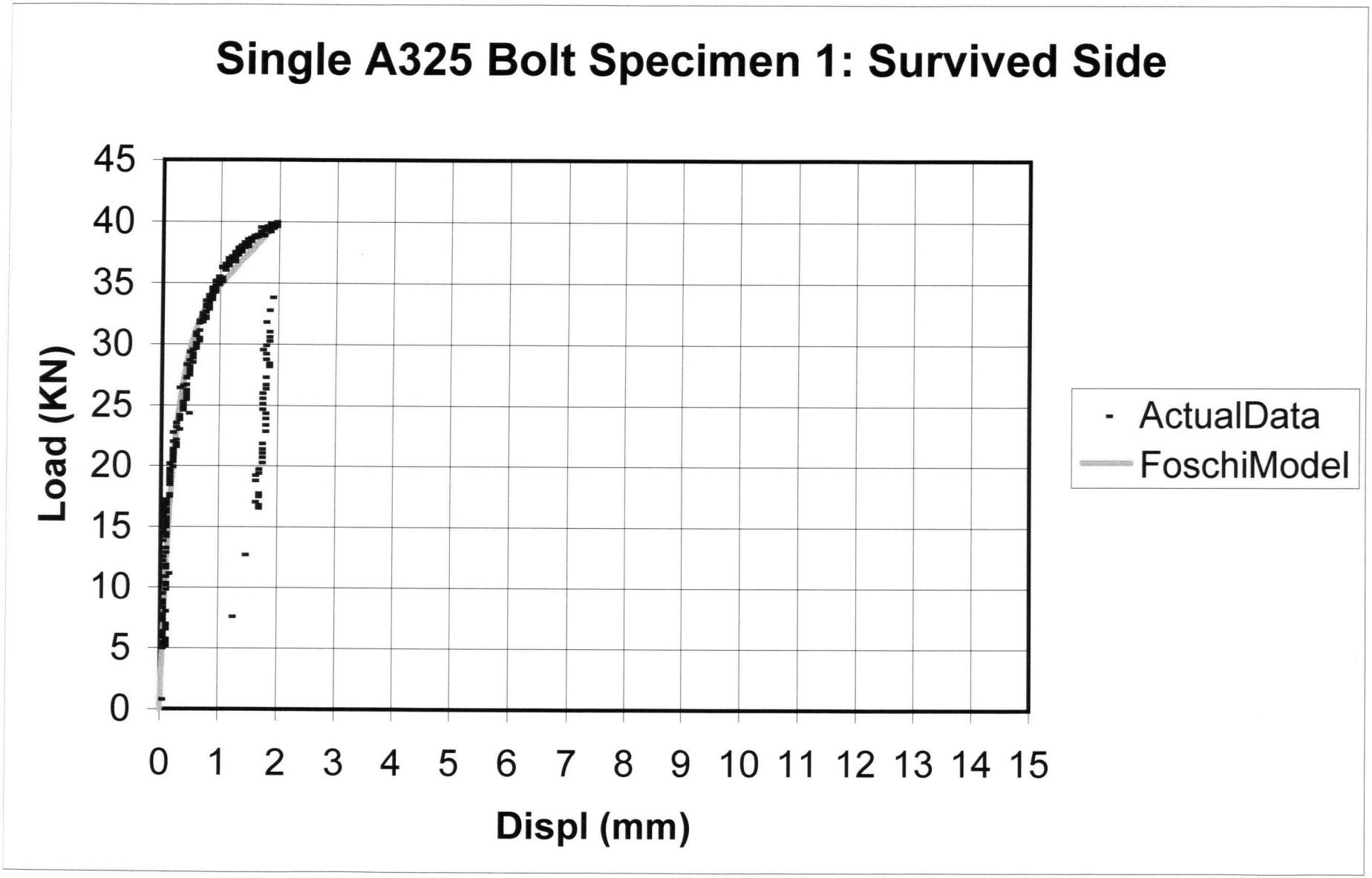
Single A325 Bolt Specimen 1: Survived Side
Load (KN)
45
40
35
30
25
20
15
10
5
0
0 1 2 3 4 5 6 7 8 9 10 11 12 13 14 15
Displ (mm)
ActualData
FoschiModel

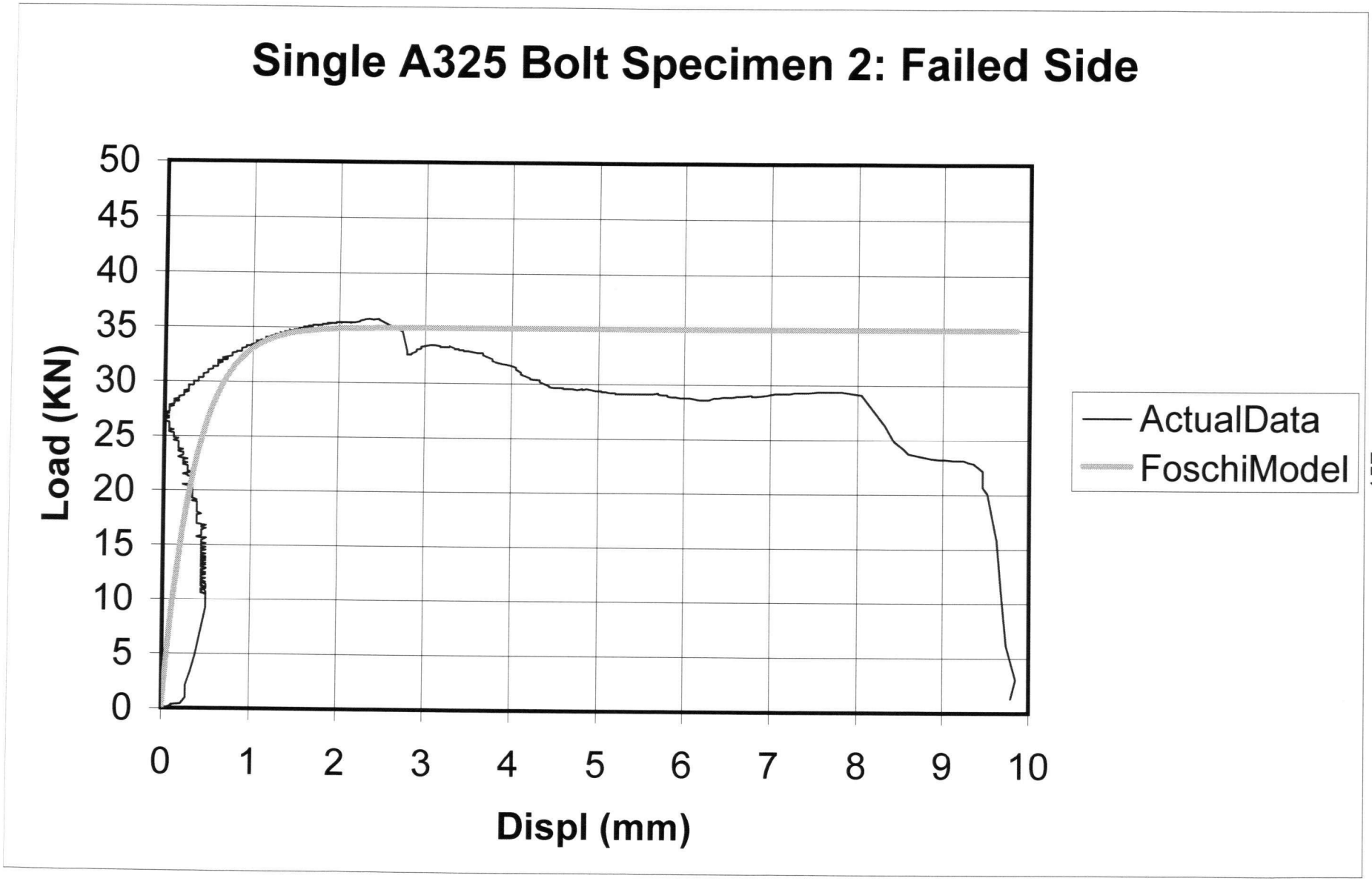
Single A325 Bolt Specimen 2: Failed Side
Load (KN)
50
45
40
35
30
25
20
15
10
5
0
0
1
2
3
4
5
6
7
8
9
10
Displ (mm)
ActualData
FoschiModel

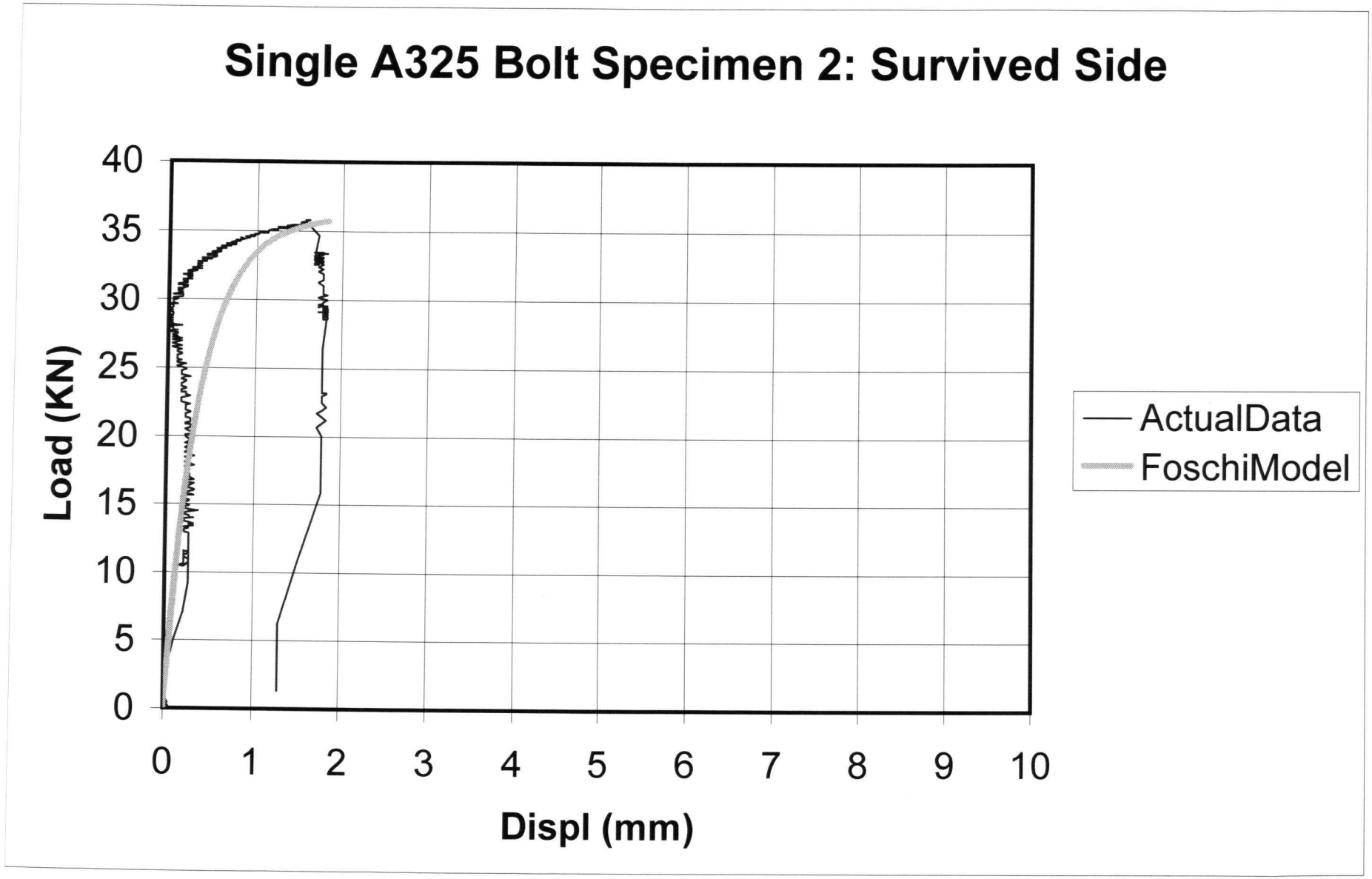
Single A325 Bolt Specimen 2: Survived Side
Load (KN)
40
35
30
25
20
15
10
5
0
0
1
2
3
4
5
6
7
8
9
10
Displ (mm)
ActualData
FoschiModel

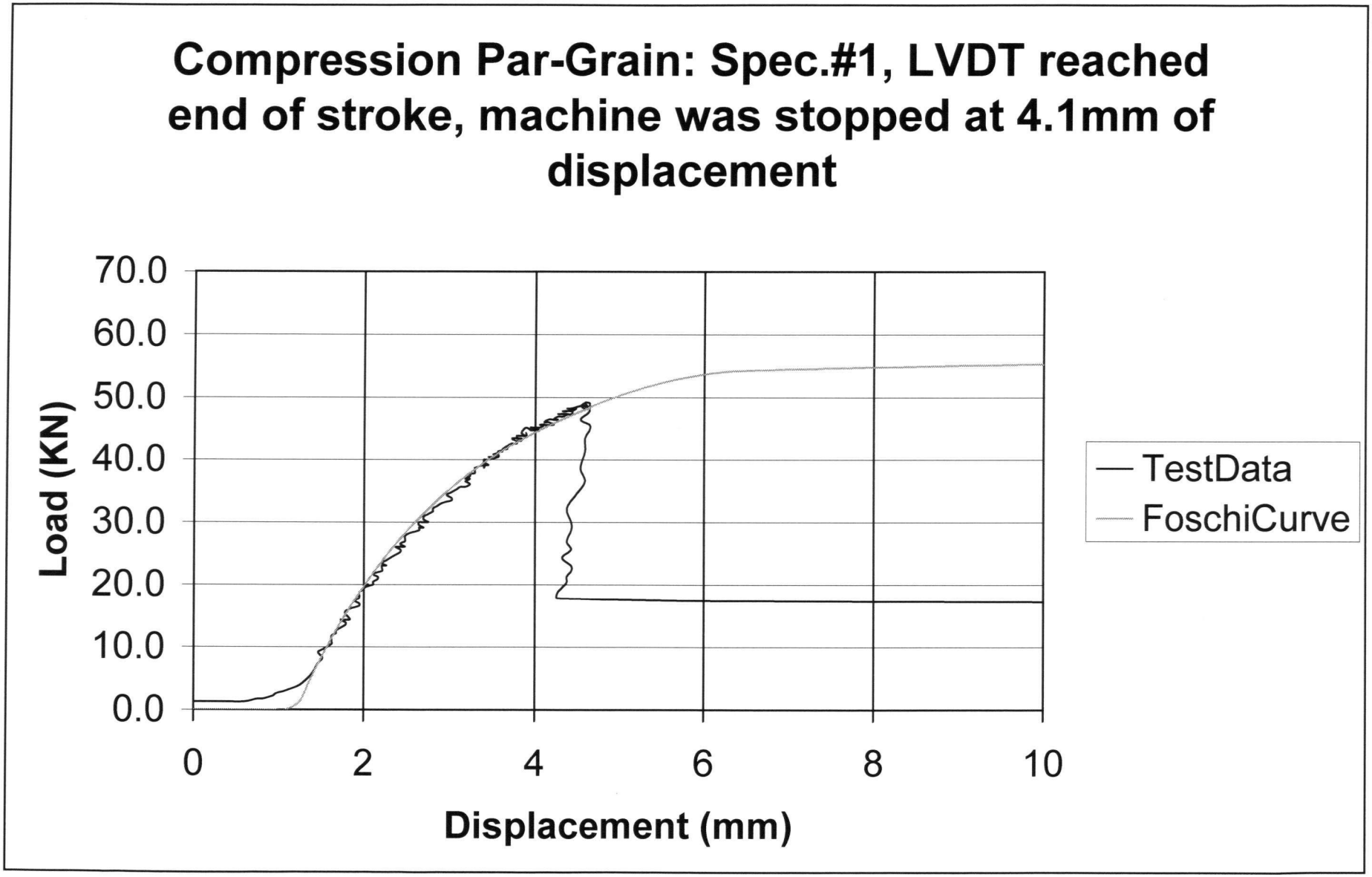
Compression Par-Grain: Spec.#1, LVDT reached end of stroke, machine was stopped at 4.1mm of displacement
70.0
60.0
50.0
40.0
30.0
20.0
10.0
0.0
Load (KN)
0
2
4
6
8
10
Displacement (mm)
TestData
FoschiCurve

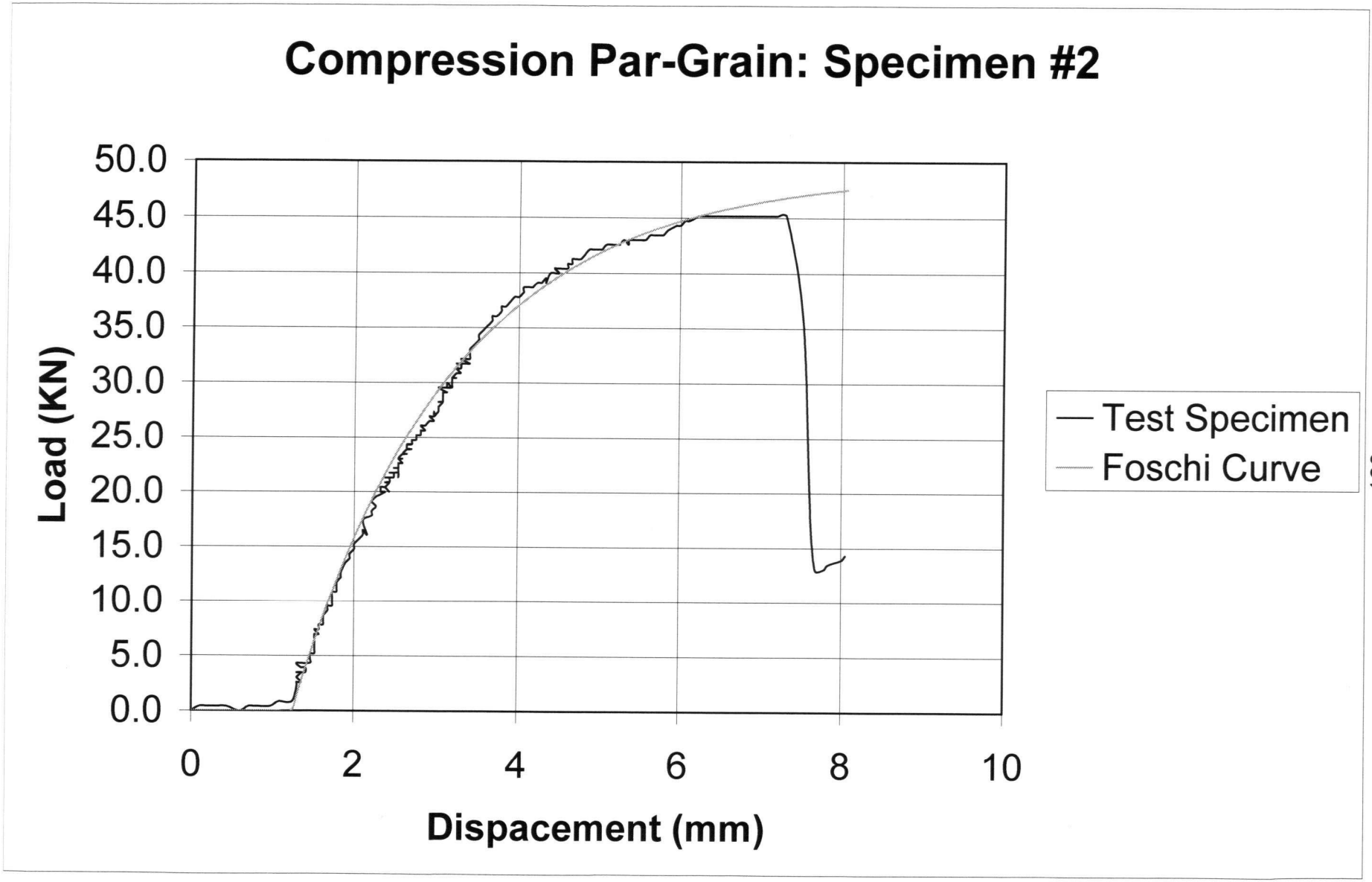
Compression Par-Grain: Specimen #2
Load (KN)
50.0
45.0
40.0
35.0
30.0
25.0
20.0
15.0
10.0
5.0
0.0
0
2
4
6
8
10
Dispacement (mm)
Test Specimen
Foschi Curve

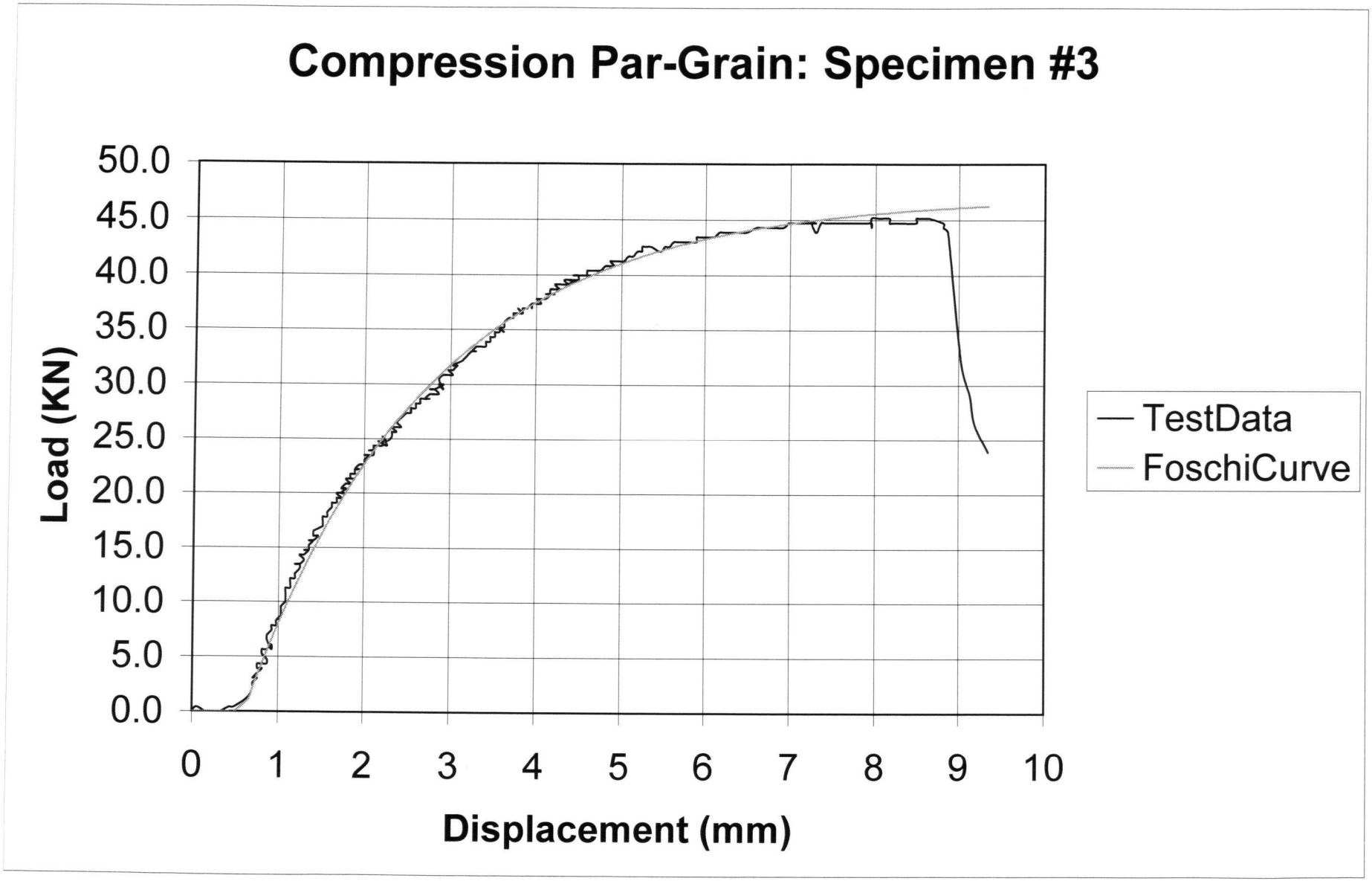
Compression Par-Grain: Specimen #3
Load (KN)
50.0
45.0
40.0
35.0
30.0
25.0
20.0
15.0
10.0
5.0
0.0
0
1
2
3
4
5
6
7
8
9
10
Displacement (mm)
TestData
FoschiCurve

Compression Par-Grain: Specimen #4, NOTE: Secondary stiffness represents bottom-out of steel

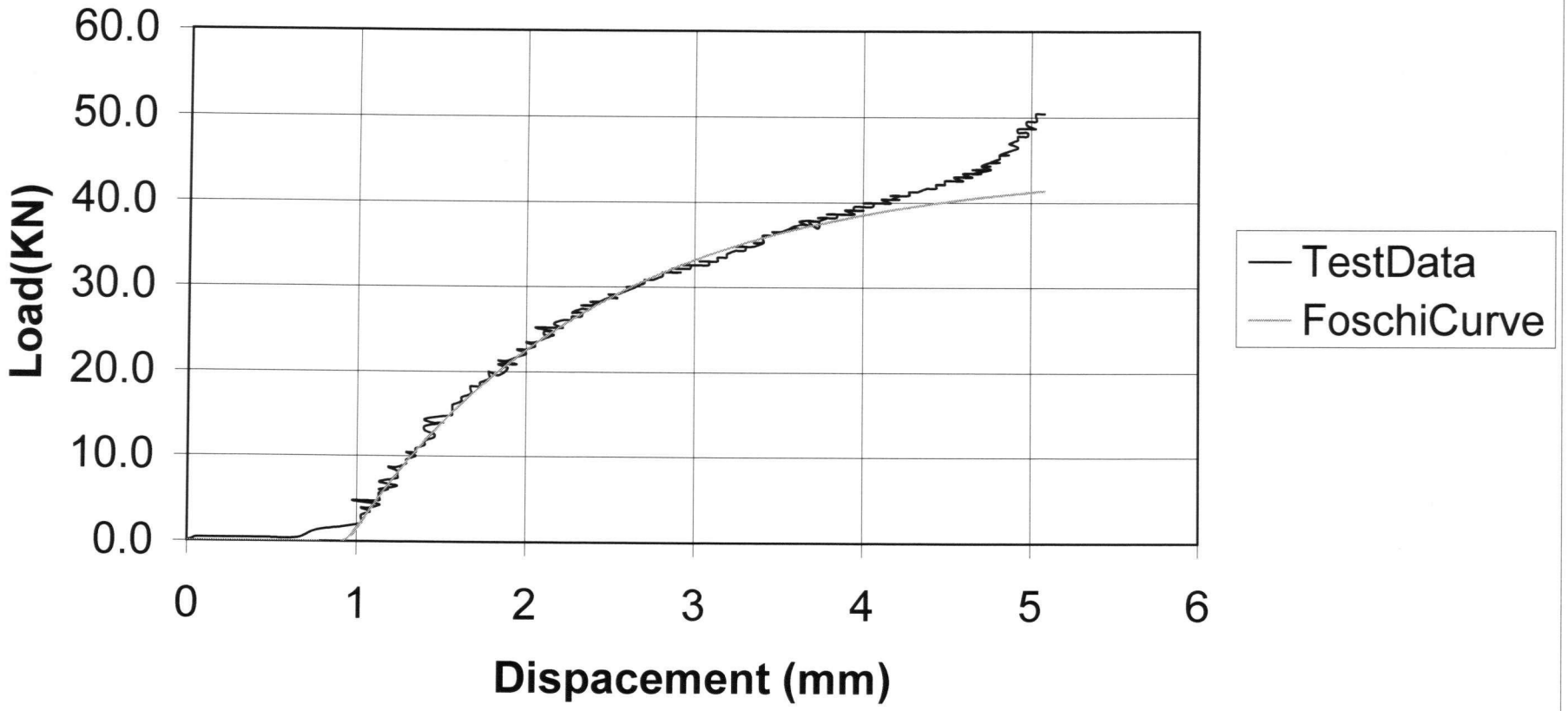

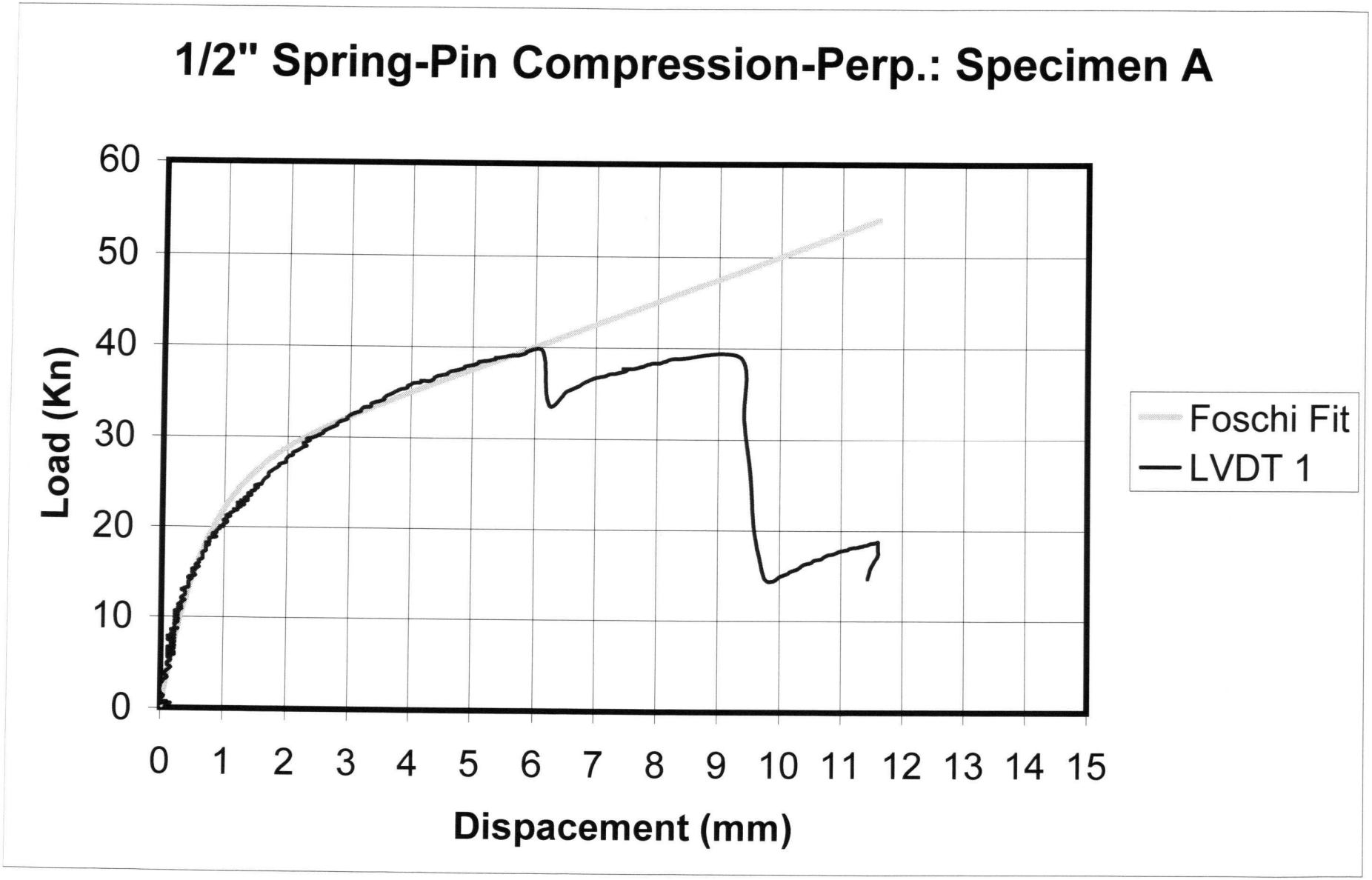
1/2" Spring-Pin Compression-Perp.: Specimen A
Load (Kn)
60
50
40
30
20
10
0
0 1 2 3 4 5 6 7 8 9 10 11 12 13 14 15
Dispacement (mm)
Foschi Fit
LVDT 1

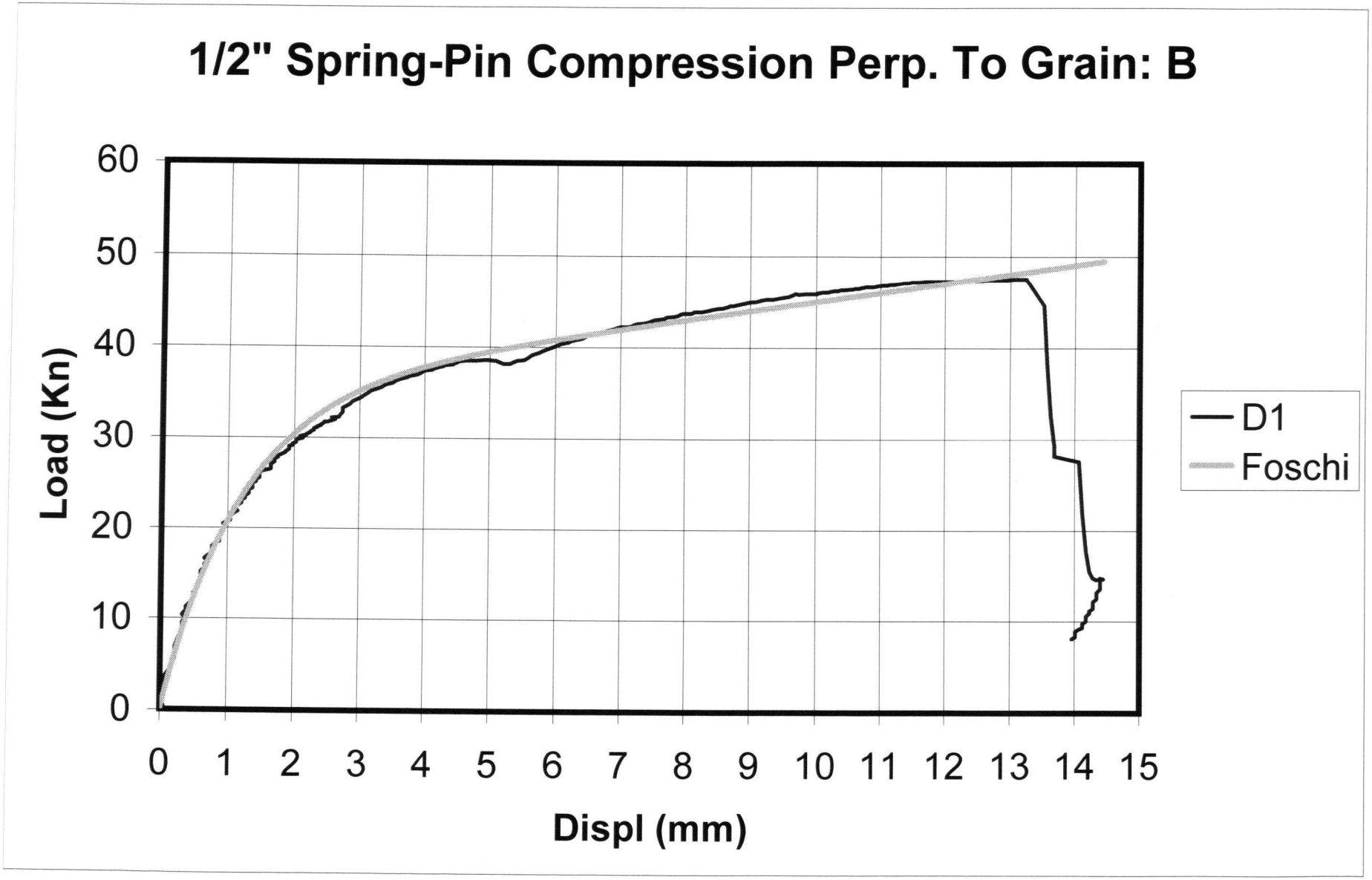
1/2" Spring-Pin Compression Perp. To Grain: B
Load (Kn)
60
50
40
30
20
10
0
0 1 2 3 4 5 6 7 8 9 10 11 12 13 14 15
Displ (mm)
D1
Foschi

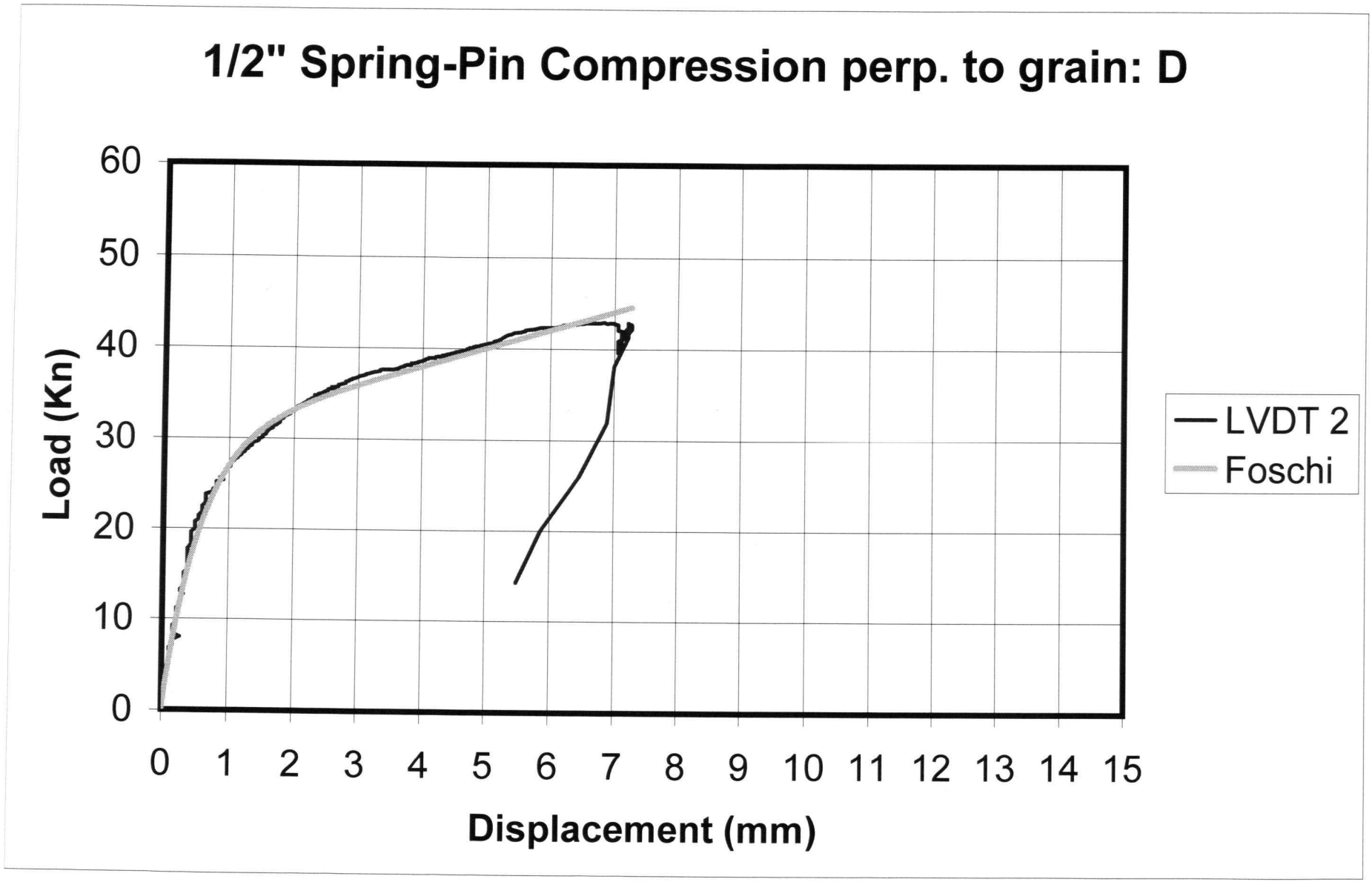
1/2" Spring-Pin Compression perp. to grain: D
Load (Kn)
60
50
40
30
20
10
0
0 1 2 3 4 5 6 7 8 9 10 11 12 13 14 15
Displacement (mm)
LVDT 2
Foschi

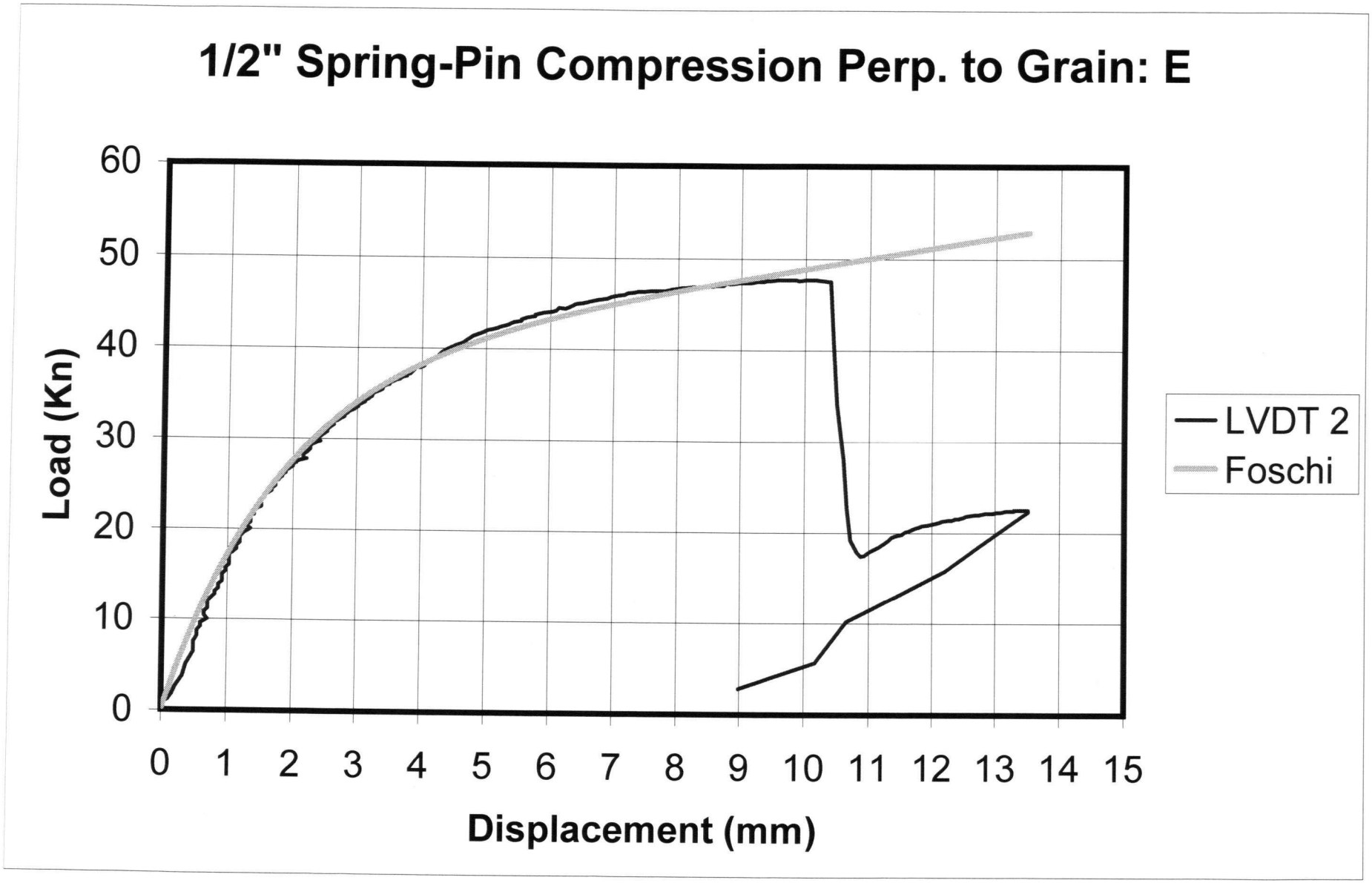
1/2" Spring-Pin Compression Perp. to Grain: E
Load (Kn)
60
50
40
30
20
10
0
0 1 2 3 4 5 6 7 8 9 10 11 12 13 14 15
Displacement (mm)
LVDT 2
Foschi

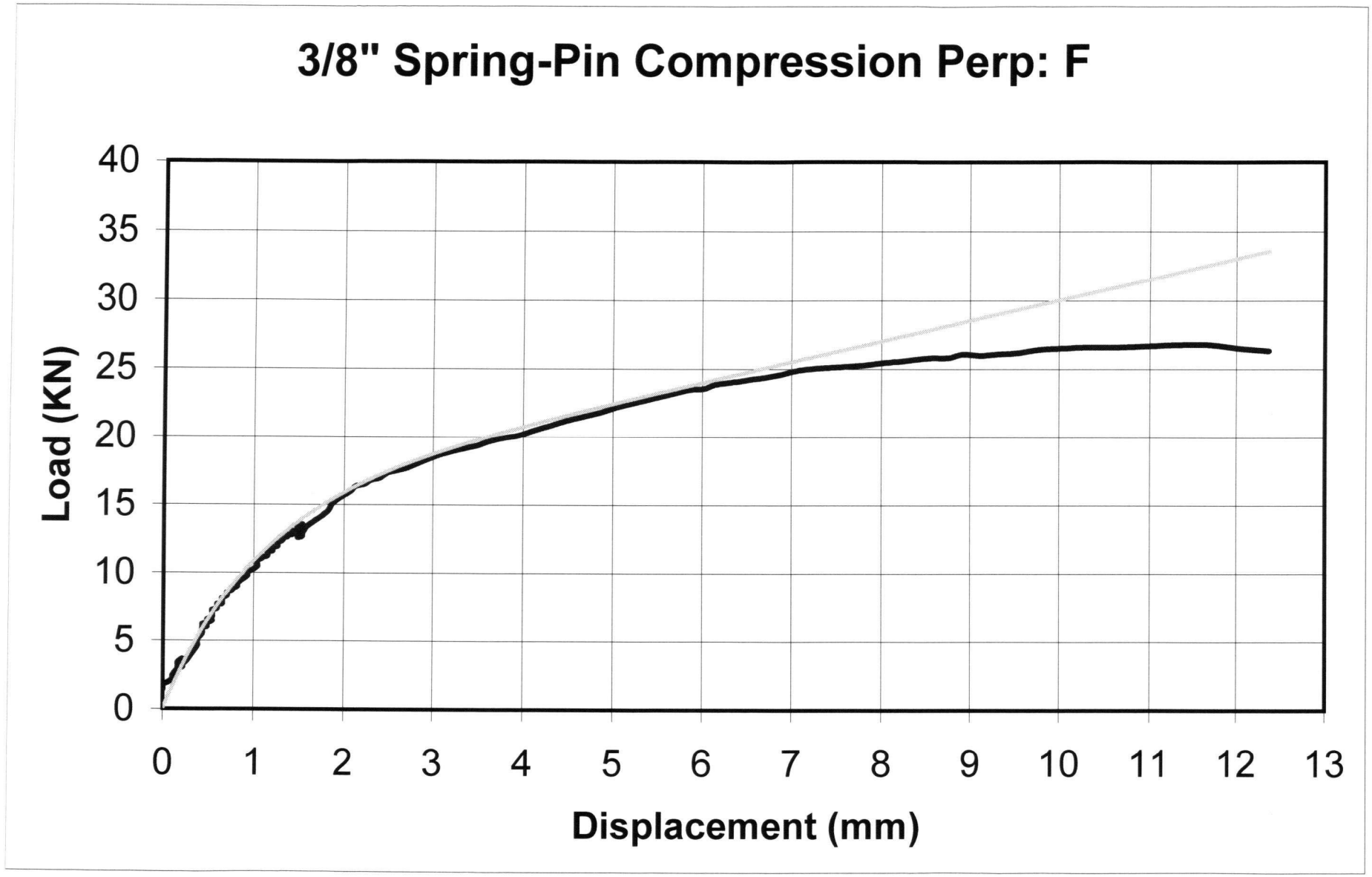
3/8" Spring-Pin Compression Perp: F
Load (KN)
40
35
30
25
20
15
10
5
0
0
1
2
3
4
5
6
7
8
9
10
11
12
13
Displacement (mm)

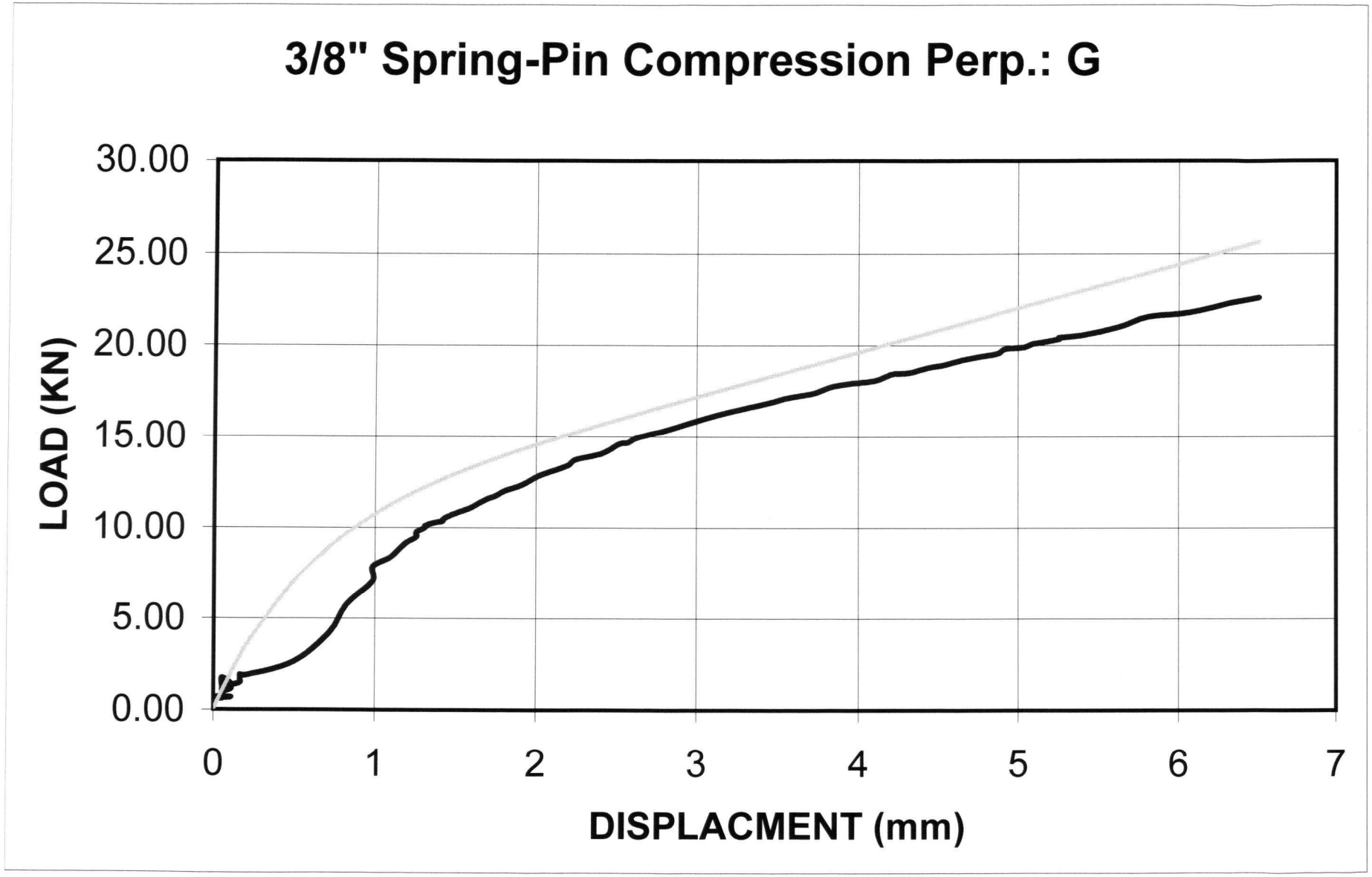
3/8" Spring-Pin Compression Perp.: G
LOAD (KN)
30.00
25.00
20.00
15.00
10.00
5.00
0.00
0
1
2
3
4
5
6
7
DISPLACMENT (mm)

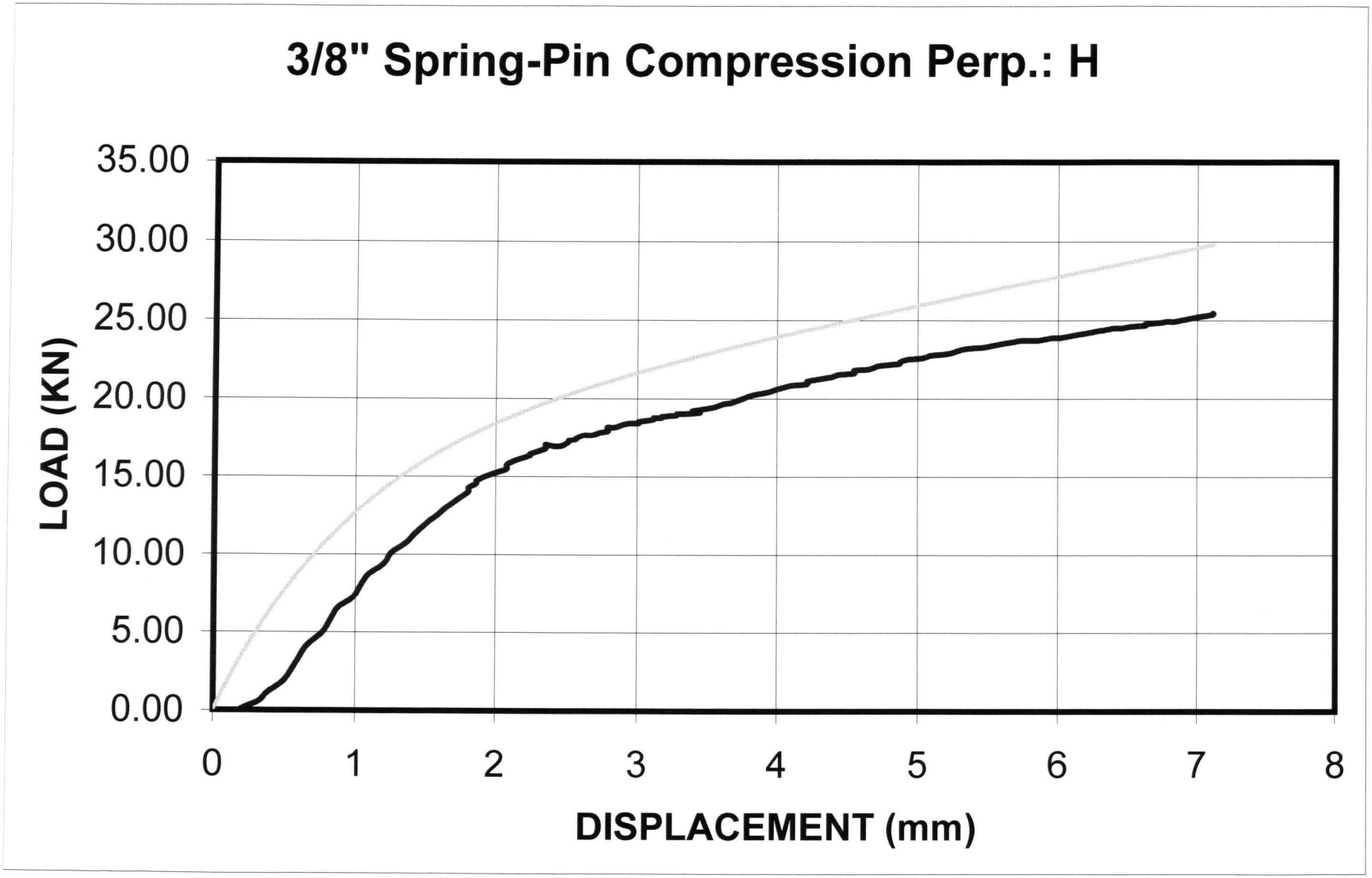
3/8" Spring-Pin Compression Perp.: H
LOAD (KN)
35.00
30.00
25.00
20.00
15.00
10.00
5.00
0.00
0
1
2
3
4
5
6
7
8
DISPLACEMENT (mm)

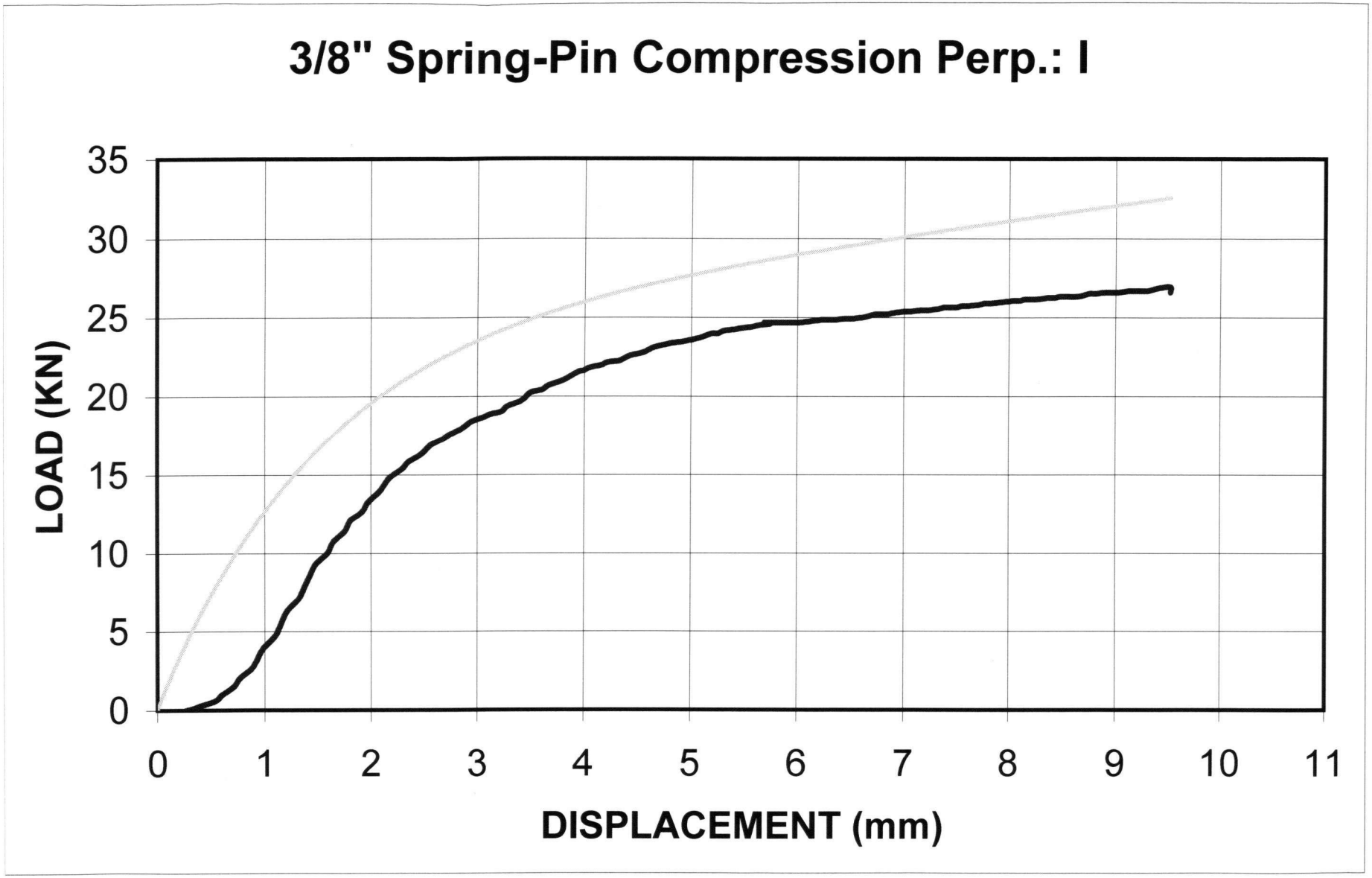
3/8" Spring-Pin Compression Perp.: I
LOAD (KN)
35
30
25
20
15
10
5
0
0
1
2
3
4
5
6
7
8
9
10
11
DISPLACEMENT (mm)

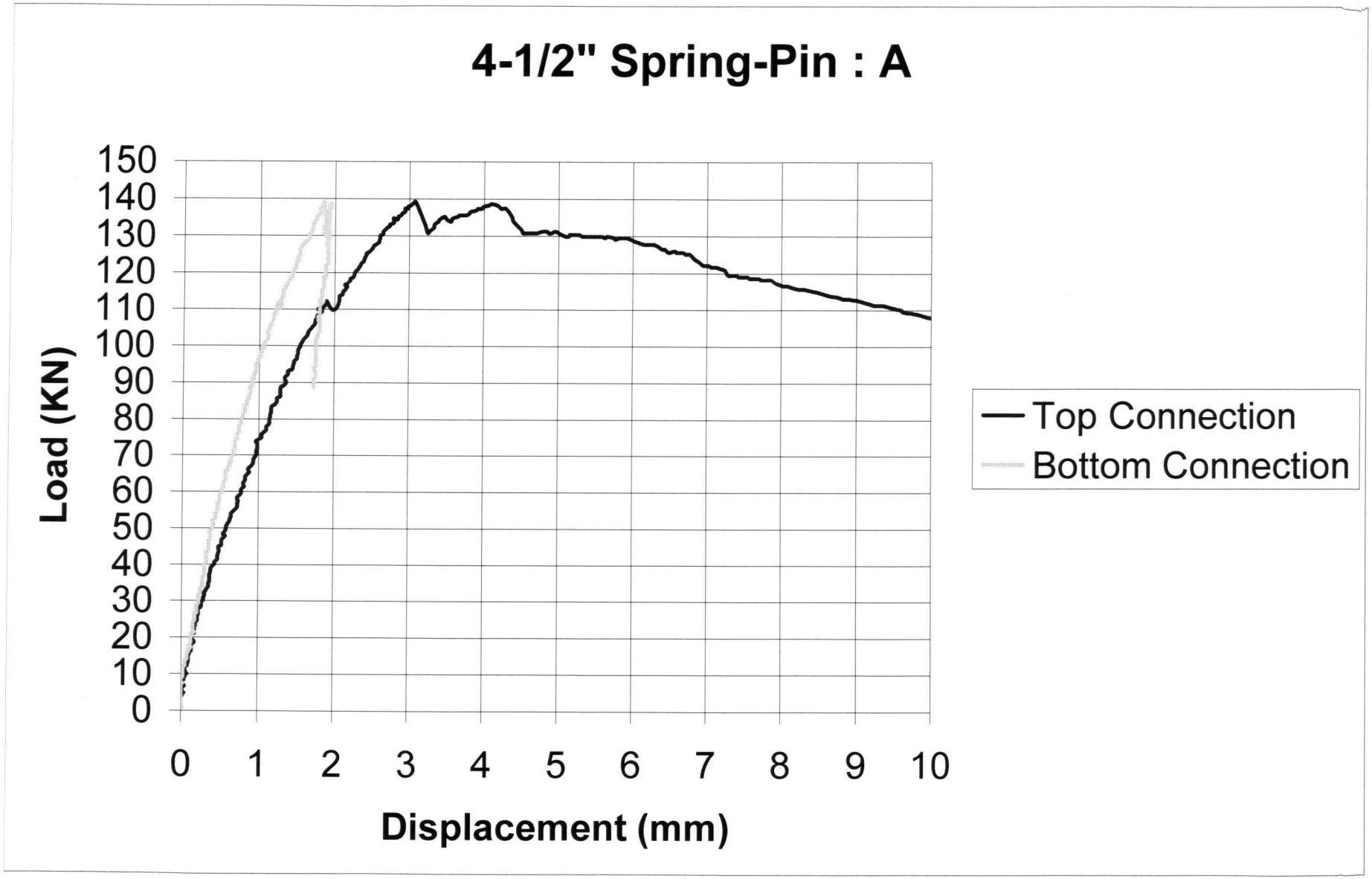
4-1/2" Spring-Pin : A
Load (KN)
150
140
130
120
110
100
90
80
70
60
50
40
30
20
10
0
0 1 2 3 4 5 6 7 8 9 10
Displacement (mm)
Top Connection
Bottom Connection

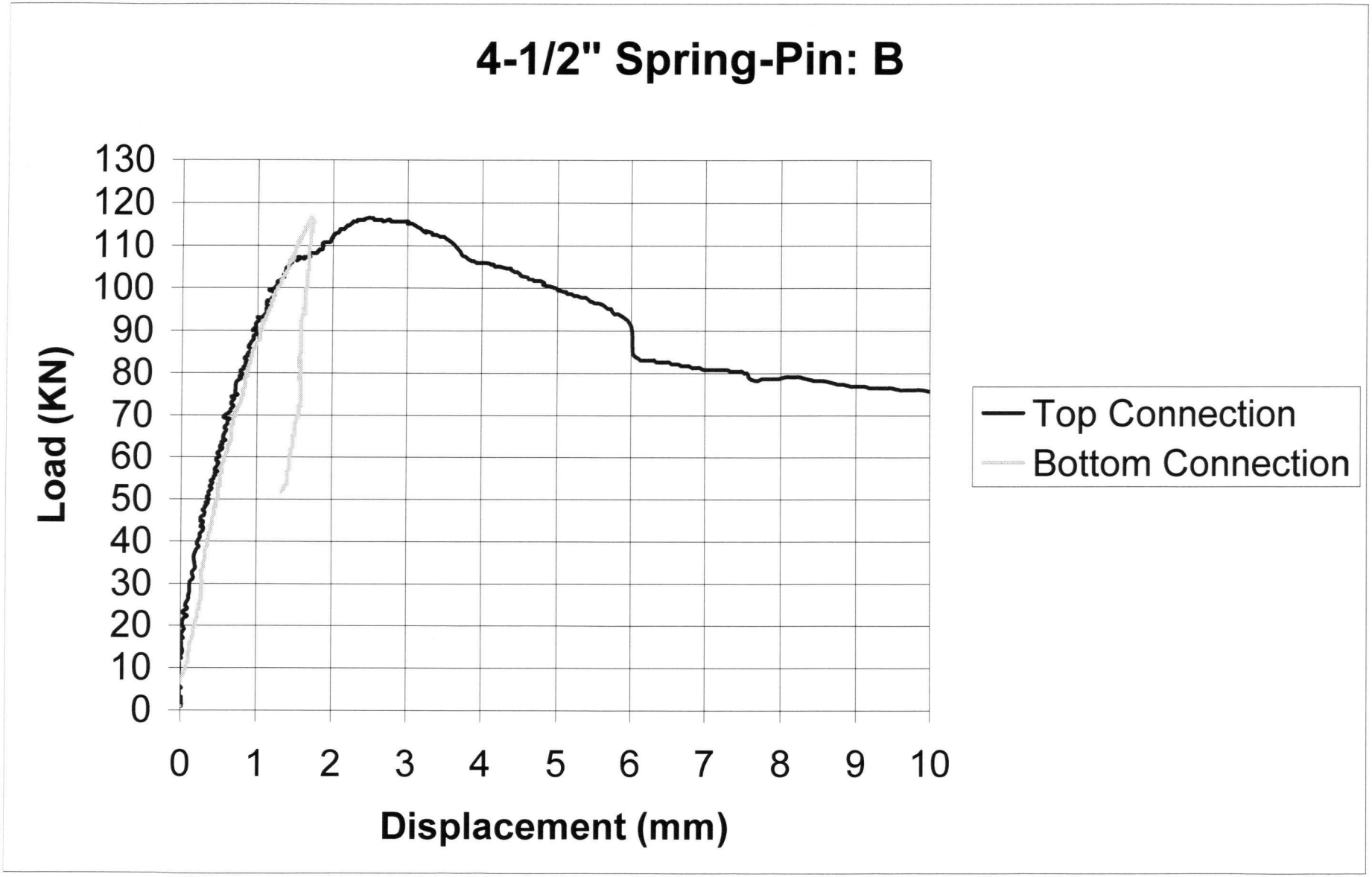
4-1/2" Spring-Pin: B
Load (KN)
130
120
110
100
90
80
70
60
50
40
30
20
10
0
0 1 2 3 4 5 6 7 8 9 10
Displacement (mm)
Top Connection
Bottom Connection

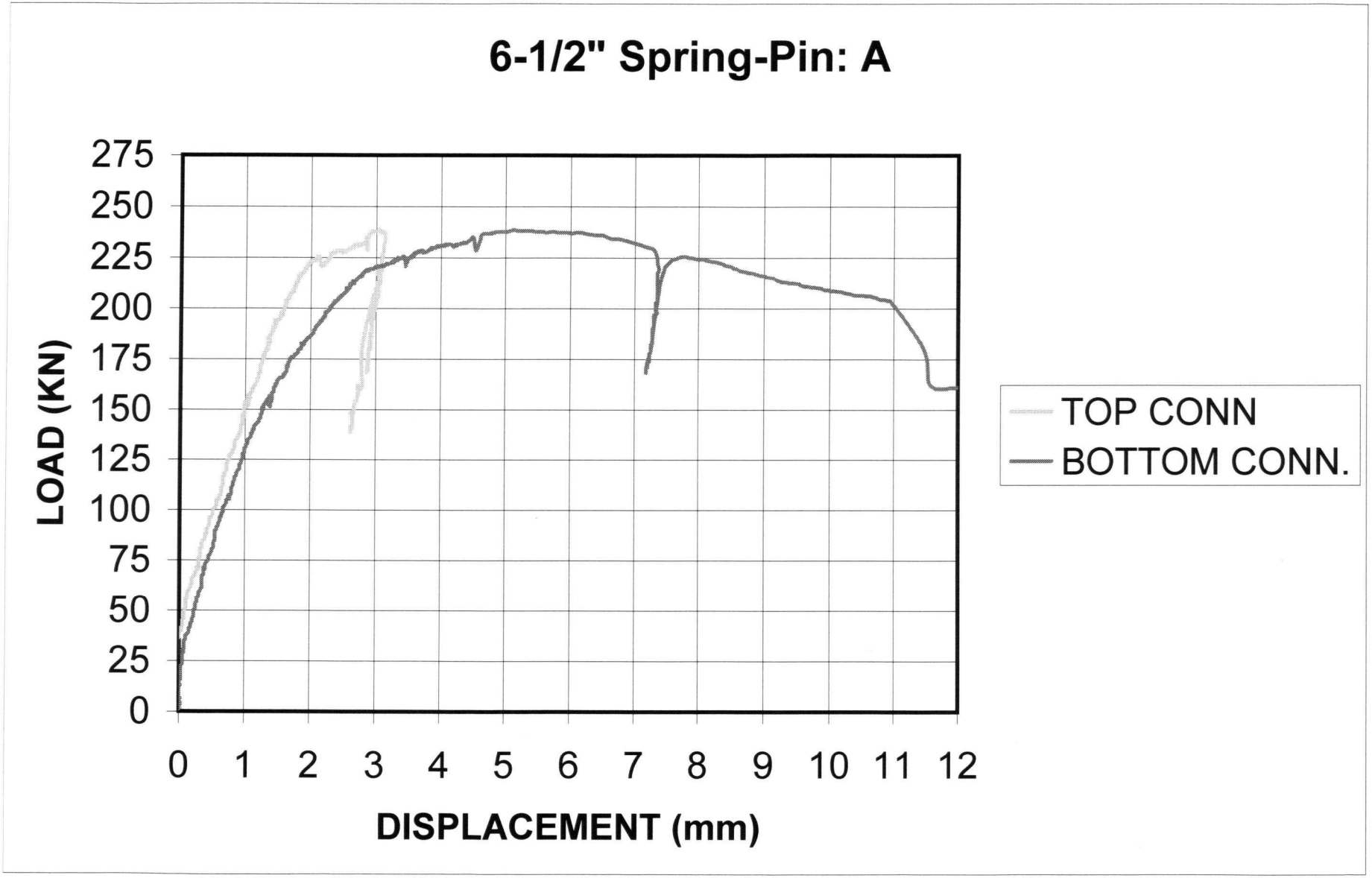
6-1/2" Spring-Pin: A
LOAD (KN)
275
250
225
200
175
150
125
100
75
50
25
0
0 1 2 3 4 5 6 7 8 9 10 11 12
DISPLACEMENT (mm)
TOP CONN
BOTTOM CONN.

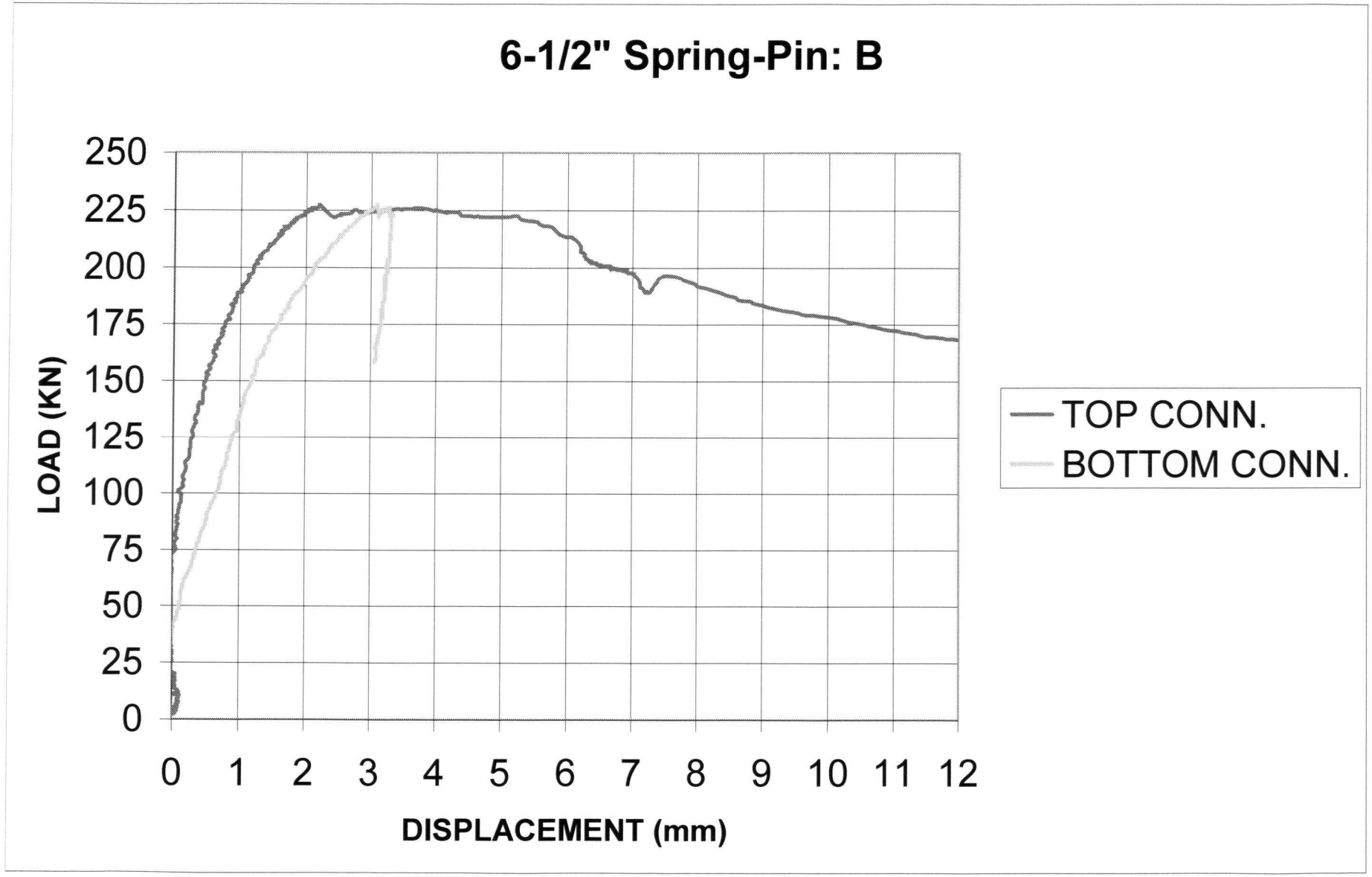
6-1/2" Spring-Pin: B
LOAD (KN)
250
225
200
175
150
125
100
75
50
25
0
0 1 2 3 4 5 6 7 8 9 10 11 12
DISPLACEMENT (mm)
TOP CONN.
BOTTOM CONN.

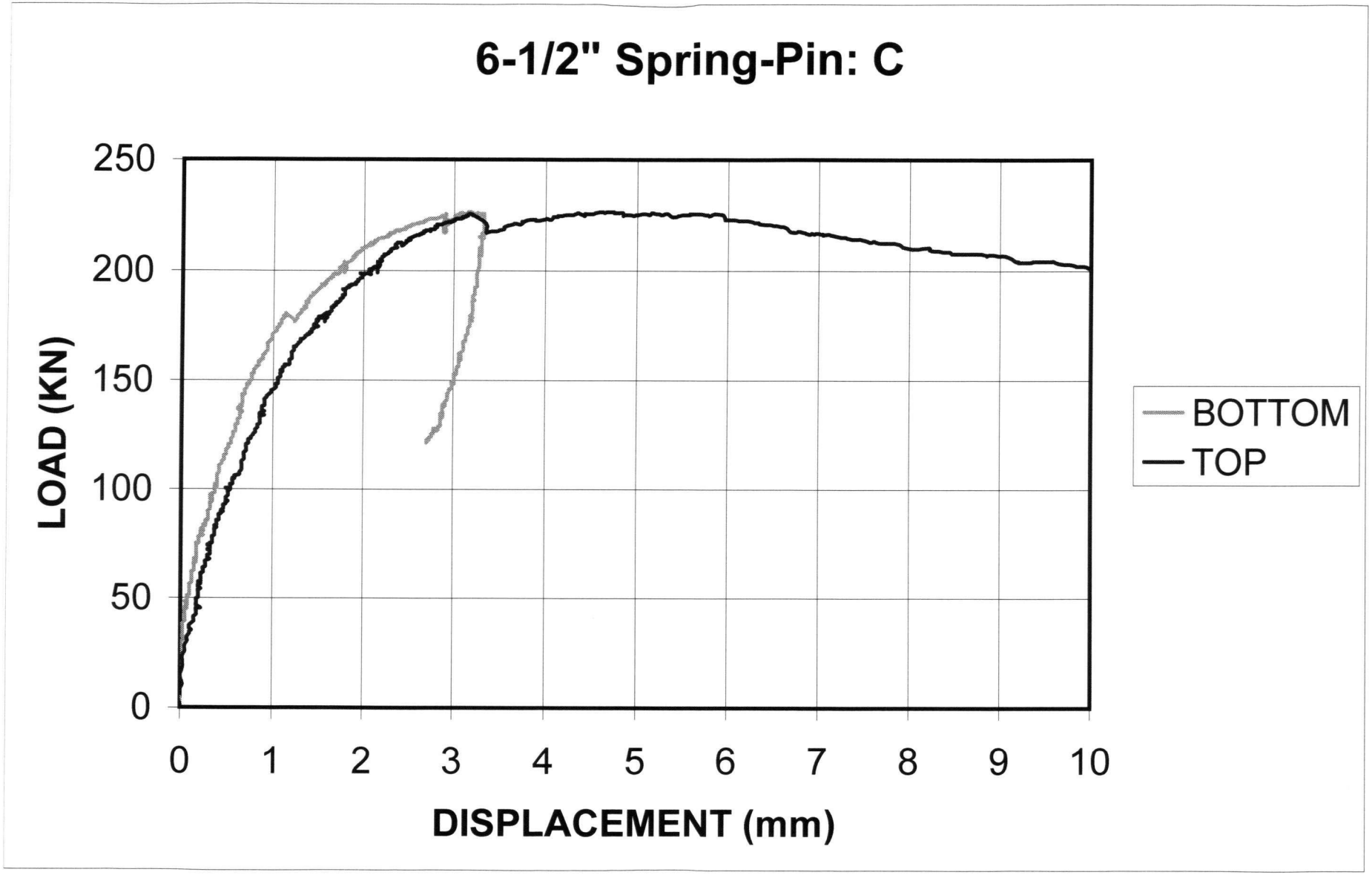
6-1/2" Spring-Pin: C
LOAD (KN)
250
200
150
100
50
0
0
1
2
3
4
5
6
7
8
9
10
DISPLACEMENT (mm)
BOTTOM
TOP

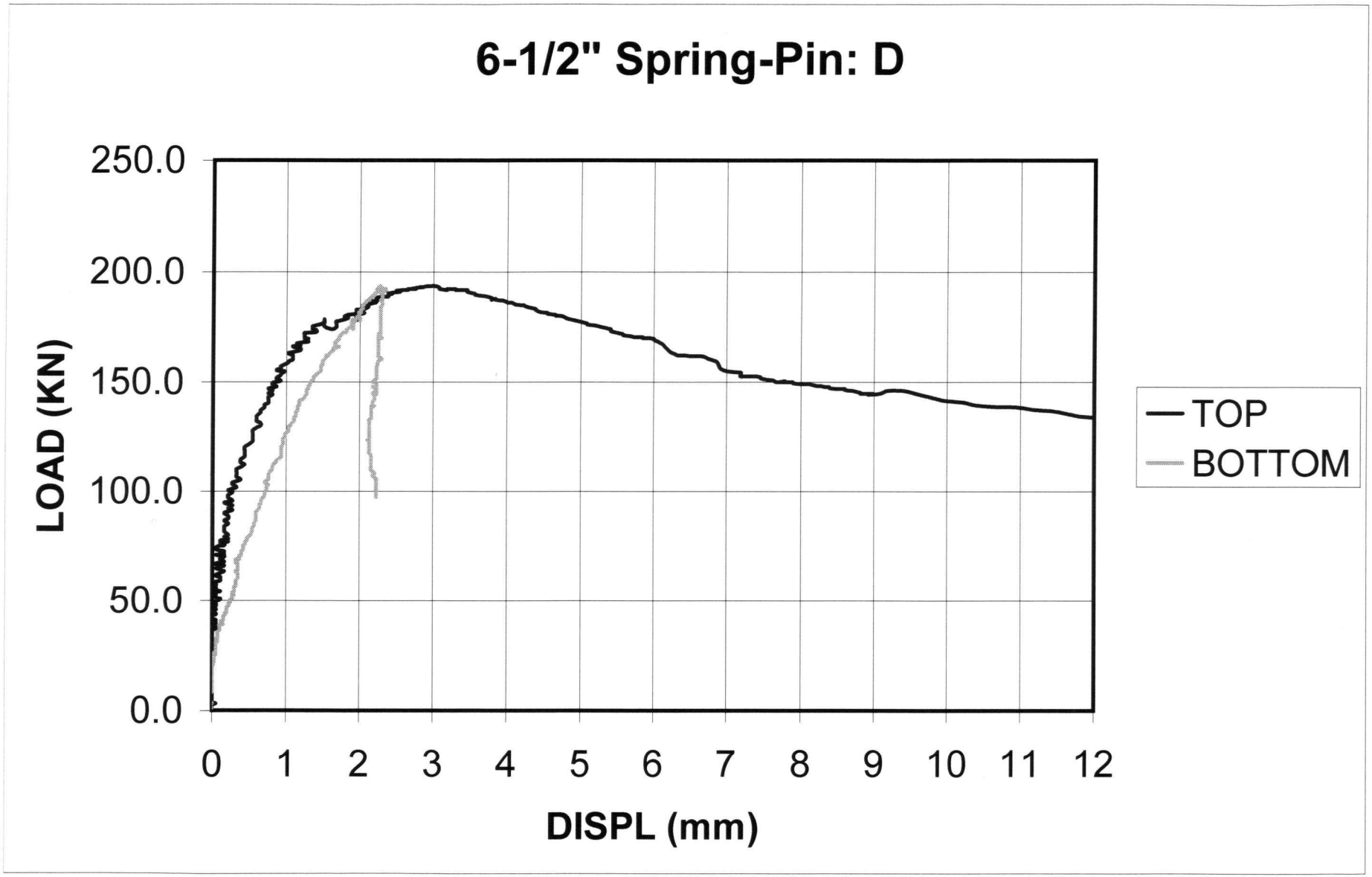
6-1/2" Spring-Pin: D
LOAD (KN)
250.0
200.0
150.0
100.0
50.0
0.0
0
1
2
3
4
5
6
7
8
9
10
11
12
DISPL (mm)
TOP
BOTTOM

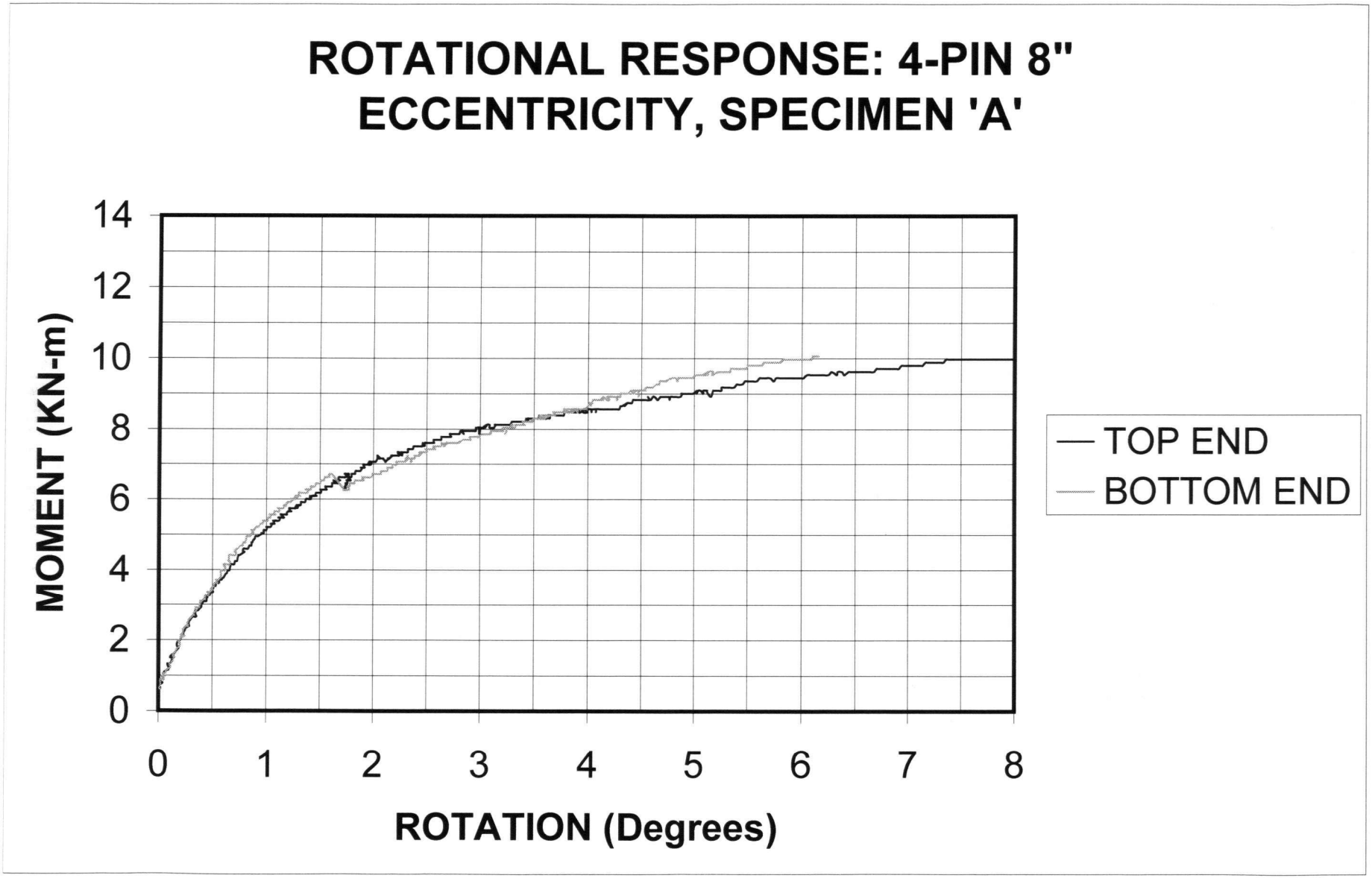
ROTATIONAL RESPONSE: 4-PIN 8" ECCENTRICITY, SPECIMEN 'A'
MOMENT (KN-m)
14
12
10
8
6
4
2
0
0
1
2
3
4
5
6
7
8
ROTATION (Degrees)
TOP END
BOTTOM END

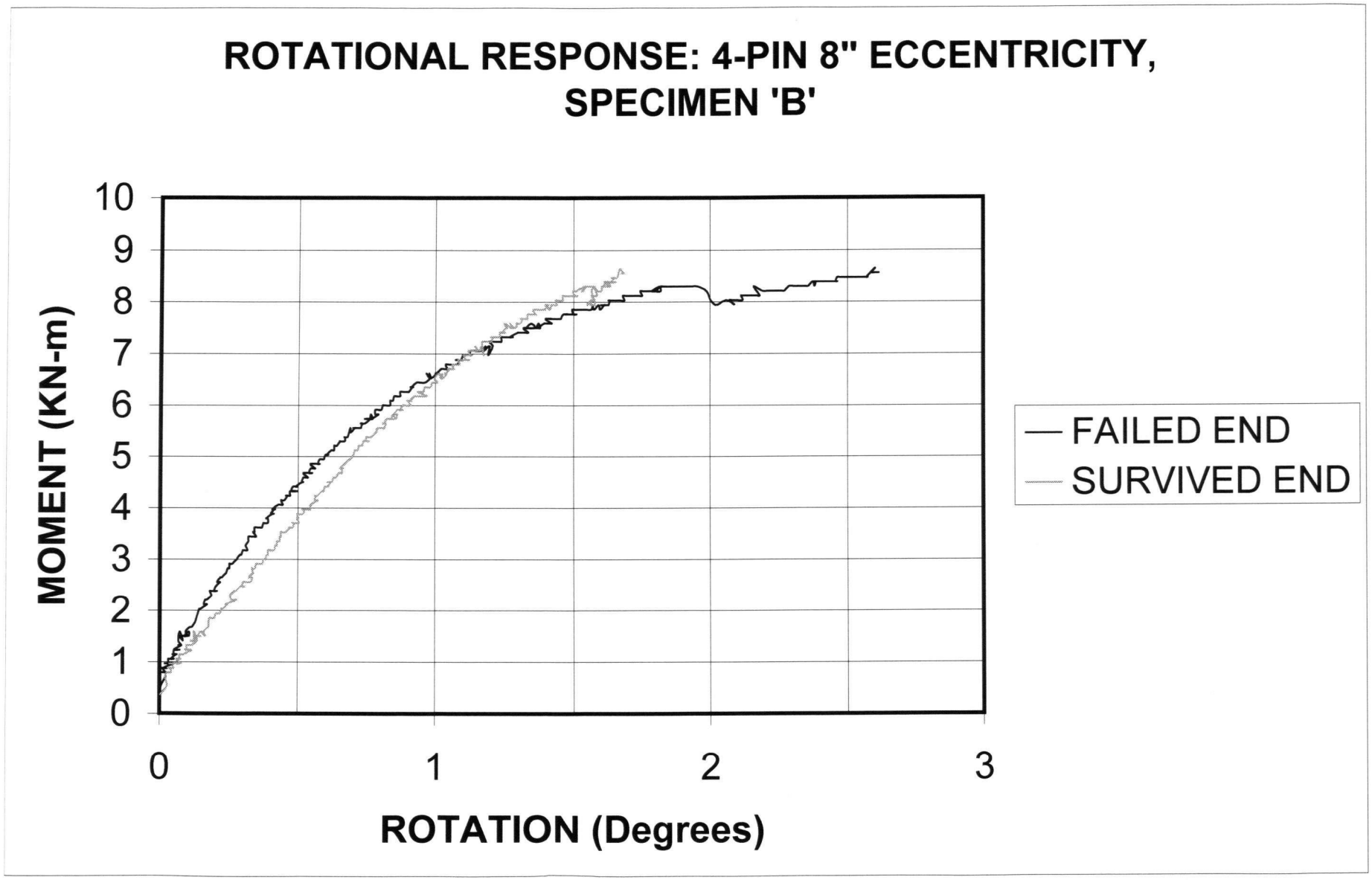
ROTATIONAL RESPONSE: 4-PIN 8" ECCENTRICITY, SPECIMEN 'B'
MOMENT (KN-m)
10
9
8
7
6
5
4
3
2
1
0
0
1
2
3
ROTATION (Degrees)
FAILED END
SURVIVED END

ROTATIONAL RESPONSE: 6-PIN 8" ECCENTRICITY, SPECIMEN 'A'

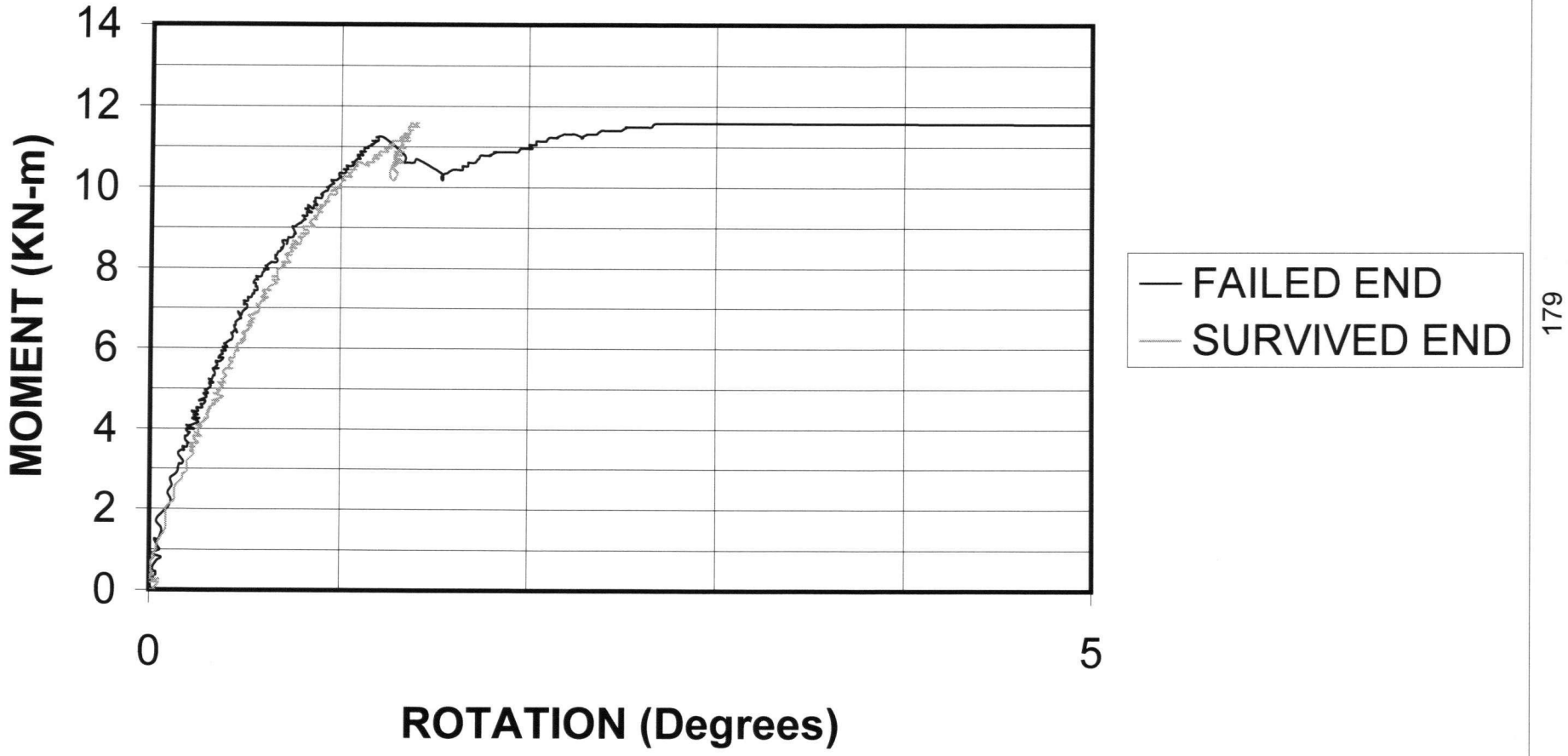

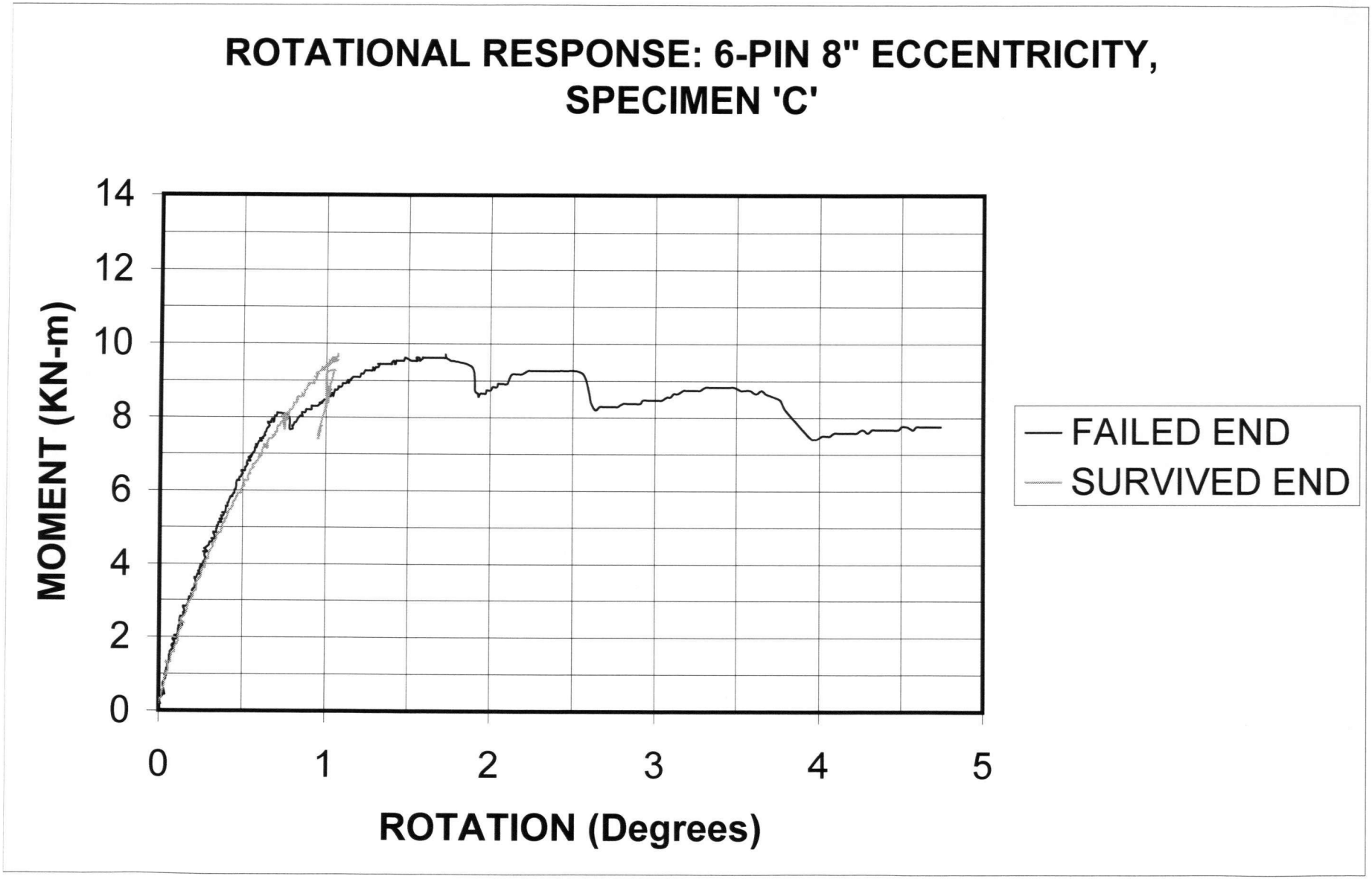
ROTATIONAL RESPONSE: 6-PIN 8" ECCENTRICITY, SPECIMEN 'C'
MOMENT (KN-m)
14
12
10
8
6
4
2
0
0
1
2
3
4
5
ROTATION (Degrees)
FAILED END
SURVIVED END

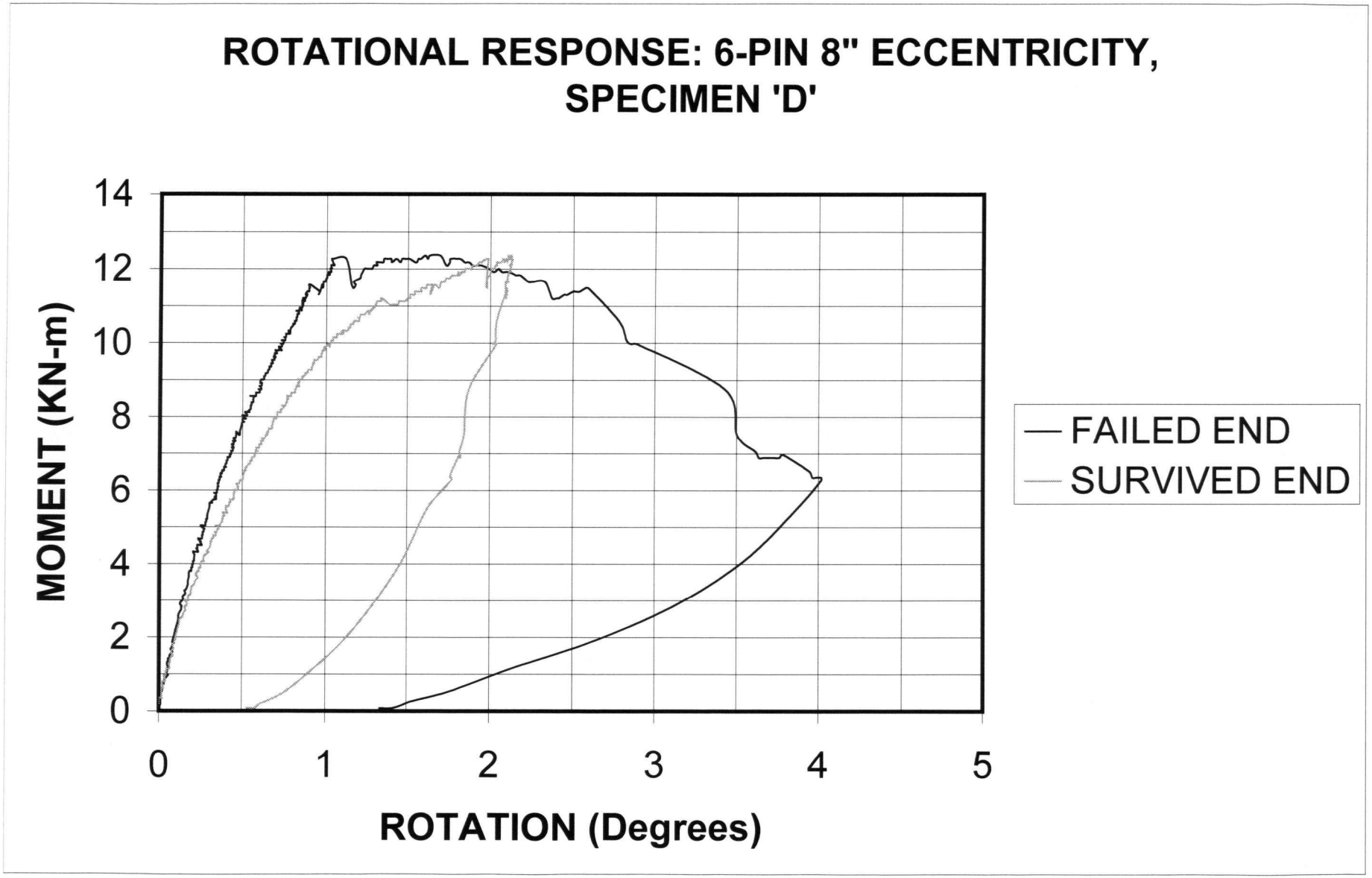
ROTATIONAL RESPONSE: 6-PIN 8" ECCENTRICITY, SPECIMEN 'D'
MOMENT (KN-m)
14
12
10
8
6
4
2
0
0
1
2
3
4
5
ROTATION (Degrees)
FAILED END
SURVIVED END

OBSERVED ROTATIONAL RESPONSE: 6-pin 5"ECCENTRICITY, SPECIMEN 'D'

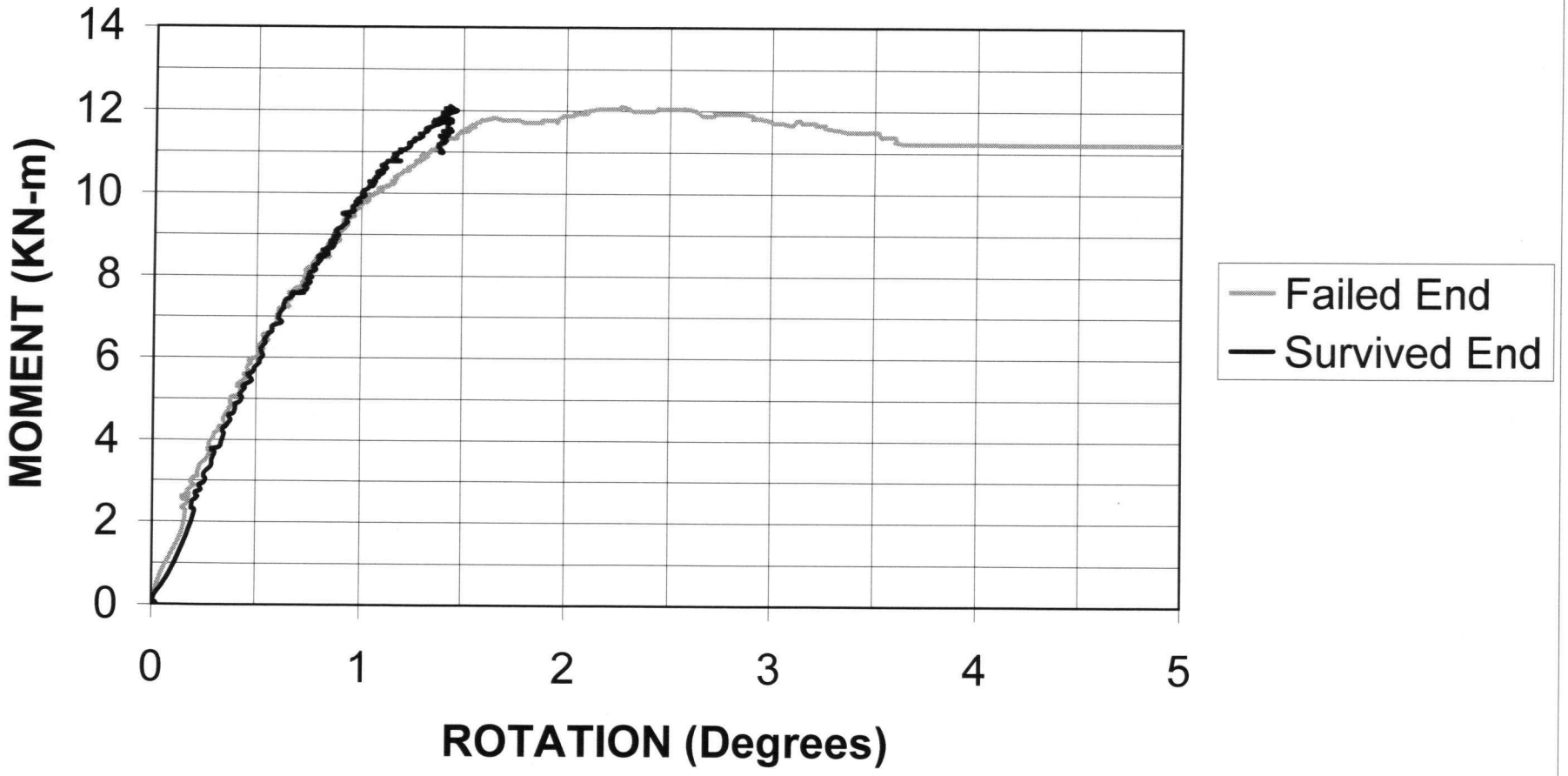

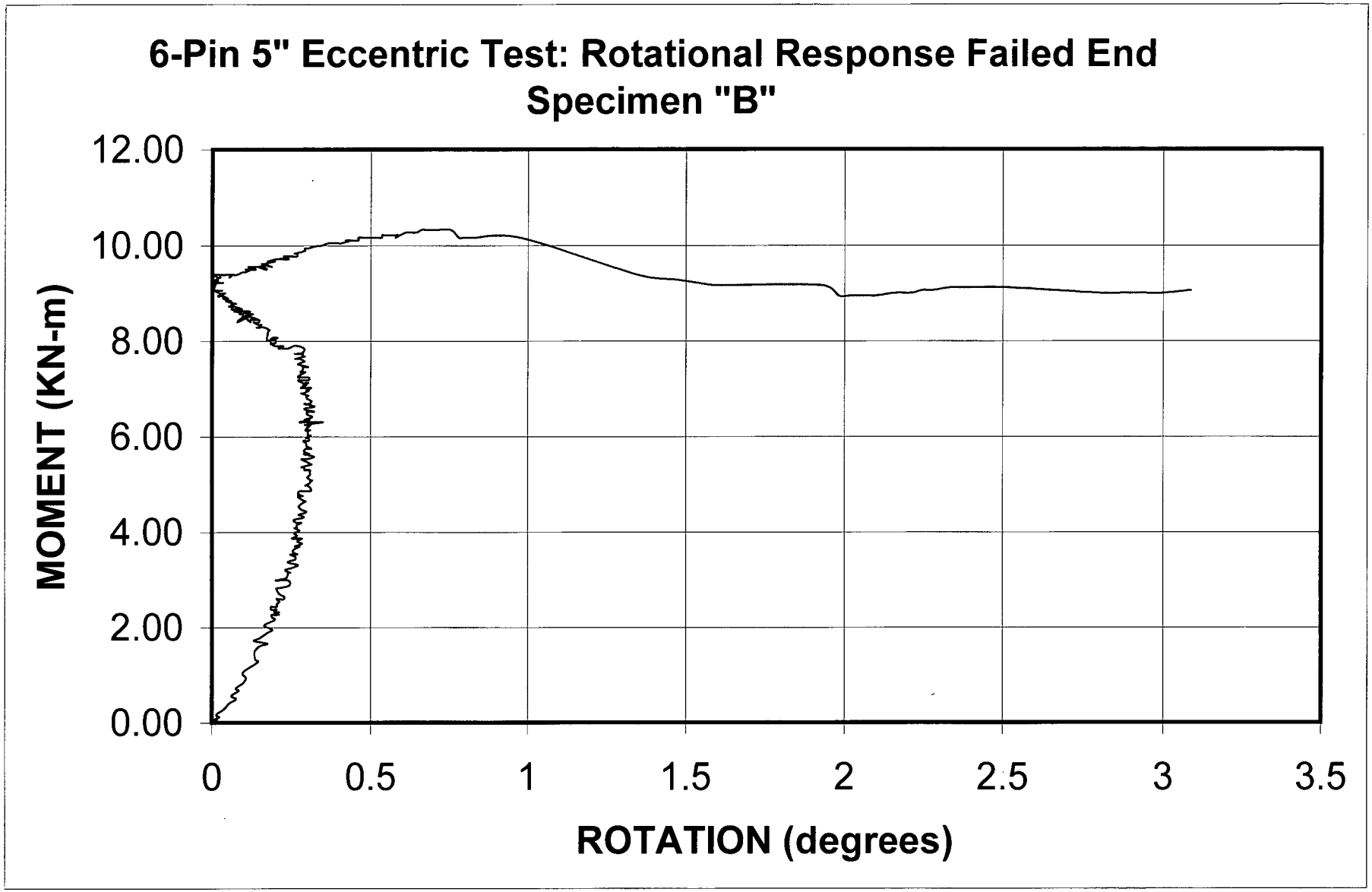
6-Pin 5" Eccentric Test: Rotational Response Failed End
Specimen "B"
MOMENT (KN-m)
12.00
10.00
8.00
6.00
4.00
2.00
0.00
0
0.5
1
1.5
2
2.5
3
3.5
ROTATION (degrees)

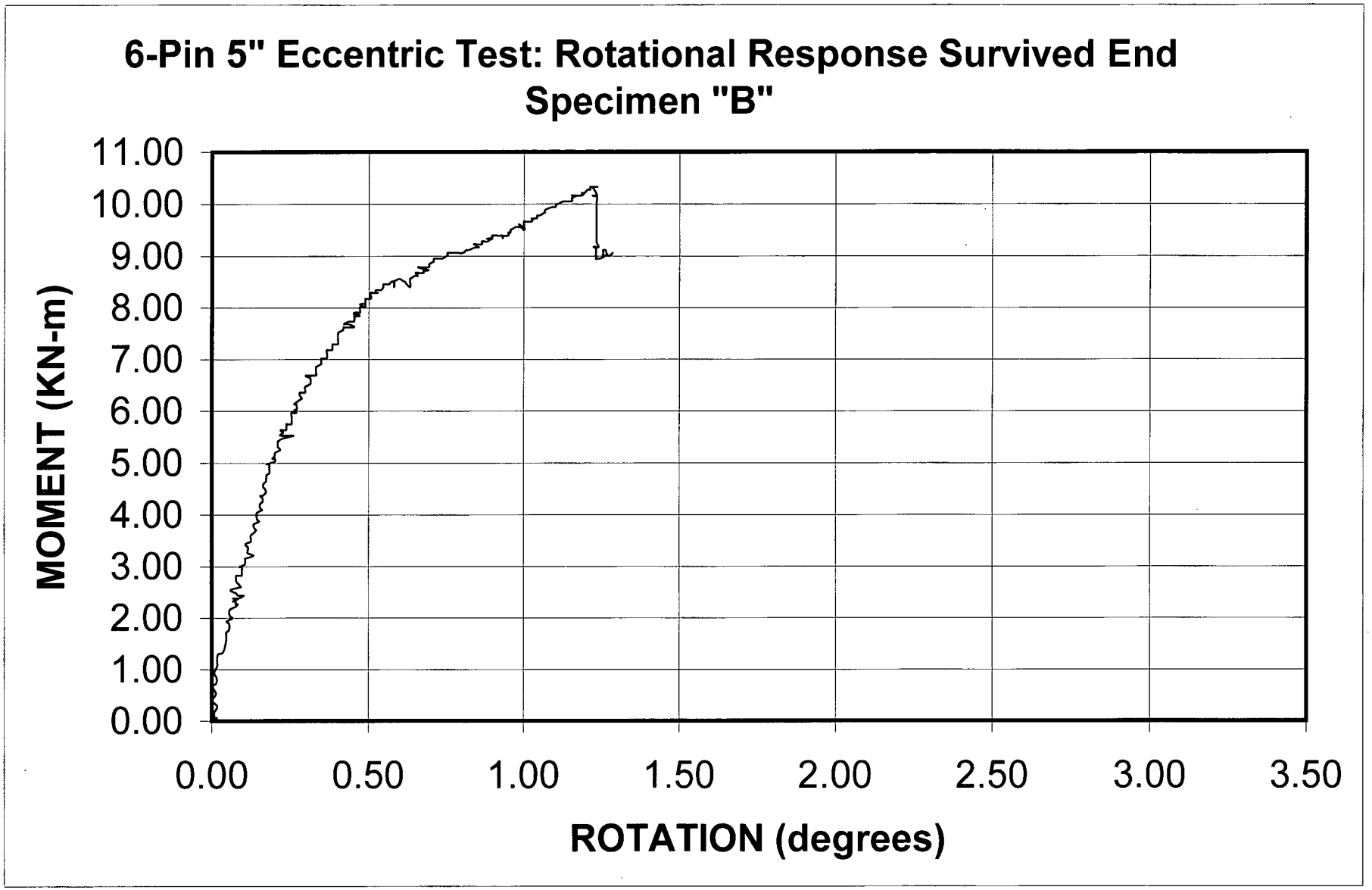
6-Pin 5" Eccentric Test: Rotational Response Survived End Specimen "B"
MOMENT (KN-m)
11.00
10.00
9.00
8.00
7.00
6.00
5.00
4.00
3.00
2.00
1.00
0.00
0.00
0.50
1.00
1.50
2.00
2.50
3.00
3.50
ROTATION (degrees)